

**The Role of Growth Hormone Secretagogue Receptor  
(GHSR) in Apoptosis**

LAU Pui Ngan

A Thesis Submitted in Partial Fulfilment  
of the Requirements for the Degree of  
Master of Philosophy

in

Pharmacology

©The Chinese University of Hong Kong  
June 2005

The Chinese University of Hong Kong holds the copyright of this thesis. Any person(s) intending to use a part or whole of the materials in the thesis in a proposed publication must seek copyright release from the Dean of the Graduate School.



## Abstract

The growth hormone secretagogue receptor (GHS-R) belongs to the G-protein coupled receptor (GPC-R) superfamily. GHS-R has two subtypes, a 7-transmembrane (7-TM) receptor named GHS-R1a and a 5-TM non-signaling receptor named GHS-R1b. Apoptosis is programmed cell death. Preliminary studies suggested that human embryonic kidney 293 (HEK293) cells stably expressing black seabream GHS-R1a (sbGHS-R1a) and transiently expressed HA-sbGHS-R1b induced anti-apoptotic and pro-apoptotic effects, respectively. This study aims to further examine the role of GHS-R in apoptosis regulation using human GHS-R (hGHS-R) and to define any functional relationship between hGHS-R subtypes. In order to reflect the apoptotic condition in the cells, caspase-3 (apoptosis executioner) activity was measured by colorimetric assay.

GHS-R1a is a G<sub>q</sub>-coupled receptor, so the properties of GHS-R1a were further examined by measuring the inositol phosphate (IP) production. There was a GHS-R1a concentration-dependent increase in the basal [<sup>3</sup>H]-IP production, which was reduced by GHS-R1a inverse agonist [D-Arg<sup>1</sup>,D-Phe<sup>5</sup>,D-Trp<sup>7,9</sup>,Leu<sup>11</sup>]-substance P (SPa), indicating that GHS-R1a is a constitutively active receptor. The GHS-R1a agonists, ghrelin and GHRP-6 were found to stimulate [<sup>3</sup>H]-IP production. In contrast to GHS-R1a, GHS-R1b is unresponsive to agonists.

In HEK293 cells transiently transfected with hGHS-R1a, adenosine was showed to be a partial agonist and induced an additive effect to ghrelin-stimulated [<sup>3</sup>H]-IP

production. To determine if part of the ghrelin- and adenosine-stimulated [ $^3\text{H}$ ]-IP production were due to any endogenous adenosine, the effect of adenosine deaminase (ADA), which breakdowns adenosine was studied. Results showed all the tested receptor-stimulated [ $^3\text{H}$ ]-IP productions were decreased. Therefore, the specificity of ADA was determined by using an adenosine blocker theophylline. However, theophylline did not block any agonist-stimulated [ $^3\text{H}$ ]-IP production. These data did not help in reaching conclusions.

To investigate the functional relationship between hGHS-R subtypes in apoptosis, one of the methods is to co-transfect the hGHS-R1a and hGHS-R1b into the cells. However, it was demonstrated that the additional plasmid DNAs in the transfection potentiated the GHS-R1a basal and agonist-stimulated [ $^3\text{H}$ ]-IP production. This phenomenon was also demonstrated in hTP $\alpha$  and transfection reagents. One of the explanations is the additional plasmid DNA increased the transfection efficiency. This potentiating effect makes data interpretation more complicated, but the unsuccessfulness in developing monoclonal HEK293 cells stably expressing hGHS-R. In addition, the properties of sbGHS-R were similar to hGHS-R. Therefore, HEK293 cells stably expressing sbGHS-R1a (HEK-sbGHS-R1a) or sbGHS-R1b (HEK-sbGHS-R1b) were used to study the role of GHS-R in apoptosis regulation.

In HEK293, HEK-sbGHS-R1a and HEK-sbGHS-R1b cells, in order to get an optimized staurosporine- and etoposide-induced caspase-3 activity in colorimetric assay, it needed to incubate these cells with staurosporine and etoposide for 8 and 24 h, respectively. The staurosporine- and etoposide-induced caspase-3 activity were



lower in these stable cell lines than in the HEK293 cells, showing that the stable expression of sbGHS-R1a and sbGHS-R1b has an anti-apoptotic effect. However, this anti-apoptotic effect did not show in transient transfection systems. It is not expected as in the preliminary study, transiently transfected HA-sbGHS-R1b having pro-apoptotic effect. One of the explanations is the difference between the HA-tagged and non-tagged sbGHS-R. Therefore, to match the preliminary study, i use the HA-sbGHS-R1b and incubate the cells with staurosporine in the absence of serum.

In summary, this study has studied the cell signaling characteristics of GHS-R1a and has assessed the control experiments needed for correct interpretation of experiments where cells are co-transfected with different receptors. In addition, it provided the optimized condition criteria for the colorimetric assay to monitor caspase-3 activity and to show that sbGHS-Rs may be involved in apoptosis regulation.

## 摘要

促生長激素分泌受體 (GHS-R) 是一種 G-蛋白聯結受體 (GPCR)。GHS-R 有兩種，其中一種有七處地方通過細胞表面，叫做 GHS-R1a，另一種有五處方通過細胞表面，叫做 GHS-R1b，它是不會傳遞信息的。細胞自毀是一種程式化的細胞死亡。初步結果提議在人類胚胎的腎 293 細胞裏 (HEK293) 穩定表出黑編 GHS-R1a (sbGHS-R1a) 和短暫轉染 HA-sbGHS-R1b 分別會引起抗細胞自毀和支持細胞自毀。這個研究目的是更進一步研究人類的 GHS-R 在調節細胞自毀和找出人類的 GHS-R 之間的關係。爲了反映細胞自毀的情況，caspase-3 (細胞自毀的行刑 caspase) 的活動力能會用色度計量度。

GHS-R1a 是聯結  $G_q$  蛋白的受體，所以觀察 GHS-R1a 的性質是量肌醇磷酸 (IP) 的生產。基本放射性的 IP ( $[^3\text{H}]\text{-IP}$ ) 的生產濃度會隨著 GHS-R1a 表出的濃度而增加，基本的  $[^3\text{H}]\text{-IP}$  生產亦會被反向催動素 [D-Arg<sup>1</sup>, D-Phe<sup>5</sup>, D-Trp<sup>7</sup>, Leu<sup>11</sup>]-substance P (SPa) 而減低，這是顯示 GHS-R1a 是一個有權採取主動的受體。GHS-R1a 的催動素，ghrelin 和 GHRP-6 被發現會刺激  $[^3\text{H}]\text{-IP}$  的生產。與 GHS-R1a 相反，GHS-R1b 是不會對催動素有反應。

在 HEK293 細胞短暫轉染人類的 GHS-R1a，証實腺嘌呤 (adenosine) 是不完全的催動素和會添加由 ghrelin 所刺激生活的  $[^3\text{H}]\text{-IP}$ 。爲了確定某部份 ghrelin 和 adenosine 刺激的  $[^3\text{H}]\text{-IP}$  生活是由於內生的 adenosine，腺嘌呤去胺的酵素 (adenosine deaminase, ADA) 的效應會研究。研究結果反映所有由測試的受體所刺激生活的  $[^3\text{H}]\text{-IP}$  都減少。因此，adenosine 的阻擋之物，theophylline 會被用作調察 ADA 的明確性。但是，theophylline 沒有阻擋任何催動素刺激的  $[^3\text{H}]\text{-IP}$



生產。這些數據不能幫助找出結論。

爲了調查人類 GHS-R 近似的分類，它們在細胞自毀的功能關係，其中一個方法是在細胞同一時間轉染人類的 GHS-R1a 和 GHS-R1b。但是，在轉染時附加的質體會刺激由 GHS-R1a 所生產的基本和催素劑刺激的 [ $^3$ H]-IP。這個現象在人類的 TP $_{\alpha}$ 和不同的轉染劑都會出現。其中一個解釋是附加的質體增加轉染的效率。因爲這個增加效果會使到解釋數據困難，但是又不能成功地製做一種穩定轉染人類 GHS-R 的 HEK293，再加上 sbGHS-R 與人類的 GHS-R 的性質相似，因此，穩定地轉染了 sbGHS-R1a (HEK-sbGHS-R1a) 或 sbGHS-R1b (HEK-sbGHS-R1b) 的 HEK293 會用作研究 GHS-R 在細胞自毀的角色。

在 HEK293, HEK-sbGHS-R1a 和 HEK-sbGHS-R1b，想有較好的 staurosporine 和 etoposide 所引起的 caspase-3 活動，在色度計的進行中，細胞分別需要醞釀在 staurosporine 和 etoposide，八小時和二十四小時。在 HEK-sbGHS-R1a 和 HEK-sbGHS-R1b, staurosporine 和 etoposide 所引起的 caspase-3 活動是少於在 HEK293 中。這顯示了穩定轉染 sbGHS-R1a 和 sb-GHS-R1b 有反向細胞自毀的效用。但是，這個效用在短暫穩定轉染的體制中不能看見。這個現象不符合初期的結果 --- 在 HEK293 短暫轉染 HA-sbGHS-R1b 會有反向細胞自毀的效用。其中一個解釋是沒有 HA 的 GHS-R 與有 HA 的 GHS-R 不同。因此，要與初步研究的結果符合，這就需要用 HA-sbGHS-R1b，和醞釀細胞在沒有血清的 staurosporine 中。

總括而言，這研究測試了 GHS-R1a 傳遞信息的特式和確定了在有附加的質體的轉染中是需要有額外的標準實驗才可有準確的判斷。另外，這個研究亦測試出

色度計中，應該要有的條件和顯示了 sbGHS-R 可能有參與細胞自毀。



## **Acknowledgement**

I would like to express my appreciation to Prof. Helen Wise, my supervisor who has so much patients and gives so much guidance throughout the study program and particularly during the preparation of the thesis. Special thanks go to Prof. Christopher H.K. Cheng from the Department of Biochemistry for his guidance and Prof. Ronald R. Fiscus from the Department of Physiology for his generosity in sharing the colorimetric assay technique.

My thanks also go to the members of the Department of Pharmacology, especially to Mr. Kevin B. S. Chow, and Ms. Penelope M. Y. Or, who facilitated my experiments based on their technical knowledge. In addition, I would like to give sincere thanks to Dr. Chi-Bun Chan, who gives technical support and valuable discussion to me.

I would also like to thank my friends, especially Chris Leung, Christina Wan, Janice Wong, Jessica Cheung, and Ray Wong, for their support and understanding.

Finally, I would like to express my deepest thanks to my family for their support and encouragement.

---

## Abbreviations

[ <sup>3</sup> H]-IP	[ <sup>3</sup> H]-inositol phosphates
TM	transmembrane
A1	adenosine 1 receptor
A3	adenosine 3 receptor
AC	adenylate cyclase
Ac-DEVD- <i>p</i> NA	Caspase-3 Substrate I
Ad	Adenosine
ADA	adenosine deaminase
Apaf-1	apoptotic protease-activating factor-1
AT2	angiotensin receptor type 2
ATP	Adenosine 5'-triphosphate
bps	base pairs
BRET <sup>2</sup>	Bioluminescence resonance energy transfer
CaCl <sub>2</sub>	Calcium chloride
CALU-1	lung carcinoma cells
cAMP	cyclic 3', 5'-adenosine monophosphate
Carb	Carbachol
CB1	cannabinoid 1 receptor
CFP	cyan fluorescent protein
CREB	cAMP responsive element binding protein
Ct	threshold cycle

CTX	cholera toxin
CXCR4	chemokine receptor
cyt c	cytochrome c
DAG	Diacylglycerol
DAPI	4',6-diamidino-2phenylidole
dsDNA	double-strand DNA
EB/AO	ethidium bromide and acridine orange
ERK1/2	extracellular regulated kinases 1/2
ET-1	endothelin receptor
EtBr	ethidium bromide
FBS	Fetal Bovine Serum
FRET	fluorescence resonance energy transfer
G	Ghrelin
GFP <sup>2</sup>	green fluorescent protein
GH	growth hormone
GHD	growth hormone deficiency
GHRP-6	Growth hormone releasing peptide-6
GHS-R	Growth hormone secretagogue receptor
GHSs	growth hormone secretagogues
GPCR	G protein-coupled receptor
HA-hTP <sub>α</sub>	Hemagglutinin influenza virus epitope-tagged Human thromboxane A <sub>2</sub>
HEK293	Human Embryonic Kidney 293 cells

---

HEK-hGHS-R1a	HEK293 cells stably expressing hGHS-R1a
HEK-hGHS-R1b	HEK293 cells stably expressing hGHS-R1b
HEK-sbGHS-R1a	HEK293 cells stably expressing seabream GHS-R1a
HEK-sbGHS-R1b	HEK293 cells stably expressing seabream GHS-R1b
hGHS-R	human GHS-R
hGHSR1a	Human growth hormone secretagogue receptor 1a
hGHSR1b	Human growth hormone secretagogue receptor 1b
INOS	Inositol
IP <sub>3</sub>	Inositol 1,4,5-trisphosphate
LiCl	Lithium chloride
MAPK	mitogen-activated protein kinases
mDP	Mouse prostaglandin D <sub>2</sub> receptor
MEK	mitogen-activated protein kinase
MOR	μ-opioid receptor
mRNA	messenger RNA
P2X7	P2X7 purinergic receptor
P <sub>2</sub> Y	purinergic P <sub>2</sub> Y receptors
P2Y2	P2Y <sub>2</sub> purinoceptor
pCFP-DEVD-YFP	FRET caspase-3 biosensor
PCR	polymerase chain reaction
pEGFP	enhanced green fluorescence protein plasmid
PGD <sub>2</sub>	Prostaglandin D <sub>2</sub>
pGFP <sup>2</sup> -DEVD-Rluc(h)	BRET Caspase-3 biosensor



---

pGFP <sup>2</sup> -Rluc(h)	positive control vector
PI3K	phosphoinositide 3-kinases
PKA	cAMP-dependent protein kinase
PKBKs	protein kinase B kinases
PKC	protein kinase C
PLC	phospholipase C
PMA	phorbol 12-myristate 13-aceate
pNA	p-nitroaniline
PtdIns-3,4,5-P <sub>3</sub>	phosphatidylinositol-3,4,5-trisphosphate
PtdIns-3,4-P <sub>2</sub>	phosphatidylinositol-3,4-bisphosphate
PtdIns-4,5-P <sub>2</sub>	phosphatidylinositol-4,5-bisphosphate
PTH/PTHrP	parathyroid hormone/ parathyroid hormone-related protein
PTHR	parathyroid hormone receptor
Rluc(h)	humanized <i>Renilla</i> luciferase
RT-PCR	reverse-transcriptase polymerase chain reaction
sbGHS-R1a	seabream GHS-R1a
SPa	[D-Arg <sup>1</sup> , D-Phe <sup>5</sup> , D-Trp <sup>7,9</sup> , D-Leu <sup>11</sup> ]-substance P
SSTR2	somatostatin receptor
Theo	theophylline
TUNEL	terminal deoxynucleotide transferase-mediated dUTP-biotin nick-end labeling
YFP	yellow fluorescent protein

## **Publications Based on Work in this thesis**

### **Abstract**

Sylvia P.N. Lau, Chris P.K. Leung, C.B. Chan, Christopher H.K. Cheng and Helen Wise (2004) Effect of co-transfected plasmid DNA on GPCR signaling in HEK293 cell. *The 8<sup>th</sup> Scientific Meeting of the Hong Kong Pharmacology Society.*





---

<b>Chapter 2</b>	<b>Materials and solutions .....</b>	<b>31</b>
2.1	Materials .....	31
2.2	Culture medium, buffer and solutions .....	37
2.2.1	Culture medium .....	37
2.2.2	Buffers.....	37
2.2.3	Solutions .....	38
<b>Chapter 3</b>	<b>Methods .....</b>	<b>41</b>
3.1	Maintenance of cell lines .....	41
3.1.1	Human Embryonic kidney (HEK293) cells.....	41
3.1.2	HEK293 cells stably expressing black seabream growth hormone secretagogues receptors (HEK-sbGHS-R1a and HEK-sbGHS-R1b).....	41
3.2	Preparation of plasmid DNA .....	42
3.2.1	Preparation of competent <i>E. coli</i> .....	42
3.2.2	Transformation of DNA into competent cells.....	42
3.2.3	Small-scale and large-scale plasmid DNA preparation .....	43
3.2.4	Confirmation of the purity and the identity of the plasmid DNA.....	43
3.3	Transient transfection of mammalian cells.....	45
3.4	Development of stable cell lines.....	46
3.4.1	Determination of the optimum concentration of each antibiotic used in selection of clones .....	46
3.4.2	Development of monoclonal stable cell line .....	46
3.4.3	Confirmation the expression of 2myc-hGHS-R1a and 2myc-hGHS-R1b .....	48
3.5	Measurement of phospholipase C activity.....	49
3.5.1	Introduction.....	49
3.5.2	Preparation of columns .....	49
3.5.3	[ <sup>3</sup> H]-inositol phosphate assay .....	49
3.5.4	Measurement of [ <sup>3</sup> H]-inositol phosphates production.....	50
3.5.5	Data analysis.....	50
3.6	Determination of transient transfection efficiency .....	51



---

3.7	Reverse-transcription polymerase chain reaction (RT-PCR).....	52
3.7.1	RNA extraction and first strand cDNA production.....	52
3.7.2	PCR and visualization of amplicons.....	52
3.7.3	Real-time PCR.....	59
3.7.3.1	Construction of standard curve.....	60
3.7.3.2	Data analysis.....	60
3.8	Measurement of caspase-3 activity.....	65
3.8.1	Determination of caspase-3 activity using colorimetric assay ... .....	65
3.8.1.1	Introduction.....	65
3.8.1.2	Induction of apoptosis.....	65
3.8.1.3	Preparation of cell lysates.....	65
3.8.1.4	Quantification of caspase-3 activity by measuring pNA absorbance.....	66
3.8.1.5	Data analysis.....	67
3.8.2	Determination of caspase-3 activity using bioluminescence resonance energy transfer (BRET <sup>2</sup> ) assay .....	67
3.8.2.1	Introduction.....	67
3.8.2.2	Quantification of caspase-3 activity using BRET <sup>2</sup> assay.....	68
3.8.2.3	Data analysis.....	69
3.8.3	Determination of caspase-3 activity using fluorescence resonance energy transfer (FRET) assay .....	70
3.8.3.1	Introduction.....	70
3.8.3.2	Quantification of caspase-3 activity using FRET assay.....	70
3.8.3.3	Data analysis.....	71
<b>Chapter 4</b>	<b>Results.....</b>	<b>72</b>
4.1	Characterization of GHS-R.....	72
4.1.1	Properties of GHS-R1a .....	72
4.1.1.1	Constitutively active receptor .....	72
4.1.1.2	Characterization of epitope-tagged hGHS-R1a .....	73

---

---

4.1.2	Properties of GHS-R1b.....	75
4.1.3	Conclusions.....	75
4.2	Effect of co-transfection of HEK293 cells.....	85
4.2.1	Effect of balancing DNA concentrations transfected into HEK293 cells.....	85
4.2.2	Effect of balancing DNA concentration using another G <sub>q</sub> -coupled receptor .....	87
4.2.3	Effect of G <sub>i</sub> - and G <sub>s</sub> -coupled receptor on GHS-R1a signaling ... ..	88
4.2.4	Potentiating effect of co-transfection appeared using different transfection reagents .....	88
4.2.5	Co-transfection improves transfection efficiency.....	89
4.2.6	Discussions .....	91
4.3	Development of cell lines stably expressing hGHS-R1a or hGHS-R1b .....	102
4.3.1	Advantages of using a monoclonal cell line .....	102
4.3.2	Sensitivity of HEK293 cells to antibiotics.....	102
4.3.3	Production of polyclonal stable cell line .....	103
4.3.4	Monoclonal stable cell line selection.....	104
4.3.5	Discussions .....	105
4.4	Effect of adenosine on GHS-R1a signaling .....	111
4.4.1	Adenosine acts as partial agonist.....	111
4.4.2	Effect of substance P analog on adenosine-mediated GHS-R1a signaling.....	112
4.4.3	Effect of adenosine deaminase (ADA) on adenosine- and ghrelin-stimulated GHS-R1a signaling.....	113
4.4.4	Specificity of ADA .....	115
4.4.5	Conclusions.....	116
4.5	Role of GHS-R in apoptosis .....	124
4.5.1	Different methods to measure caspase-3 activity .....	124
4.5.1.1	Colorimetric assay .....	124
4.5.1.1.1	Time course for staurosporine and	

---



	etoposide in HEK293 cells .....	125
4.5.1.1.2	Effect of 2myc-hGHS-R1a on staurosporine- and etoposide-induced caspase-3 activity.....	127
4.5.1.1.3	Time course for staurosporine and etoposide in sbGHS-R monoclonal stable cell line.....	128
4.5.1.1.4	Effect of sbGHS-Rs on staurosporine- and etoposide- induced caspase-3 activity in HEK 293 cells.....	129
4.5.1.1.5	Effect of sbGHS-Rs on staurosporine-induced caspase-3 activity in sbGHS-R monoclonal stable cell line .....	130
4.5.1.1.6	Differences between epitope-tagged and non-tagged sbGHS-Rs in staurosporine-induced caspase-3 activity .....	131
4.5.1.1.7	The role of epitope-tagged sbGHS-R1b in staurosporine-induced caspase-3 activity ..	132
4.5.1.1.8	Effect of staurosporine and etoposide on GHS-R1a signaling.....	133
4.5.1.2	BRET <sup>2</sup> assay .....	135
4.5.1.3	FRET assay .....	136
4.5.1.4	Conclusions.....	136
4.6	Determination of GHS-R amount in terms of mRNA .....	155
4.6.1	Determination of GHS-R amount in stable cell lines .....	155
4.6.2	Transfected DNA amount match with stable cell lines.....	155
<b>Chapter 5</b>	<b>Discussion, Conclusions and Future Plan.....</b>	<b>159</b>
5.1	General Discussion and Conclusions .....	159
5.2	Future Plan and Experimental Design.....	168
<b>References.....</b>		<b>171</b>

# Chapter 1

## Introduction and project overview

The growth hormone secretagogue receptor (GHS-R) belongs to the G protein-coupled receptor (GPCR) superfamily (Howard *et al.*, 1996). Many GPCRs have been shown to be involved in regulating apoptosis. In addition, many synthetic compounds and endogenous ligands, which act on GHS-R, were found to regulate apoptosis.

Preliminary study showed that the staurosporine-induced caspase-3 activity in HEK293 cells was higher than the HEK293 cells stably expressing the seabream GHS-R1a (sbGHS-R1a) receptor, it suggested that sbGHS-R1a might be anti-apoptotic. When HEK293 cells were transfected with epitope-tagged sbGHS-R1b, the staurosporine-induced caspase-3 activity was higher than that in HEK293 cells, it suggested that epitope-tagged sbGHS-R1b might be apoptotic. In addition, the apoptotic effect of epitope-tagged sbGHS-R1b was reduced by stably expressing sbGHS-R1a in HEK293 cells.

In this project, the role of human GHS-R (hGHS-R) subtypes, namely hGHS-R1a and hGHS-R1b and their functional relationship in regulating apoptosis were studied. In order to investigate the interaction between GHS-R1a and GHS-R1b, it is necessary to co-transfect GHS-R1a and GHS-R1b into HEK293 cells. Therefore, it is



important to look for possible artifactual results caused by the co-transfection of two different plasmids. It was found that co-transfection resulted in a variable potentiating effect in both basal and agonist-stimulated [ $^3\text{H}$ ]-inositol phosphate ([ $^3\text{H}$ ]-IP) production. This potentiating effect makes data interpretation more complicated, so we tried to develop HEK293 cells stably expressing hGHS-R1a (HEK-hGHS-R1a) or hGHS-R1b (HEK-hGHS-R1b). Using the stable cell line to study the receptor subtypes interaction, there is only one of the receptor subtype plasmid DNA to be transfected into the cells and then the potentiating effect of co-transfection is avoided. However, the development of stable cell lines was unsuccessful, therefore HEK293 cells stably expressing seabream GHS-R1a (HEK-sbGHS-R1a) or GHS-R1b (HEK-sbGHS-R1b) were used to study the role of GHS-R in apoptosis regulation.

Before studying the role of GHS-R in apoptosis regulation by monitoring the caspase-3 activity, we need to find out which is the best assay to monitor caspase-3 activity in HEK293 cells and optimize the assay conditions by determining which agonists and apoptotic inducers to use. In addition, we also need to have same expression level of sbGHS-R in both transiently transfected cells and the stable cell lines, so the amount of sbGHS-R in the stable cell lines and in the transient transfection were determined by real-time polymerase chain reaction (PCR). Finally, the apoptotic inducer stimulated caspase-3 activities in HEK-sbGHS-R1a and HEK-sbGHS-R1b was measured, it will reflect the role of sbGHS-R1a and sbGHS-R1b in apoptosis regulation. Also these cells were transfected with sbGHS-R1a or sbGHS-R1b and then the caspase-3 activities were monitored, it will

indicate the functional relationship of sbGHS-R1a and sbGHS-R1b. HEK293 cells and the cells transfected with sbGHS-R1a and sbGHS-R1b were used as a control.

## 1.1 Ghrelin structure and its synthesis

Ghrelin is a 28 amino acid peptide and is the endogenous ligand for GHS-R. Under the influence of an unknown acyl-transferase, ghrelin has a unique n-octanoyl modification on the hydroxyl group of the serine 3 residue (Fig. 1.1) (Kojima *et al.*, 1999; Kojima *et al.*, 2001; Smith, 2005). This modification appears to be essential for most of its biological activities, such as endocrine activities (Bresson-Bepoldin *et al.*, 1994), and activation of GHS-R1a (Kojima *et al.*, 1999) as the unmodified ghrelin does not possess these functions. In the human hypothalamus and pituitary gland, the binding of [<sup>125</sup>I]-ghrelin was displaced by ghrelin (Asakawa *et al.*, 2001). It only showed that ghrelin may bind to GHS-R1a or other non-GHS-R. In COS-7 cells transfected with hGHS-R1a, ghrelin stimulated [<sup>3</sup>H]-IP production and competed against [<sup>125</sup>I]-ghrelin binding (Holst *et al.*, 2003), it showed ghrelin is an agonist of GHS-R1a. Although the octanoylated form has more functions than the non-octanoylated form, in human, the major circulating form of ghrelin is the non-octanoylated form (Broglia *et al.*, 2003). Not only the non-octanoylated ghrelin is the major form in human, but also in other animals, such as rat (Hosoda *et al.*, 2000).

Ghrelin is produced and secreted from the stomach, and may circulate in the blood stream in order to reach the pituitary where ghrelin stimulates growth hormone release (Kojima *et al.*, 1999; Kojima *et al.*, 2001). Ghrelin is not only found in the

stomach, but also in most other organs in a relatively small amount, such as intestine, pancreas, adrenal, pituitary, lung (Gnanapavan *et al.*, 2002; Kojima *et al.*, 2001) and in different human neoplastic tissues and related cancer cell lines, such as pancreatic endocrine tumor (Volante *et al.*, 2002) and thyroid tumor (Volante *et al.*, 2003)

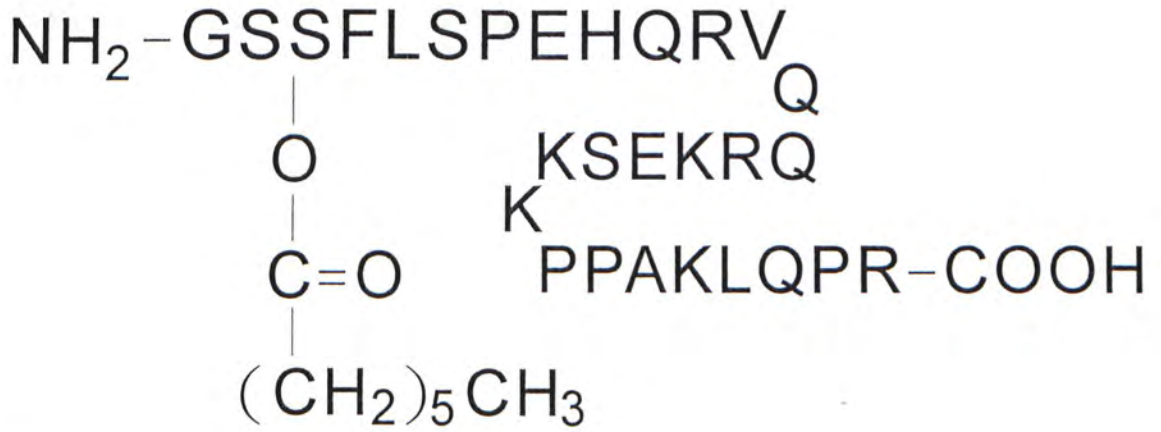


Figure 1.1 Chemical structure of ghrelin. The octanoyl group is attached to serine-3.



## 1.2 Types of growth hormone secretagogues (GHSs)

In the eighties, a small synthetic hexapeptide, named GHRP-6, was developed and based on its structure, many other GHSs with better oral bioavailability and potency were developed (Smith, 2005). GHSs can be divided into two groups, synthetic peptide and synthetic non-peptide. GHRP-6 and hexarelin belong to the peptide group. For the non-peptide group, it can be further sub-divided into benzolactams and spiroindanylpiperidines. Benzolactams includes L-692,429 and L692,585, spiroindanylpiperidine includes MK-0677. In general, the potency and the oral availability are in the following order: synthetic peptide < benzolactams < spiroindanylpiperidine. These GHSs are highly selective, even at a concentration above 10  $\mu\text{M}$  (Smith, 2005). Besides ghrelin, GHSs can also bind to and activate GHS-R1a. COS-7 cells transfected with hGHS-R1a showed GHS (L-692,429)-stimulated [ $^3\text{H}$ ]-IP production, but L-692,429 did not displace [ $^{125}\text{I}$ ]-ghrelin (Holst *et al.*, 2003). Some of the GHSs, such as MK-0677 were able to displace [ $^{125}\text{I}$ ]-ghrelin in human hypothalamic membranes (Muccioli *et al.*, 2001). Labeling the porcine GHS-R1a with radioactive GHS ([ $^{35}\text{S}$ ]-MK-0677), a series of GHSs (GHRP-6, L-692,429, MK-0677) displaced the [ $^{35}\text{S}$ ]-MK-0677 (Pomes *et al.*, 1996). These indicated that most of the GHSs can bind to and activate GHS-R1a, but in the case of L-692,429 another non-GHS-R1a receptor appears to be involved.

## **1.3 Characterization of GHS-R**

### **1.3.1 Cloning of GHS-R1a and GHS-R1b**

#### **1.3.1.1 GHS-R subtypes**

There are two forms of GHS-R produced by an alternative splicing from a single gene (Fig. 1.2). The gene is composed of two exons, named exon 1 and exon 2, and there is an intron between the exons. TM I to TM V and TM VI to TM VII are encoded by exon 1 and exon 2 respectively. One form of GHS-R contains seven transmembrane domains and is encoded by two exons, and is named GHS-R1a. The other form of GHS-R contains five transmembrane domains and is encoded by one exon together with a part of the intron containing a stop codon, and is named GHS-R1b. In human and seabream, the amino acid sequence of GHS-R1b diverges from GHS-R1a starting at Leu which locates within TM VI (Kojima *et al.*, 1999; Smith, 2005).

#### **1.3.1.2 Properties of GHS-R subtypes**

GHS-R1a is a  $G_q$ -coupled receptor which responds to agonists and causes IP production, as described in sections 1.1 and 1.2. GHS-R1a also stimulates IP production in the absence of agonists that means GHS-R1a is a constitutively active receptor. COS-7 cells were transiently transfected with different concentrations of hGHS-R1a, the [ $^3$ H]-IP production was measured in the presence and absence of ghrelin. There was a gene dose-dependent increase in the [ $^3$ H]-IP production, both in the presence and absence of ghrelin (Holst *et al.*, 2004). The constitutive activity was not only observed in hGHS-R1a, but also demonstrated in sbGHS-R1a, as in the



HEK293 cells stably expressing sbGHS-R1a, there was a relatively high level of basal [<sup>3</sup>H]-IP production when compared with HEK293 cells (Chan *et al.*, 2004b). The use of the inverse agonist is also a good tool to show that GHS-R1a is a constitutively active receptor. Inverse agonist means an agonist which reduces the constitutive activity of a receptor and has a negative efficacy (Rang, 2003). [D-Arg<sup>1</sup>,D-Phe<sup>5</sup>,D-Trp<sup>7,9</sup>,Leu<sup>11</sup>]-substance P (SPa) was found to function as a high efficacy and high potency inverse agonist of GHS-R1a. One of the evidence is SPa inhibited the spontaneous, ligand-independent [<sup>3</sup>H]-IP production in hGHS-R1a expressed in COS-7 cells (Holst *et al.*, 2003). SPa is not a specific inverse agonist for GHS-R1a, it also acts on the tachykinin NK1 (Palma *et al.*, 2000) and bombesin receptors (Djanani *et al.*, 2003).

In contrast to GHS-R1a, GHS-R1b is unresponsive to ghrelin or GHS (Ghigo *et al.*, 2005; van der Lely *et al.*, 2004). In COS-7 cells transfected with hGHS-R1b, high-affinity saturable binding of [<sup>35</sup>S]-MK-0677 was not evident. It indicated that GHS-R1b does not respond to GHS (Smith *et al.*, 1997). Also, there was no induction of a Ca<sup>2+</sup>-activated Cl<sup>-</sup> current in response to MK-0677 in oocytes injected with GHS-R1b cRNA (Howard *et al.*, 1996). Although GHS-R1b is unresponsive, it can attenuate the signal transduction capacity of GHS-R1a. It was found that there was a decrease in the GHS (GHRP-6, L163,540 or L692,585) induced intracellular calcium release in HEK293 cells stably expressing sbGHS-R1a, when these cells were transfected with sbGHS-R1b (Chan *et al.*, 2004a).



### 1.3.1.3 Evidence of non-GHS-R1a stimulated by ghrelin and GHSs

If administration of ghrelin or GHSs causes an alteration in cellular response, it does not necessarily imply the presence of GHS-R1a. There are many evidences indicating that ghrelin and GHSs can act on a receptor which is different from GHS-R1a. [<sup>125</sup>I]-Tyr-Ala-hexarelin binding to human breast tumor membranes was displaced by different unlabeled GHSs (hexarelin and MK-0677) and human ghrelin, as well as by non-octanoyl ghrelin, indicating that there is other receptors which are different from GHS-R1a present in human breast tumor, as the non-octanoyl ghrelin does not act on GHS-R1a as mention in section 1.1 (Cassoni *et al.*, 2001). In addition, in three different human breast carcinoma cell lines (MCF7, T47D, and MDA-MB231), GHSs, ghrelin and even non-octanoyl ghrelin caused a significant inhibition of cell proliferation, however, there was no GHS-R1a mRNA demonstrated by RT-PCR (Cassoni *et al.*, 2001). Other than breast tumor, lung carcinoma cells (CALU-1) and human prostate tumors showed the existence of non-GHS-R1a. In CALU-1 cells, GHS-R1a is absent, but CALU-1 cells respond to peptidyl GHS resulting in inhibition of cell proliferation (Ghe *et al.*, 2002). In human prostate tumors and some prostate cancer cell lines, [<sup>125</sup>I]-Tyr<sup>4</sup>-ghrelin binding was detected in the cell membranes and the binding was displaced by ghrelin, synthetic GHS and des-octanoyl ghrelin (Cassoni *et al.*, 2004).

Non-GHS-R1a was not only present in tumor cells, but also in normal tissues, such as cardiovascular tissues, pancreas and thyroid, as the binding of [<sup>125</sup>I]-Tyr-Ala-hexarelin was displaced by unlabeled non-octanoyl ghrelin (Ghigo *et al.*, 2005).

#### 1.3.1.4 Distribution of GHS-R

Distribution of GHS-R can be studied using different methods, such as radioactive binding assay, northern blotting, immunohistochemistry and RT-PCR. Different methods have different specificity and sensitivity, therefore results can be variable. GHS-R1a is highly expressed in the hypothalamus and pituitary gland (Ghigo *et al.*, 2005). GHS-R1a was also reported in other areas with relatively lower expression level (Gnanapavan *et al.*, 2002) by real-time RT-PCR.

In human, using real-time RT-PCR, GHS-R1a mRNA was found in hypothalamus, pituitary gland, thyroid gland, pancreas, spleen, myocardium and adrenal gland. In contrast to hGHS-R1a, hGHS-R1b was not only found in these tissue, but also in atrium, bladder, breast, buccal, mucosa, colon, duodenum, fallopian tubes, fat, fundus, gall bladder, ileum, jejunum, kidney, liver, lung, lymph node, lymphocytes, muscle, esophagus, ovary, placenta, skin, testis or vein (Gnanapavan *et al.*, 2002). In all the prostate cancer cell lines studied, GHS-R1a and GHS-R1b are co-expressed (van der Lely *et al.*, 2004). Using RT-PCR, hGHS-R has been observed in liver, T cells, B cells and neutrophils (Hattori *et al.*, 2001; Murata *et al.*, 2002), but it did not distinguish the presence of hGHS-R1a or hGHS-R1b or both. Using [<sup>125</sup>I]-Try-Ala-hexarelin, there was widespread binding in adrenal gland, gonads, arteries, lung, liver, skeletal muscle, kidney, thyroid, adipose tissue, veins, uterus, skin and lymph node, but not in the stomach and colon (Papotti *et al.*, 2000). Using [<sup>125</sup>I]-His<sup>9</sup>-ghrelin binding assay, binding was found in the aorta, coronary, pulmonary, arcuate arteries in the kidney and saphenous veins (Katugampola *et al.*,



2001). The presence of binding do not necessarily suggest the presence of hGHS-R1a, since hexarelin and ghrelin can bind to non-GHS-R1a receptor, as described in section 1.3.1.3.

In seabream, using radioactive PCR, sbGHS-R1a was predominantly found in pituitary, followed by hypothalamus, telencephalon and spinal cord (Chan *et al.*, 2004a). sbGHS-R1a was also found in peripheral tissues, such as heart, liver, spleen, gill, kidney, stomach, intestine, gall bladder, muscle, testis and ovary. The distribution of sbGHS-R1b was similar to sbGHS-R1a, but sbGHS-R1b had the highest expression level in telencephalon, followed by hypothalamus, pituitary, optic-tectum and thalamus and spinal cord. All the periphery tissues had a very low expression level of sbGHS-R1a and sbGHS-R1b.

### **1.3.2 Signal transduction pathways of GHS-R**

Ghrelin or GHSs activates GHS-R1a, and then the ligand-activated GHS-R1a interacts with  $G_q$  protein and leads to activation of phospholipase C (PLC) / protein kinase C (PKC) signaling pathway, results in an increase in IP production and intracellular calcium level. This has been shown in transfection systems, for example, COS-7 cells transiently transfected with hGHS-R1a and incubated with ghrelin and GHS (L-692,429), produced an increase in IP production (Holst *et al.*, 2003). CHO cells, which stably expressed hGHS-R1a, caused intracellular calcium increase in response to ghrelin (Kojima *et al.*, 1999). HEK293 cells stably expressed sbGHS-R1a caused an increase in intracellular calcium level by GHRP-6. PLC inhibitor, U73122, and PKC activator, phorbol 12-myristate 13-aceate (PMA),



inhibited GHRP-6 stimulated intracellular calcium (Chan *et al.*, 2004b).

Ghrelin and GHSs not only activates PLC/PKC signaling pathway, but also cyclic 3', 5'-adenosine monophosphate (cAMP) / cAMP-dependent protein kinase (PKA) pathway. Which pathway will be stimulated depends on the species and cells types? In rat pituitary somatotrophs, the GHRP-6 stimulated intracellular calcium increase was inhibited by depleting PKC using PMA (Bresson-Bepoldin *et al.*, 1994). It indicated that in rat somatotrophs, intracellular calcium increase was a PKC-dependent response. In pig pituitary cells, ghrelin-stimulated growth hormone (GH) release was reduced by the blockade of PLC, PKC, as well as adenylate cyclase (AC) or PKA (Malagon *et al.*, 2003). It indicated that ghrelin-stimulated GH release requires PLC/PKC and cAMP/PKA pathways. In porcine pituitary cells, the ghrelin-stimulated intracellular calcium increase also involved PLC and AC pathways (Glavaski-Joksimovic *et al.*, 2003). In ovine somatotrophs, there is a crosstalk between PKC and cAMP/PKA pathway in the action of GHRP-2 (Wu *et al.*, 1997). In these experiments, one can not concluded that the activation of PLC/PKA and cAMP/PKA pathways by ghrelin or GHSs, is through the direct activation of GHS-R1a or other non-GHS-R1a.

### **1.3.3 Comparison between human and seabream GHS-R**

sbGHS-R is very similar to hGHS-R, in terms of the subtype structures and their signaling properties. As the same as hGHS-R, sbGHS-R has two subtypes, namely, sbGHS-R1a and sbGHS-R1b, results from the alternative splicing of the single gene (Chan *et al.*, 2004a). sbGHS-R1a with seven transmembrane domains, while

sbGHS-R1b is a truncated receptor, only has five transmembrane domains. Like hGHS-R1a, sbGHS-R1a is a constitutively active receptor and responds to GHSs such as GHRP-6 and L163,540, leading to elevation of [<sup>3</sup>H]-IP production and intracellular calcium level (Chan *et al.*, 2004b). It also showed that the GHS induced an increase in the intracellular calcium level was PLC- and PKC-dependent. However, the potency of these GHSs was less than that showed in human GHS-R1a studies (Palyha *et al.*, 2000). Besides GHSs can activate sbGHS-R1a, ghrelin was also demonstrated to be an agonist of sbGHS-R1a. Unlike hGHS-R1a, ghrelin is a weak ligand of sbGHS-R1a, it needed 10  $\mu$ M ghrelin to give a measurable signal (Chan *et al.*, 2004b).

## Genomic DNA (3q26.2)

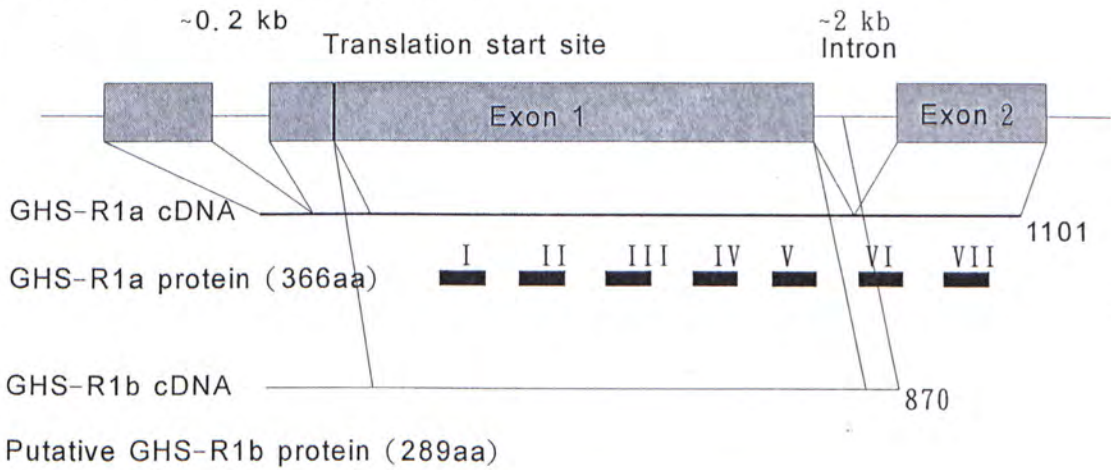


Figure 1.2 Component of GHS-R gene and the alternative splicing of GHS-R subtypes. Gray boxes represent exons. Black boxes represent the seven transmembrane domains marked with roman numbers. Figure adapted from Korbonits *et al.* (2004).



## 1.4 Is adenosine a partial agonist at GHS-R1a?

Adenosine induces intracellular calcium release by acting directly onto GHS-R1a, as the GHS-R1a inverse agonist ([D-Arg<sup>1</sup>, D-Phe<sup>5</sup>, D-Trp<sup>7,9</sup>, D-Leu<sup>11</sup>]-substance P) inhibited the adenosine-mediated calcium release in HEK293 or BHK cells stably expressing hGHS-R1a (Carreira *et al.*, 2004; Tullin *et al.*, 2000). In BHK/hGHS-R1a cells, the 100 nM adenosine-induced calcium response was measured by Fura-2, and was not blocked by 200  $\mu$ M theophylline, which is an adenosine receptor blocker (Tullin *et al.*, 2000). In contrast to BHK/hGHS-R1a cells, in HEK293 cells stably expressing pig GHS-R1a with bioluminescence reporter gene, aequorin, the 2  $\mu$ M adenosine-stimulated calcium response was blocked by 10  $\mu$ M theophylline, as shown by the decrease in the bioluminescence signal (Smith *et al.*, 2000; Ungrin *et al.*, 1999). The contradictory results from theophylline may be due to the different concentrations of adenosine and theophylline, different sensitivity in the two assays for calcium measurement and different GHS-R1a species.

It has been suggested that adenosine binds to GHS-R1a and then GHS-R1a couples to G<sub>s</sub> protein, it was supported by the inhibition effect of cholera toxin (CTX), an activator of G<sub>s</sub>, on the adenosine-stimulated calcium response (Carreira *et al.*, 2004). Also it was showed the adenosine-stimulated calcium response passes through the typical G<sub>s</sub> pathway involving the activation of AC and PKA, results in the production of cAMP. In HEK-hGHS-R1a cells, the calcium signal elicited by adenosine was blocked by an AC inhibitor, MDL-12,330A, and a PKA inhibitor, H-89. Also, there was cAMP level elevated in response to adenosine (Carreira *et al.*, 2004). These

indicated adenosine-induced calcium response through  $G_s$  pathway. The signaling pathway of adenosine is different from the one activated by ghrelin and GHS. It suggested that depending on the agonist that activates GHS-R1a, different intracellular signaling pathways were activated.

Partial agonist means a drug with a lower efficacy than full agonist and it only induces a submaximal cellular response even there is 100% receptor occupation (Rang, 2003). By comparing the potency and the maximum response of GHS and adenosine, it indicated that adenosine is less potent and the adenosine agonist activation curves reach a plateau at a lower level than the one activated by GHS. In addition, at the concentrations of adenosine that maximized activation of GHS-R1a, GHS did not provide additional stimulation. These suggested that adenosine is a partial agonist of GHS-R1a (Smith *et al.*, 2000).

## 1.5 Physiological effects of ghrelin

Ghrelin has lots of physiological actions, including GH-releasing activity, food intake stimulation, glucose metabolism, sleep behaviors, proliferation regulation and apoptosis regulation (Ghigo *et al.*, 2005; Korbonits *et al.*, 2004; van der Lely *et al.*, 2004). Therefore, ghrelin has been suggested to act as a drug to cure the growth hormone deficiency (GHD) in childhood, obesity, and cancer. In this section, it focuses on the regulation of proliferation and apoptosis.

Ghrelin inhibits cell proliferation in some cancer cells. In human breast cancer cell lines, after incubating the cells with ghrelin for 48 hours, there was a significant decrease in the cell number (Cassoni *et al.*, 2001). In human medullary thyroid carcinomas, ghrelin binding sites were significantly higher density than the normal thyroid tissue (Kanamoto *et al.*, 2001) and ghrelin inhibited cell proliferation in thyroid tumor cell lines (Volante *et al.*, 2003). However, ghrelin also promotes cell proliferation in other cancer cells. In human pancreatic cancer cell lines, the cells were incubated with ghrelin, there was a dose-dependent increase in cell proliferation up to 10 nM (Duxbury *et al.*, 2003). This cell proliferation effect of ghrelin was also observed in prostate cancer cell lines (Jeffery *et al.*, 2002) and hepatoma (Murata *et al.*, 2002). Besides cancer cells, ghrelin also promotes cell proliferation on adrenal (Andreis *et al.*, 2003), cardiac (Pettersson *et al.*, 2002), adipose cells (Choi *et al.*, 2003; Kim *et al.*, 2004; Thompson *et al.*, 2004) and pituitary (Nanzer *et al.*, 2004). In general, ghrelin promotes cell proliferation in normal cells, and inhibits cell proliferation in abnormal cells.



Ghrelin protects different types of cells from apoptosis, such as cardiomyocytes, endothelial cells (Baldanzi *et al.*, 2002; Benso *et al.*, 2004) and adipocytes (Kim *et al.*, 2004). Taking adipocytes as an example, in 3T3-L1 preadipocytes, apoptosis was induced by 48 hours serum starvation. In the presence of ghrelin, the DNA fragmentation caused by serum starvation decreased, suggesting that ghrelin protects preadipocytes from apoptosis. Ghrelin can also induce a pro-apoptotic effect to the cells. In human aldosteronoma, ghrelin enhances apoptosis, as indicated in the TUNEL assay, more DNA fragments in the adrenocortical carcinoma-derived cell lines than in the normal human adrenocortical cells, so ghrelin can be a drug to cure cancer (Belloni *et al.*, 2004).

## **1.6 Apoptosis**

### **1.6.1 Introduction**

The word apoptosis is derived from Greek and means “falling off”, as of leaves from trees. Apoptosis is an active process of gene-directed cellular self-destruction, which is important in homeostasis function providing the balance between cell survival and cell death (Tomei *et al.*, 1991). Apoptosis is very important to mammals, as it can maintain a relatively constant cell population by balancing between apoptosis and mitosis. Apoptotic cell death plays an important role in eliminating the cells whose survival may be harmful to the body, such as the cells are mutants, DNA-damaged or virus-infected (Tomei *et al.*, 1991). Furthermore, apoptosis plays an important role in embryo development, for example, in the formation of interdigital webs (Hammar *et al.*, 1971). As apoptosis is a process, which causes cell death, if it is not normally regulated, it will cause harm to our organs.

Mitogens and survival factors have been shown to play important roles in regulating cell proliferation and apoptosis. These factors, first binding to cell surface receptors, trigger phosphorylation of various molecular targets, which activate the downstream signaling cascades, leading to changes in cell death-regulating proteins and resulting in the survival or death of a cell (Wu-Wong *et al.*, 2000).

### **1.6.2 Apoptosis versus necrosis**

The onset of apoptosis is heralded by compaction and segregation of chromatin into sharply uniform masses that lie against the nuclear envelope, condensation of the cytoplasm and mild convolution of nuclear and cellular outlines. In the next few

minutes, there is nuclear and DNA fragmentation and marked convolution of the cellular surface with budding. In the final stage, separation of the membrane-bound apoptotic bodies occurs, which are then phagocytosed and digested by macrophages (Tomei *et al.*, 1991). In contrast, the onset of necrosis is heralded by the injured cells, which cannot be repaired. At the beginning stage, chromatin clumps into less uniform masses and the organelles swell. At final stage, cell membranes break down and the nuclear chromatin disappears, that is, cell disintegration occurs (Tomei *et al.*, 1991).

Apoptosis is a programmed cell death, which is different from necrosis. By comparing these two, necrosis involves the swelling of the organelles, while apoptosis involves condensation only. Both contain the DNA fragmentation, while in apoptosis, the cleavage of DNA occurs at the linker regions between nucleosomes to produce fragments with approximately 185 base pairs (Tomei *et al.*, 1991), but in necrosis, the cleavage of DNA is in a random manner. Apoptosis is not associated with inflammation, as there have not internal constituents released into the cell's surroundings, all the materials are phagocytosed by macrophages. Whereas necrosis is accompanied by inflammation, as after the disorganized disintegration of cells, the resulting products which are released trigger the inflammatory response (Rang, 2003).

### **1.6.3 Mechanisms of apoptosis**

There are many apoptosis pathways which have been discovered. Here, it just focus on two main pathways, one involving the stimulation of death receptors and the other



one involving the mitochondria, both of them involve the activation of caspases (Rang, 2003).

Caspase refers to ICE/CED-3 family of cysteine proteases, and is highly conserved among species. In human, about two-third of caspases have been suggested to function in apoptosis (Hengartner, 2000) and the other caspases have another physiological functions, for example, caspase-12 has been suggested to be involved in regulating inflammation (Tracey *et al.*, 2004). It cleaves its substrates after an aspartate residue at the carboxyl terminal and the caspase's distinct substrate specificity is determined by the four residues amino-terminal to the cleavage site. All caspases exist as zymogens, which are composed of three domains, they are the N-terminal prodomain, and the p20 and p10 domains. Zymogens require proteolytic processing to become active, it usually involves the removal of the N-terminal pro-domain (Hengartner, 2000). Once activated, caspase can initiate a diverse cleavage of other cellular proteins, and then lots of physiological effects occur, including apoptosis. In human, eleven caspases have been identified (caspase 1 to caspase 11) to be involved in apoptosis regulation and they can be divided into two classes according to the presence of the amino-terminal pro-domain. Class I caspases (caspase-1, 2, 4, 5, 8, 9, 10 and 11) contain long pro-domain. They are usually in the upstream part of the apoptotic cascade, so they are also called initiator caspases. Class II caspases (caspase-3, 6, 7) contain short or absent pro-domains. They are usually in the downstream part of the apoptotic cascade, so they are also called effector caspases. The activity of caspases can be regulated by transcription, proteolytic activation, alternative splicing to produce truncated protein and

localization of caspases (Tomei *et al.*, 1991).

One of the main apoptosis pathways is the death receptor pathway. Death receptors have 'death domain' in their cytoplasmic tail (Rang, 2003). Upon binding of an external ligand, adapter protein is recruited and associated with the death domain on the membrane. Then this complex recruits many procaspase-8. Under this close proximity, procaspase-8 gets activated by mutual cleavage and then activates each other. The activated caspase-8 is an initiator caspase, it activates effector caspases and induces apoptosis (Hengartner, 2000).

Mitochondrial pathway is another major apoptosis pathway. It involves the release of cytochrome c from the mitochondria by the activity of the Bcl-2 protein family. Bcl-2 family can be divided into three groups, based on their structural similarities. The first group includes bcl-2 and bcl-x<sub>L</sub>, all of them possess anti-apoptotic activity. They are characterized by four short, conserved bcl-2 homology domains (BH1 - BH4). They also possess a C-terminal hydrophobic tail, by which this group members can localize on the outer surface of the mitochondria. The second group possesses apoptotic activity, includes bax and bak. Their structure is similar to the first group, except the missing of BH4. The third group also possesses apoptotic activity, include bid and bik. Their structure is very diverse and they only have a BH3 domain in common with the previous groups. Among these three groups, they can form heterodimer between groups and homodimer within group. These groups meet at the surface of the mitochondria, if the pro-apoptotic signals from the second and third group are stronger than the anti-apoptotic signals from the first group, and



then cytochrome c is released from the mitochondria. In the cytosol, the released cytochrome c will associate with apoptotic protease-activating factor-1 (Apaf-1) and procaspase-9 to form an apoptosome. In the apoptosome, procaspase-9 gets activated. Procaspase-3 is activated by caspase-9, and apoptosis is executed (Hengartner, 2000) (Fig. 1.3).

#### **1.6.4 Methods to study apoptosis**

There are many methods to study apoptosis, such as recognition of the apoptotic cells morphology, assessment of internucleosomal DNA fragmentation, quantification of the Bcl-2 family proteins amount and detection of caspases activity. The objective of the study determines which techniques are chosen.

To recognize the apoptotic cell morphology, several stains are used such as ethidium bromide and acridine orange (EB/AO) (Cohen, 1993; Coligan, 1995), 4',6-diamidino-2phenylidole (DAPI) (Coligan, 1995) or Hoechst staining (Coligan, 1995). After staining, the apoptotic cells were different from the normal cells. Take the EB/AO staining as an example, after staining, the live cells have a normal green nucleus; early apoptotic cells have bright green nucleus with condensed or fragmented chromatin; late apoptotic cells display condensed and fragmented orange chromatin; cells that have died from direct necrosis have a structurally normal orange nucleus (Renvoize *et al.*, 1998; Ribble *et al.*, 2005; Wang *et al.*, 2005).

To assess the DNA fragmentation from apoptosis, the most common methods are DNA laddering on an agarose gel and the terminal deoxynucleotide



transferase-mediated dUTP-biotin nick-end labeling, usually known by the acronym TUNEL. TUNEL assay is based on the specific binding of the enzyme and the incorporation of biotin. Then the biotinylated-labelled bases on the fragmented DNA are detected by the anti-biotin immunoglobulins (Gavrieli *et al.*, 1992).

There are several ways to detect the Bcl-2 family members, such as immunoblotting, northern blot analysis, reverse-transcriptase polymerase chain reaction (RT-PCR) and immunohistochemical detection.

Detection of the apoptosis induction by the measurement of the caspases activity, usually makes use of the specific cleavage sites of each caspase and a fluorogenic or chromogenic compound, such as a colorimetric assay using compound (Ac-DEVD-pNA) (Chae *et al.*, 2004). If there is an activation of caspase, and then the cleavage site will be recognized and cleaved by the caspase, as a result a release of the fluorogenic or chromogenic compound, which can be detected.

### **1.6.5 Different types of apoptotic inducers**

Apoptotic inducers pass through various mechanisms to disturb the cells and initiate apoptosis. These mechanisms include the death receptor, calcium influx, oxidative stress, inhibition of protein synthesis, perturbation of DNA integrity and inhibition of protein kinases, therefore, apoptotic inducers can be divided based on their mechanism.

Intracellular calcium increase can lead to apoptosis, it is indicated in the parathyroid

hormone/ parathyroid hormone-related protein (PTH/PTHrP) receptor. PTH-induced apoptosis through PTH/PTHrP receptor was inhibited by a calcium-binding protein, calbindin (Turner *et al.*, 2000). This group of apoptotic inducers includes the calcium ionophore.

In murine lymphoma cell line, apoptosis was induced by nitric oxide (Hu *et al.*, 2005). Nitric oxide induces apoptosis by imposing an oxidative stress to the cells. Apoptotic inducers using this pathway include some of the nitric oxide donors (Fiscus *et al.*, 2002).

DNA breaks result in apoptosis. One of the methods to produce DNA breaks is to inhibit topoisomerase. For examples, etoposide inhibits topoisomerase II by forming a ternary complex with the cleaved DNA, in order to prevent the religation of double-strand DNA breaks (Sai Krishna *et al.*, 2005). The other apoptotic inducers fall into this group include topoisomerase I inhibitors.

Some of the drugs induce apoptosis by inhibiting protein kinases. For example, phosphoinositide 3-kinases (PI3K) inhibitor blocks the PI3K/Akt anti-apoptotic pathway to induce apoptosis. Other apoptosis inducers of this group include staurosporine.

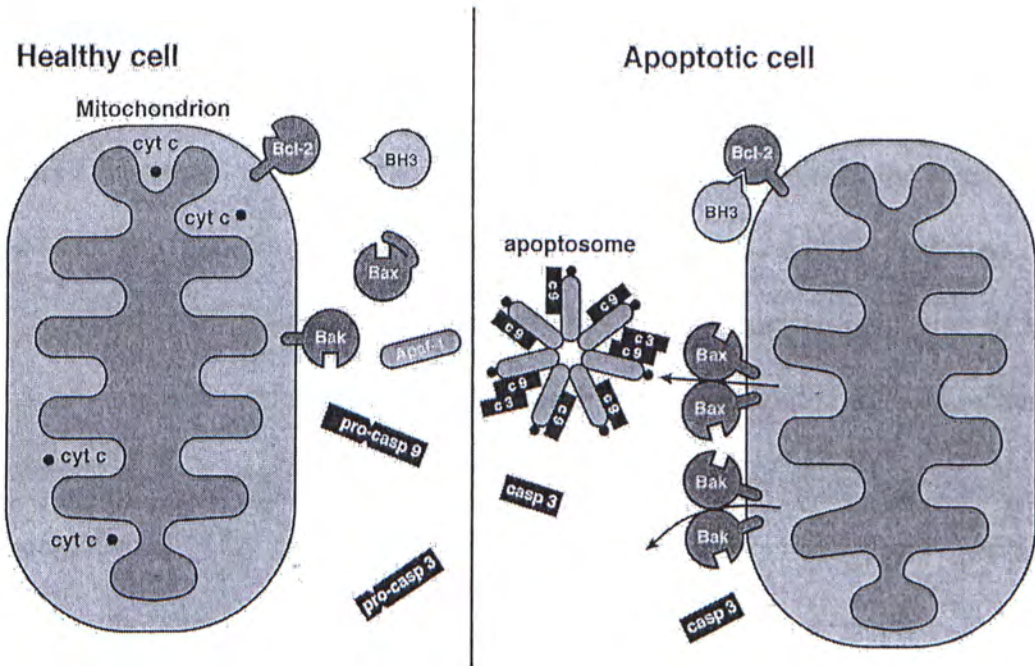


Figure 1.3 Mitochondrial pathways of apoptosis. In the apoptotic cells, on the mitochondria surface, the pro-apoptotic subtype (BH3) of Bcl-2 family inhibits the anti-apoptotic subtype (bcl-2). It causes the release of cytochrome c (cyt c) and then the apoptosome (composed of caspase-3: c3, caspase-9: c9 and cyt c) formed. In the apoptosome, the pro-caspase-3 gets activated and the caspase-3 induced apoptosis occurs in the cells. Figure modified from Adams, (2003).



## **1.7 Apoptotic and anti-apoptotic pathways regulated by GPCRs**

### **1.7.1 Bcl-2 family pathway**

GPCRs have been demonstrated to regulate apoptosis by determining the expression level and the phosphorylation of bcl-2 family. GPCRs induce apoptosis by down-regulation of pro-apoptotic member in bcl-2 family and up-regulation of the apoptotic member, it has been demonstrated in cannabinoid 1 (CB1) receptor (Fernandez-Ruiz *et al.*, 2004), somatostatin (SSTR2) receptor (Kumar *et al.*, 2004) and angiotensin (AT2) receptor (Tejera *et al.*, 2004). GPCRs induce anti-apoptotic effect by the opposite pattern as the apoptotic pathway, that is by increasing the expression level of proapoptotic bcl-2 family and decreasing the expression level of apoptotic bcl-2 family, such as P2Y<sub>2</sub> purinoceptor (P2Y2) (Chorna *et al.*, 2004), adenosine 1 (A1) and adenosine 3 (A3) (Das *et al.*, 2005). GPCRs regulate the bcl-2 family by activating PI3K/Akt pathway (Das *et al.*, 2005; Di Iorio *et al.*, 2004; Iwai-Kanai *et al.*, 2004) as described in section 1.7.4, and mitogen-activated protein kinases (MAPK), such as extracellular signal-regulated kinases (ERK1/2) pathways (Di Iorio *et al.*, 2004; Iwai-Kanai *et al.*, 2004) as described in section 1.7.3, or inhibiting the caspase cascades as described in section 1.7.2 (Kippenberger *et al.*, 2005). cAMP responsive element binding (CREB) protein-dependent pathway can induce (Iwai-Kanai *et al.*, 2004) or inhibit (Chorna *et al.*, 2004; Das *et al.*, 2005) apoptosis, depending on the cell types.

### **1.7.2 Caspase pathway**

GPCRs regulate apoptosis through caspases cascade. One of the pathways is through

the G<sub>q</sub>-coupled receptor to raise the intracellular calcium level, and then the calcium activates caspase-1 and caspase-3 activity through mitochondria pathway, as described in section 1.6.3. P2X7 purinergic receptor (P2X7) (Kippenberger *et al.*, 2005) and parathyroid hormone receptor (PTHr) (Turner *et al.*, 2000) were shown to make use of this pathway to execute apoptosis. The other two pathways in which GPCRs initiate or inhibit caspases cascade are the MAPK kinase pathways, such as ERK1/2 and p38, and PI3K/Akt pathway. Some of the GPCRs reduce the activity of ERK1/2, results in the increasing caspase-3 activity in the cells (Jaleel *et al.*, 2004; Katsuma *et al.*, 2005). Similar to ERK1/2, inhibition of PI3K/Akt pathway results in an increase of caspase-3 activity (Bar-Yehuda *et al.*, 2005; Germack *et al.*, 2004a; Vassiliou *et al.*, 2004).

### 1.7.3 ERK pathway

GPCR activation can lead to activation of ERKs. ERK1 (44 kDa) and ERK2 (42 kDa) are well-established mitogen-activated protein kinase (MEK) substrates (Sugden *et al.*, 1997). Activation of ERK1 and ERK2 leads to activation of several transcription factors and causes cellular proliferation and cell survival (Somai *et al.*, 2002). Many of the GPCRs were shown to protect the cells against apoptosis through the activation of ERK1/2 pathways, such as endothelin receptor (ET-1) (Iwai-Kanai *et al.*, 2004; Wu-Wong *et al.*, 2000), GPR120 (Katsuma *et al.*, 2005)), chemokine receptor (CXCR4) (Jaleel *et al.*, 2004) and neurotensin receptor (Somai *et al.*, 2002). For example, in MCF-7 cells, activation of neurotensin receptor inhibited apoptosis and stimulated cell proliferation through activation of ERK1 and ERK2 (Widmann *et al.*, 1999). Studies showed that stimulation of neurotensin receptor activated ERK1 and



ERK2 (Ehlers *et al.*, 2000) and bcl-2 gene expression was promoted by ERK1 and ERK2 (Liu *et al.*, 1999). As a result, bcl-2 inhibits apoptosis. That is, GPCR activates ERK1 and ERK2 and leads to cell survival by promoting gene expression of anti-apoptotic factor.

#### 1.7.4 PI3K/Akt pathway

On the interior cell surface, phosphoinositide 3-kinases (PI3K) converts phosphatidylinositol-4,5-bisphosphate (PtdIns-4,5-P<sub>2</sub>) into phosphatidylinositol-3,4,5-trisphosphate (PtdIns-3,4,5-P<sub>3</sub>), and then it is further converted to phosphatidylinositol-3,4-bisphosphate (PtdIns-3,4-P<sub>2</sub>) by phospholipids phosphatase. Akt is a serine/threonine protein kinase. Akt recruits to the membrane and gets conformational change. Then Akt gets activation by phosphorylation at serine and threonine by protein kinase B kinases (PKBKs). Subsequently, the phosphorylated Akt is released from the membrane and phosphorylates its specific targets (Hemmings, 1997). One of the effects is the induction of an anti-apoptotic effect in the cells. There are many GPCRs which can induce anti-apoptotic effect through PI3K/Akt pathway, including adenosine A<sub>3</sub> receptor (Das *et al.*, 2005; Germack *et al.*, 2004b), ET-1 (Iwai-Kanai *et al.*, 2004), EP<sub>2</sub> and EP<sub>4</sub> (Vassiliou *et al.*, 2004), and β<sub>2</sub>-adrenergic receptor (Singh *et al.*, 2001). In adult mouse cardiac myocytes, β<sub>2</sub>-adrenergic receptors activate PI3K/Akt through PTX-sensitive G<sub>i</sub> proteins. This activation is a cell survival signal, because inhibition of G<sub>i</sub> protein by PTX or inhibition of PI3K by LY294002 caused DNA fragmentation (Zhu *et al.*, 2001). Therefore, PI3K/Akt is an important cell survival intermediate. Akt mediates survival effect by several mechanisms, which include phosphorylation of BAD,



releasing Bcl-2 family member (Datta *et al.*, 1997), phosphorylation and inactivation of caspase-9 (Datta *et al.*, 1999) and phosphorylation of the forkhead transcription factor, FKHL1 (Romashkova *et al.*, 1999).

## Chapter 2

### Materials and solutions

#### 2.1. Materials

**0.25% Trypsin/EDTA** (Sigma)

**1 kb DNA ladder** (0.5 mg DNA/ml, Fermentas)

**2myc-hGHSR1a plasmid DNA** (HW/8/72) was cloned in pcDNA3.1(+) expression vector.

**2myc-hGHSR1b plasmid DNA** (HW/8/72) was cloned in pcDNA3.1(+)/Zeocin expression vector.

**6x loading buffer** (Fermentas)

**Adenosine** (Sigma)

**Adenosine deaminase** (Sigma)

**Agar powder** (Sigma)

**Agarose** (genetic technology grade, FMC)

**Ammonia solution** (25%, BDH)

**Ammonium formate** (Sigma)

**Ampicillin** (Sigma) was dissolved in ultra-pure water at 50 mg/ml, aliquoted and stored at -20°C and thawed no more than twice.

**Antibiotic G418 sulfate, geneticin** (USB) was dissolved in autoclaved ultra-pure water at 50 mg/ml, aliquoted and stored at -20°C and thawed no more than twice.

**ATP** (Adenosine 5'-triphosphate, Sigma) was freshly prepared by dissolving in

ultra-pure water at 100 mM.

**Bam HI** (New England Biolab)

**Buffer B** (Roche)

**Buffer H** (Roche)

**Calcium chloride, dihydrate** ( $\text{CaCl}\cdot 2\text{H}_2\text{O}$ , Sigma)

**Caspase-3 biosensor** (pGFP<sup>2</sup>-DEVD-Rluc(h), BioSignal Packard) was reconstituted at 1.0  $\mu\text{g}/\text{ml}$  with 10 mM Tris-HCl, pH 8.0, 1 mM EDTA, and stored at  $-20^\circ\text{C}$ .

**Caspase-3 Substrate I** (Ac-DEVD-pNA, Calbiochem) was dissolved in 100% DMSO at 100 mM, aliquoted and stored at  $-20^\circ\text{C}$  and thawed no more than twice.

**CHAPS** (Calbiochem)

**Chloroform** (Sigma)

**D-(+)-Glucose** (Sigma)

**DAMGO** ([D-Ala<sup>2</sup>, NMe-Phe<sup>4</sup>, Gly-ol<sup>5</sup>] enkephalin DAGO, Tocris)

**DeepBlueC** (50  $\mu\text{g}$ , BioSignal Packard) was dissolved in absolute ethanol at 1 mM and stored at  $-20^\circ\text{C}$ .

**DMEM** (Dulbecco's Modified Eagle Media, Cat no. 12800-017, Gibco)

**DMSO** (Dimethyl sulfoxide, Sigma)

**DTT** (Dithiothreitol, Pharmacia Biotech)

**Dulbecco's Modified Eagle Medium without serum, glutamine and phenol red**  
(Cat no. 31053-028, Gibco)

**Eco RI** (Roche)

**EDTA** (Ethylenediamine-tetraacetic acid, disodium salt; Dihydrate, Sigma)

**Escherichia coli DH5a**

**Escherichia coli Top10F'**



**Ethanol** (absolute, Merck)

**Ethidium bromide** (Sigma)

**Etoposide** (Biomol) was dissolved in DMSO at 40 mM, aliquoted and stored at -20 °C.

**Fetal bovine serum** (Gibco) was heat treated 65°C, aliquoted and stored at -20°C and thawed no more than twice.

**Fluorescence resonance energy transfer (FRET) caspase-3 biosensor** (pCFP-DEVD-YFP, a gift from Prof. Donald C. Chang, HKUST)

**Formic acid** (BDH)

**Ghrelin** (Bachem) was dissolved in ultra-pure water at 1 mM, aliquoted and stored at -20°C and thawed no more than twice.

**GHRP-6** (Growth hormone releasing peptide 6, Bachem) was dissolved in ultra-pure water at 30 mM, aliquoted and stored at -20°C and thawed no more than twice.

**Glacial acetic acid** (Riedel-de Haen)

**Glycerol** (Sigma)

**G<sub>α</sub>qRC plasmid DNA** (a gift from Prof. Y.H. Wong, HKUST) was cloned in pcDNA1 expression vector.

**HA-tagged Human thromboxane A<sub>2</sub> (HA-hTP<sub>α</sub>) receptor plasmid DNA** (a gift from Takuya Kobayashi, Kyoto University) was cloned in pcDNA3.1(+).

**HEPES** (N-(2-Hydroxyethyl)piperazine-N<sup>1</sup>-(2-ethanesulfonic acid, Sigma)

**HindIII** (Roche)

**Human growth hormone secretagogue receptor 1a (hGHSR1a) plasmid DNA** (Guthrie) was cloned in pcDNA3.1(+) expression vector.

**Human growth hormone secretagogue receptor 1b (hGHSR1b) plasmid DNA**

(Guthrie) was cloned in pcDNA3.1(+) expression vector.

**Hydrochloric acid** (35.4%, BDH)

**Isopropanol** (BDH)

**Kanamycin** (Sigma) was dissolved in ultra-pure water at 40 mg/ml and stored at -20 °C.

**Lipofectamine2000 reagent** (Invitrogen)

**Lithium chloride** (Sigma) was prepared as a 1 M solution in ultra-pure water and stored at 4°C.

**Magnesium chloride, hexahydrate, ACS** ( $\text{MgCl}_2 \cdot 6\text{H}_2\text{O}$ , USB)

**mDP (mouse prostaglandin D<sub>2</sub> receptor) plasmid DNA** (a gift from Takuya Kobayashi, Kyoto University) was cloned in pCMV expression vector.

**Micro BCA<sup>TM</sup> Protein Assay Kit** (PIERCE)

**MOR ( $\mu$ -opioid receptor) plasmid DNA** (a gift from Prof. Y.H. Wong, HKUST) was cloned in pRcCMV expression vector.

**Myo-inositol-[2-<sup>3</sup>H(N)]** (specific activity 22.2 Ci/mmol, NEN) stored at 4°C.

**Na<sub>2</sub>HPO<sub>4</sub>** (Sodium phosphate, dibasic, anhydrous, Sigma)

**Not I** (Roche)

**Opti-Mem I reduced serum medium** (Gibco)

**Optiphase Hisafe-3** (Pharmacia Biotech)

**pBK-CMV vector DNA** (Stratagene)

**pcDNA3.1(+)/Zeocin vector DNA** (Invitrogen)

**pcDNA3.1(+)-vector DNA** (Invitrogen)

**pEGFP-N1 plasmid DNA** (clontech)

**Penicillin/Streptomycin solution** (Sigma) was reconstituted with 20 ml sterile

ultra-pure water and stored at 4°C.

**PIPES** (1,4-Piperazinediethanesulfonic acid, Sigma)

**p-nitroaniline** (Sigma) was dissolved in absolute ethanol at 5 mM, aliquoted and stored at -70°C.

**Poly-D-lysine** (Sigma) was dissolved in PBSA at 5 mg/ml, aliquoted and stored at -20°C.

**Positive control vector for bioluminescence resonance energy transfer (BRET<sup>2</sup>) assay** (pGFP<sup>2</sup>-Rluc(h), BioSignal Packard)

**Potassium chloride** (KCl, Sigma)

**Potassium dihydrogen phosphate** (KH<sub>2</sub>PO<sub>4</sub>, Merck)

**Prostaglandin D<sub>2</sub>** (PGD<sub>2</sub>, Cayman) was dissolved in ethanol at 1 mM and stored at -20°C.

**QIAGEN Plasmid Maxi Kit** (QIAGEN)

**Sal I** (Roche)

**Seabream growth hormone secretagogue receptor 1a (sbGHSR1a) plasmid DNA** (a gift from Dr Chi-Bun Chan, CUHK) was cloned in pBK-CMV expression vector.

**Seabream growth hormone secretagogue receptor 1b (sbGHSR1b) plasmid DNA** (a gift from Dr Chi-Bun Chan, CUHK) was cloned in pBK-CMV expression vector.

**Sodium bicarbonate** (NaHCO<sub>3</sub>, Sigma)

**Sodium chloride** (NaCl, Sigma)

**Sodium hydroxide** (NaOH, Sigma)

**Staurosporine** (Biomol) was dissolved in DMSO at 10 mM, aliquoted and stored at -20°C.

**Substance P analog** (D-Arg<sup>1</sup>,D-Phe<sup>5</sup>,D-Trp<sup>7, 9</sup>,Leu<sup>11</sup>)-Substance P, Bachem) was



dissolved in ultra-pure water at 10 mM, aliquoted and stored at -20°C and thawed no more than twice.

**SuperScript™ First-Strand Synthesis System** (Invitrogen)

**SYBR Green RT-PCR Kit** (Applied Biosystems)

**Tetracycline** (Sigma) was dissolved in ultra-pure water at 10 mg/ml and stored at -20°C.

**Theophylline** (Sigma) was freshly prepared by dissolving in ultra-pure water at 0.02 M.

**Tris-base** (Sigma)

**Trizma-hydrochloride** (Sigma)

**TRIZOL reagent** (Invitrogen) stored at 4°C.

**Trypan blue** (Sigma)

**Tryptone** (Oxoid)

**U46619** (Sigma) was dissolved in absolute ethanol at 2.85 mM and stored at -20°C.

**Wizard® Plus SV Minipreps DNA Purification System** (Promega)

**XhoI** (New England Biolab)

**Yeast extract** (Oxoid)

**Zeocin** (Invitrogen)

All the disposable culture dishes and culture plates were supplied by Corning.

## 2.2. Culture medium, buffers and solutions

### 2.2.1. Culture medium

**Dulbecco's Modified Eagle's Medium DMEM** (Gibco) was reconstituted with 1000 ml ultra pure water, and supplemented with  $\text{NaHCO}_3$  (3.7 g/L). The pH was adjusted to 7.2 with 1 M HCl and filter sterilized through a 0.22  $\mu\text{m}$  filter into 1000 ml bottle to give a final pH of around 7.4. It was stored at 4°C. Heat-treated fetal bovine serum (10% v/v) was added to form complete medium.

### 2.2.2. Buffers

**Assay buffer** for caspase-3 colorimetric assay was prepared with the following reagents: HEPES (50 mM), NaCl (100 mM), CHAPS (0.1%), DTT (10 mM), EDTA (0.1 mM) and glycerol (10%) in ultra-pure water. The pH was adjusted to 7.4 and the solution was stored at -70°C.

**Cell lysis buffer** for caspase-3 colorimetric assay was prepared with the following reagents: HEPES (50 mM), NaCl (100 mM), CHAPS (0.1%), DTT (1 mM) and EDTA (0.1 mM) in ultra-pure water. The pH was adjusted to 7.4 and the solution was stored at -70°C.

**Dulbecco's PBS** (PBSA:  $\text{Ca}^{2+}/\text{Mg}^{2+}$  free) was prepared with the following ACS reagents supplied by Sigma: KCl (2.7 mM),  $\text{KH}_2\text{PO}_4$  (1.4 mM), NaCl (137 mM) and  $\text{Na}_2\text{HPO}_4$  (8.1 mM) in ultra-pure water. The pH was adjusted to 7.5 with 1 M NaOH and the solution was filter sterilized giving a final pH of 7.4 and stored at 4°C.

**HEPES buffered saline (HBS)** was prepared with the following ACS reagents supplied by Sigma:  $\text{CaCl}_2 \cdot 2\text{H}_2\text{O}$  (2.2 mM), HEPES (15 mM), KCl (4.7 mM),  $\text{KH}_2\text{PO}_4$  (1.2 mM),  $\text{MgCl}_2 \cdot 6\text{H}_2\text{O}$  (1.2 mM), NaCl (140 mM) in ultra-pure water. The pH was adjusted to 7.5 with 1 M NaOH and the solution was filter sterilized giving a final pH of 7.4 and stored at 4°C. Glucose (11 mM) was added on the day of experiment.

### 2.2.3. Solutions

**1 M formic acid** was prepared by adding 37.73 ml 26.5 M formic acid stock solution to ultra-pure water and the volume was made up to 1000 ml. The solution was stored at room temperature.

**20 mM formic acid** was prepared by adding 20 ml 1 M formic acid to ultra-pure water and the volume was made up to 1000 ml. The solution was stored at 4°C.

**2 M ammonium formate / 0.1 M formic acid** was prepared by dissolving 252.24 g ammonium formate in 200 ml 1 M formic acid, and the volume was made up to 2000 ml using ultra-pure water. The solution was stored at room temperature.

**40 mM ammonium formate / 0.1 M formic acid** was prepared by dissolving 5.04 g ammonium formate and adding 200 ml 1 M formic acid, and the volume was made up to 2000 ml using ultra-pure water. The solution was stored at room temperature.



**0.05% ammonia solution** was prepared by adding 2 ml 25% ammonia solution to ultra-pure water and the volume was made up to 1000 ml. The solution was stored at room temperature.

**LB broth** was prepared by dissolving 10 g NaCl, 10 g tryptone and 5 g yeast extract in 1000 ml ultra-pure water. The LB broth was autoclaved and antibiotic was added as required to the solution after cooling. The solution was stored at 4°C.

**LB broth (low salt)** was prepared by dissolving 5 g NaCl, 10 g tryptone and 5 g yeast extract in 1000 ml ultra-pure water. The LB broth was autoclaved and antibiotic was added as required to the solution after cooling. The solution was stored at 4°C.

**Agar plates** were prepared by dissolving 10 g NaCl, 10 g tryptone, 5 g yeast extract and 15 g agar powder in 1000 ml ultra-pure water. The agar solution was autoclaved and the antibiotic was added as required to the solution after cooling. 15 ml agar solution was poured into each 100 mm dish and left to solidify at room temperature. The agar plates were stored up side down at 4°C.

**Agar plates (low salt)** were prepared by dissolving 5 g NaCl, 10 g tryptone, 5 g yeast extract and 15 g agar powder in 1000 ml ultra-pure water. The agar solution was autoclaved and the antibiotic was added as required to the solution after cooling. 15 ml agar solution was poured into each 100 mm dish and left to solidify at room temperature. The agar plates were stored up side down at 4°C.

**50 X TAE** was prepared by dissolving 48.4 g Tris-base, 11.71 ml glacial acetic acid and 7.44 g EDTA in 200 ml ultra-pure water and stored at room temperature.

**1 X TAE** was prepared by adding 20 ml 50 X TAE to 980 ml ultra-pure water and stored at room temperature.

**TE** was prepared as 10 mM Trizma-hydrochloride and 1 mM EDTA in ultra-pure water at pH 8.0 and stored at 4°C.

## Chapter 3

### Methods

#### 3.1. Maintenance of cell lines

##### 3.1.1. Human Embryonic Kidney (HEK293) cells

HEK293 cells were cultured in DMEM medium supplemented with 10% FBS, 100 units/ml penicillin and 100 µg/ml streptomycin in a humidified atmosphere of 5% CO<sub>2</sub>/95% air at 37°C. Cells were passaged weekly at 90% confluency, and the medium was refreshed every two to three days. When subculturing the cells, the medium was removed from 100 mm culture dish and the cells were rinsed with 10 ml PBSA. Then, PBSA was aspirated and 1 ml trypsin/EDTA was added to the dish for 3 to 5 min at room temperature. When the cells were completely detached from the dish, 9 ml complete DMEM was added to neutralize the trypsin. The cell suspension (1 ml) was added to a new dish with 9 ml complete DMEM (split ratio 1 : 10 ). When counting cells, 10 µl of cell suspension was mixed with 10 µl of trypan blue solution. Then, 10 µl of the mixture was transferred to a hemocytometer slide and counted under a microscope. Normal viability was over 90%.

##### 3.1.2. HEK293 cells stably expressing black seabream growth hormone secretagogue receptors (HEK-sbGHS-R1a and HEK-sbGHS-R1b)

HEK-sbGHS-R1a and HEK-sbGHS-R1b cells were cultured as described in section 3.1.1 but with the addition of 500 µg / ml G418.



## **3.2. Preparation of plasmid DNA**

### **3.2.1. Preparation of competent *E. coli***

Five ml of the non-competent *E. coli* (Top10F' or DH5 $\alpha$ ) was added to 200 ml LB with appropriate antibiotic as necessary. The growth of *E. coli* was monitored until the absorbance at 600 nm reached between 0.4 and 0.6. The *E. coli* culture was aliquoted into prechilled falcon tubes and incubated on ice for 10 min. The *E. coli* were then centrifuged at 1600 x g at 4°C for 7 min. The supernatant was removed and the pellet was resuspended in 10 ml ice-cold CaCl<sub>2</sub> solution (60 mM CaCl<sub>2</sub>, 10 mM PIPES and 15% glycerol). The *E. coli* suspension was centrifuged at 1100 x g at 4°C for 5 min and the pellet was resuspended in 20 ml ice-cold CaCl<sub>2</sub> solution. Then, the resuspended *E. coli* were incubated on ice for 30 min followed by centrifugation at 1100 x g at 4°C for 5 min and the pellet was resuspended in 3 ml ice-cold CaCl<sub>2</sub> solution. The competent cells were aliquoted and stored at -70°C.

### **3.2.2. Transformation of DNA into competent cells**

Plasmid DNA (10 ng) was mixed with 100  $\mu$ l suitable competent cells and incubated on ice for 30 min to allow the plasmid DNA to surround the competent cells. Then, the competent cells were heat shocked at 42°C for 2 min, so the plasmid DNA enters the competent cells. The heat shocked competent cells were incubated with 500  $\mu$ l LB at 37°C with shaking for 1 h and collected by centrifugation at maximum speed (about 13000 x g) for 30 sec using micro-centrifuge (Sigma 113). The cell pellet was resuspended in approximately 100  $\mu$ l LB and spread on an agar plate which contained suitable antibiotic for selection of positive clones. Colonies were

developed by overnight incubation at 37°C and individual colonies were picked and inoculated to 5 ml of antibiotic-containing LB for small scale DNA preparation.

### **3.2.3. Small-scale and large-scale plasmid DNA preparation**

Wizard® *Plus* SV Minipreps DNA Purification System was used to prepare small-scale plasmid DNA suitable for characterizing the plasmid DNA and transfection. QIAGEN Plasmid Maxi Kit was used to prepare a large-scale plasmid DNA. All the procedures followed supplier's instructions.

### **3.2.4. Confirmation of the purity and the identity of the plasmid DNA**

In order to confirm the purity of the plasmid DNA, the ratio of the absorbance measurements at 260 nm and 280 nm were used. As the absorbance at 260 nm and 280 nm indicate the amount of DNA and protein present in the sample respectively. An absorbance ratio between 1.6 and 2.0 was regarded as suitable plasmid DNA purity for use.

Restriction enzyme digestion was used to confirm the identity of plasmid DNA. Restriction enzymes used in each plasmid DNA digestion and the band sizes of each DNA fragment after restriction enzyme digestion are shown in Table 3.1.

---

Plasmid	Restriction enzyme(s)	Size of DNA fragment(s) (kb)
hGHS-R1a	Eco RI + Xho I	1.1, 5.4
hGHS-R1b	Eco RI + Xho I	0.9, 5.4
pBK-CMV	Hind III	4.5
pcDNA3.1(+)	Hind III	5.4
pEGFP-N1	Hind III	4.7
pGFP-DEVD-Rluc(h)	Hind III + Bam HI	1.0, 4.2
sbGHS-R1a	Not I and Sal I	1.2, 4.4
sbGHS-R1b	Not I and Sal I	0.9, 4.4

---

Table 3.1. Band sizes of plasmid DNA after digestion by different restriction enzymes.



### **3.3. Transient transfection of mammalian cells**

Cells were seeded in the plates and maintained in complete medium without antibiotic for 2 days. Cells were transfected at 80% to 90% confluency using Lipofectamine2000 reagent and Opti-Mem I reduced serum medium following manufacturer's instructions. Briefly, 0.8 µg DNA and 2 µl lipofectamine2000 reagent were each diluted in 25 µl Opti-Mem I medium. After 5 min, the solutions were combined to form a transfection cocktail and allowed to stand at room temperature for 20 min. After that, the correct DNA concentration was achieved by adding suitable volume of Opti-Mem I medium to the transfection cocktail. The resulting transfection cocktail was added to the cells in the culture dishes or culture plates which were then incubated at 37°C for 5 h before replacing the cocktail with complete medium without antibiotic. Cells were assayed 48 h post-transfection.

### **3.4. Development of stable cell lines**

#### **3.4.1. Determination of the optimum concentration of each antibiotic used in selection of clones**

Cells in 100 mm dish at 80 – 90% confluency were split at 1:50 or 1:300 dilutions, and seeded in 6-well plates. After 24 h, the cells were incubated with different concentrations of G418 (0, 200, 300, 400, 500, 600, 800 and 1 µg/ml) for one and a half weeks. The medium containing G418 was refreshed every 3 – 4 days. At last, the percentages of the surviving cells at each G418 concentration were estimated under microscope.

Cells were seeded in 24-well plate (300,000 cells per well). After 24 h, the cells were incubated with different concentrations of Zeocin (0, 100, 150, 200, 250, 300, 350, 400, 500, 600, 800 µg/ml) for one and a half weeks. The medium contained Zeocin was refreshed every 3 – 4 days. At last, the percentages of the surviving cells at each Zeocin concentration were estimated under microscope.

#### **3.4.2. Development of monoclonal stable cell line**

Two transfection methods were used in developing stable cell lines. The first one was that the cells were seeded in 100 mm dish and transfected with 0.25 µg/ml 2myc-hGHS-R1a plus 0.75 µg/ml pcDNA3.1(+) or 1 µg/ml 2myc-hGHS-R1b, as described in section 3.3.

The other method was that the cells were seeded in 6-well plates and transfected with



2 µg/ml either linearized or circular hGHS-R1a or hGHS-R1b using lipofectamine. Using lipofectamine transfection reagent, the procedures are similar to the use of lipofectamine2000. Basically, 2 µg DNA and 4 µl lipofectamine were diluted in 100 µl Opti-Mem I reduced serum medium separately. Then the two solutions were mixed together and incubated at room temperature for 30 min. At last, the transfection cocktail was made up to 1 ml by adding Opti-Mem I reduced serum medium and overlaid onto the cells. The cells were incubated at 37°C for 6 h and then the transfection cocktail was replaced by complete medium without antibiotic.

After 48 h post-transfection, the cells transfected in 100 mm dish were split at 1:8 or 1:50, and transferred to a new 100 mm dish. After 72 h post-transfection, the cells transfected with 2myc-hGHS-R1a in the 100 mm dish and 6-well plate were incubated with 600 µg/ml G418. The cells transfected with 2myc-hGHS-R1b were incubated with 300 µg/ml Zeocin. The medium was refreshed every 3 – 4 days, and the antibiotic selection was last for two and a half weeks, until no more cells died. The remaining surviving cells were called polyclonal stable cell line.

After antibiotic selection, surviving cells were transferred to 96-well plate at a cell density of 1 cell per well. After 2 weeks, single colonies were selected and each colony was transferred to a well in the 12-well plate. When the cells grew to 90% confluency in 12-well plate, cells were transferred to 6-well plate. At last, the cells grew in 100 mm dish. Besides using 96-well plate to select single colonies, clonal ring is another technique that was used to select single colonies. In this method, after antibiotic selection, surviving cells were seeded in 100 mm dish at different cell



numbers (10, 20, 30, 50, 100 cells per dish). After one week, delineated single colony border by drawing a circle on the bottom of the culture dish around each colony. Then the medium was aspirated from the dish and a clonal ring (the top of the pipette tip) with silicon grease at the bottom was placed onto the dish, in order to surrounding an individual clone. Single colony inside the clonal ring was detached by adding 100  $\mu$ l complete medium and pipetting up and down. The single colony was transferred to 96-well plate for growth.

#### **3.4.3. Confirmation the expression of 2myc-hGHS-R1a and 2myc-hGHS-R1b**

To check the expression of 2myc-hGHS-R1a and 2myc-hGHS-R1b in the monoclonal stable cell lines, [ $^3$ H]-inositol phosphates assay and RT-PCR were carried out respectively, as described in sections 3.5 and 3.7.

## 3.5. Measurement of phospholipase C activity

### 3.5.1. Introduction

Activation of a G<sub>q</sub>-coupled receptor results in the stimulation of phospholipase C (PLC). The activity of PLC leads to the formation of inositol 1,4,5-trisphosphate (IP<sub>3</sub>) and diacylglycerol (DAG). IP<sub>3</sub> can be further metabolized to a variety of inositol bis- and monophosphates. IP degradation is inhibited by the presence of lithium chloride (LiCl). Therefore, the accumulation of [<sup>3</sup>H]-inositol phosphates was measured in this assay by inclusion of LiCl.

### 3.5.2. Preparation of columns

Dowex resin (Bio-Rad AG 1 – X8) was washed twice with distilled water. Resin suspension was transferred to each polyprep column (Bio-Rad), until there was approximately 1 ml resin packed in each polyprep column.

### 3.5.3. [<sup>3</sup>H]-inositol phosphate assay

Cells were transfected as described in section 3.3, in 12-well plates coated with 50 µg/ml poly-D-lysine (300 µl per well), using 300 µl transfection cocktail per well. After 24 h post-transfection, cells were labeled with 2 µCi/ml *myo*-[<sup>3</sup>H]-inositol at 37°C overnight. The medium was then aspirated and the cells were washed twice with 1 ml HBS buffer to remove the free *myo*-[<sup>3</sup>H]-inositol. Then the cells were incubated in 1 ml assay buffer containing 20 mM LiCl for 10 min at 37°C. The assay buffer was replaced by another 1 ml assay buffer and 10 µl tested compound, and then incubated for 1 h at 37°C. The reactions were terminated by aspiration of assay buffer and the addition of 750 µl ice-cold 20 mM formic acid solution. Cells samples



were kept at 4°C for at least 1 h before processing.

#### 3.5.4. Measurement of [<sup>3</sup>H]-inositol phosphates production

[<sup>3</sup>H]-inositol phosphates were separated from total [<sup>3</sup>H]-inositol by column chromatography using dowex resin. Before loading the cells lysates onto the dowex columns, the columns were washed with 5 ml 2 M ammonium formate/0.1 M formic acid, 2 ml of distilled water and then 2 ml 0.05% ammonia solution. The washed dowex columns were positioned on the top of a set of scintillation vials, then each cell lysate was loaded onto the column, followed by the immediate addition of 3 ml ammonia solution. The fraction collected in the vials contained [<sup>3</sup>H]-inositol and was mixed with 7.5 ml scintillant (Optiphase Hisafe-3). The columns were then placed over a waste container and washed with 4 ml 40 mM ammonium formate/0.1 M formic acid. Next, the washed columns were positioned on the top of another set of scintillation vials, and 5 ml 2 M ammonium formate/0.1 M formic acid was added to each column. The fraction collected in the vial is [<sup>3</sup>H]-inositol phosphates, which were then mixed with 10 ml scintillant. Blank samples (i.e. no cells) were processed in parallel to the test cells samples, in order to determine the background count for the columns; these values were subtracted from all the test values. All the samples in the vials were counted in a liquid scintillation counter (Packard LS2900TR).

#### 3.5.5. Data analysis

Assays were performed in duplicate or triplicate. [<sup>3</sup>H]-inositol phosphates production is expressed as  $(IP/[INOS+IP]) \times 100$ , where IP is inositol phosphates and INOS is inositol.



### **3.6. Determination of transient transfection efficiency**

Cells were transfected with enhanced green fluorescence protein plasmid (pEGFP) in 24-well plates as described in section 3.3, using 200  $\mu$ l transfection cocktail per well. After 48 h post-transfection, the medium was aspirated and the cells in each well were washed with 1 ml HBS. Then another 1 ml HBS was added to each well. Cells were observed under fluorescent microscope and the images of the cells were captured. If cells express EGFP, they glow in green colour under fluorescent microscope, as the fluorescent microscope excite the EGFP at 488 nm and then EGFP will have emission at 510 nm. By estimating the percentage of the fluorescent cells per field, the transfection efficiency can be estimated. The fluorescence of the same batch of cells was quantified and also counted by a counter (Victor-2 multilabel counter).

### **3.7. Reverse-transcription polymerase chain reaction (RT-PCR)**

#### **3.7.1. RNA extraction and first strand cDNA production**

Cells were transfected in 6-well plates as described in section 3.3, using 600  $\mu$ l transfection cocktail per well. After 48 h post-transfection, total RNA from the cells were extracted by TRIzol reagent, following manufacturer's instructions. Three  $\mu$ g of the extracted total RNA was used to make the first-strand cDNA, using SuperScript<sup>TM</sup> II reverse transcriptase and oligo-dT<sub>12-18</sub> as primer. All the procedures followed "SuperScript<sup>TM</sup> First-Strand Synthesis System" manufacturer's instructions.

#### **3.7.2. PCR and visualization of amplicons**

PCR was carried out in 50  $\mu$ l volume containing 1 - 1.5 mM MgCl<sub>2</sub>, 200  $\mu$ M dNTP, 200 - 400 nM primers, 2.5 U Taq polymerase, and 150 ng first-strand cDNA. Using the primers listed in table 3.2 to amplify part of the hGHS-R1a, hGHS-R1b, 2myc-hGHS-R1b, sbGHS-R1a and sbGHS-R1b. The places where the primers bind to are illustrated in figure 3.1 to figure 3.4. After an initial denaturation at 94°C 5 min, the PCR for GHS-Rs except the 2myc-hGHS-R1b, were performed at 94°C for 45 sec, 55°C for 45 sec and 72°C 1.5 min. The PCR for 2myc-hGHS-R1b was performed at 94°C for 45 sec, 59°C for 1 min and 72°C 1 min. At the end of each PCR cycle, there was an elongation step performed at 72°C for 10 min. The PCR cycle number used is 25. Amplification of cellular hGADPH was carried out in parallel as an internal positive control.

The PCR products were loaded and resolved in 1% agarose gel at 110V for 45 min.

The gel was then stained in ethidium bromide (EtBr) solution for about 15 min and the EtBr stained PCR products were visualized by UV exposure and the bands were photographed. DNA ladder (1kb) was used as a marker.



Gene Name	Primer	PCR product size (bps)
hGHS-R1a	Forward: <b>TAT AGA ATT</b> CAT GTG GAA CGC GAC GCC CAG Reverse: CAC CAC TAC AGC CAG CAT TTT C	806
hGHS-R1b	Forward: <b>TAT AGA ATT</b> CAT GTG GAA CGC GAC GCC CAG Reverse: GCT GAG ACC CAC CCA GCA	807
2myc-hGHS-R1b	Forward: CAC AAA GAT TAT GGA GCA GAA G Reverse: TCA GAG AGA AGG GAG AAG GCA CA	983
sbGHS-R1a	Forward: <b>CAC AGT CGA</b> CAT GCC CTC TTG GCC AAA T Reverse: <b>CAC ATC TAG ATT</b> AGA AGC TGA TTG TGGA	1200
sbGHS-R1b	Forward: <b>CAC AGT CGA</b> CAT GCC CTC TTG GCC AAA T Reverse: CAC ATC TAG ACT ACA TGG ATA AAG TTA TG	900

Table 3.2 Primers for PCR and the PCR product size. The bolded sequences are for the restriction enzyme sites.

```

atgtggaacg cgacgcccag cgaagagccg gggttcaacc tcacactggc cgacctggac
tgggatgctt cccccggcaa cgactcgctg ggcgacgagc tgctgcagct cttccccgcg
ccgctgctgg cgggcgtcac agccacctgc gtggcactct tcgtgggtggg tategctggc
aacctgctca ccatgctggg ggtgtcgcgc ttcgcgagc tgcgcaccac caccaacctc
tacctgtcca gcatggcctt ctccgatctg ctcatcttcc tctgcatgcc cctggacctc
gttcgcctct ggcagtaccg gccctggaac ttcggcgacc tcctctgcaa actcttccaa
ttcgtcagtg agagctgcac ctacgccacg gtgctcacca tcacagcgct gagcgtcgag
cgctacttcg ccatctgctt cccactccgg gccaaaggtgg tggtcaccaa ggggcgggtg
aagctggtca tcttcgtcat ctgggccgtg gccttctgca gcgccgggcc catcttcgtg
ctagtcgggg tggagcacga gaacggcacc gacccttggg acaccaacga gtgccgcccc
accgagtttg cgggtgcgctc tggactgctc acggtcatgg tgtgggtgtc cagcatcttc
ttcttccttc ctgtcttctg tctcacggtc ctctacagtc tcateggcag gaagctgtgg
cggaggaggc gcggcgatgc tgtcgtgggt gcctcgctca gggaccagaa ccacaagcaa
accgtgaaaa tgctggctgt agtgggtgtt gccttcatcc tctgctggct ccccttccac
gtagggcgat atttatcttc caaatcttt gagcctggct ccttggagat tgctcagatc
agccagtact gcaacctcgt gtcctttgtc ctcttctacc tcagtgtctgc catcaacccc
attctgtaca acatcatgtc caagaagtac cgggtggcag tgttcagact tctgggatc
gaacccttct cccagagaaa gctctccact ctgaaagatg aaagtctctg ggcctggaca
gaatctagta ttaatacatg a

```

Figure 3.1. Coding sequence for hGHS-R1a (1101 bps, genebank no:NM198407).

Key: Arrows above the coding sequence are the position of primers for amplification of 806 bps PCR product.



atgtggaacg cgacgcccag cgaagagccg gggttcaacc tcacactggc cgacctggac  
 tgggatgctt cccccggcaa cgactcgctg ggcgacgagc tgctgcagct cttccccgag  
 ccgctgctgg cgggcgtcac agccacctgc gtggcactct tctgtggtggg tatcgctggc  
 aacctgctca ccatgctggt ggtgtcgcgc ttccgcgagc tgcgcaccac caccaacctc  
 tacctgtcca gcatggcctt ctccgatctg ctcatcttcc tctgcatgcc cctggacctc  
 gttcgcctct ggagctaccg gccctggaac ttccggcgacc tctctgcaa actcttccaa  
 ttctgcagtg agagctgcac ctacgccacg gtgctcacca tcacagcgtg gagcgtcgag  
 cgctacttgc ccatctgctt cccactccgg gcccaaggtgg tggtcaccaa ggggagggtg  
 aagctggtca tcttcgtcat ctgggccgtg gccttctgca gcgccggggc catcttcgtg  
 ctatgcgggg tggagcacga gaacggcacc gacccttggg acaccaacga gtgccgcccc  
 accgagtttg cgggtgcgctc tggactgctc acggtcatgg tgtgggtgtc cagcatcttc  
 ttcttcttc ctgtcttctg tctcacggtc ctctacagtc tcatcggcag gaagctgtgg  
 cggaggaggc gcggcgatgc tgtcgtgggt gcctcgtc ggaaccagaa ccacaagcaa  
 accgtgaaaa tgctgggtgg gtctcagcgc gcgctcaggc ttctctcgc gggtcctatc  
 ctctccctgt gccttctccc ttctctctga

Figure 3.2. Coding sequence for hGHS-R1b (870 bps, genebank no:NM004122) Key:  
 Arrows (▶) above the coding sequence are the position of primers for amplification  
 of 807 bps hGHS-R1b PCR product. Arrow (---▶) above the coding sequence is the  
 position of reverse primer for amplification of 943 bps 2myc-hGHS-R1b PCR  
 product, the position of the forward primer has not been shown, because the forward  
 primer bind to the 2myc sequence.





tgc 
  
 cctcttggcc aaatctctcg gaggcctct cccttaactg cagctgggag gagaccgca
   
 acgccacaag gaagtttgat ctggcctgc ctctctcaa ctactactca atccctcttc
   
 ttacaggcat caccatcgcc tgcacgctgc tgtttctggt cggggtggcc ggtaatgtca
   
 tgaccatfff ggtggtcagt aagtaccggg acatgcgcac aaccactaac ctttacctgt
   
 gcagcatggc agtatccgac ctgctcatct tcctctgtat gccgctggac ctctaccgta
   
 tgtggaggta caggccctgg cggtttgggg acgcgctctg caagctcttt cagttcgtgt
   
 cagagtcatg cacctactcc accatctca gcatcaccgc gctgtcagtg gagagatacc
   
 tagcgatctg tttcccgtg cgtgccaaag ctttggttac caaaaggcgg gtacgcgccc
   
 tcattcttct tctctggaca gtgtctctac tgagcgccgg tcccgtgttt gtcattggtgg
   
 gaggggagcg tgacagcatg tggccaggaa atctcagttg ggtgggaatg aatgggactg
   
 ggttcttccc ggaggaagga gacaccggg agtgtaaaat gaccattac gcagtggagt
   
 ccggcctgat gggggccatg gtgtggctga gctctgtgtt cttcttcatg ccggtgttct
   
 gtctcacagt gctctacagc ctcatcggtc ggcggctgtg gcaaagacac agagaaacga
   
 acataaactc ccgtgtggcg catcgggaga aaagcaacag acagaccatc aagatgttgg
   
 tgggtgggtg gttggccttt gtctgtgct ggctgccgtt tcatgtagga cgctacctgc
   
 agttccgttc tctggacgct ccattccccg tgcgtctctt gttgtccgag tactgcagct
   
 tagtgtctgt ggttctcttc tacctgagcg ccgcatcaa ccccatctc tacaacatca
   
 tgtctggaa ataccggggc gcagcggcgc gtctcttcgg cctgatcgac agccagccgc
   
 cccgaggccg cacagccagc accgtgaagg gagacggctc gaacggctgg acggaatcca 
  
 caatcagctt ctaa

Figure 3.3. Coding sequence for sbGHS-R1a (1157 bps, genebank no:AY151040)

Key: Arrows ( $\rightarrow$ ) above the coding sequence are the position of primers for amplification of 1200 bps sbGHS-R1a PCR product.

```

atgccctct
tggccaaatc tctcggagtg cctctccctt aactgcagct gggaggagac cgcgaacgcc
acaaggaagt ttgatcttgg cctgcctcct ctcaactact actcaatccc tcttcttaca
ggcatcacca tgcctgcac gctgctgttt ctggtcgggg tggccggtaa tgcatgacc
atfttggtgg tcagtaagta ccgggacatg cgcacaacca ctaaccttta cctgtgcagc
atggcagtat ccgacctgct catcttctc tgtatgccgc tggaccteta ccgtatgtgg
aggtacaggc cctggcggtt tggggacgcg ctctgcaagc tcttccagtt cgtgtcagag
tcatgcacct actccacat cctcagcacc accgcgctgt cagtggagag atacctagcg
atctgtttcc cgctgcgtgc caaagctttg gttaccaaaa ggcgggtacg cgcctcatt
cttcttctct ggacagtgtc tctactgagc gccggteccg tgtttgtcat ggtgggagtg
gagcgtgaca gcatgtggcc aggaaatctc agttgggtgg gaatgaatgg gactgggttc
tccccggagg aaggagacac ccgggagtgt aaaatgacct attacgcagt ggagtcgggc
ctgatggggg ccatggtgtg gctgagctct gtgttcttct tcatgccggt gttctgtctc
acagtgtctt acagcctcat cggtcggcgg ctgtggcaaa gacacagaga aacgaacata
aactcccgtg tggcgcacg ggagaaaagc aacagacaga ccatcaagat gttgggtaag
ttacgcaaat tacgcacacg cataacttta tccatgtag

```

Figure 3.4. Coding sequence for sbGHS-R1b (887 bps genebank no:AY151041) Key: Arrows (→) above the coding sequence are the position of primers for amplification of 900 bps sbGHS-R1b PCR product.



### 3.7.3. Real-time PCR

SYBR Green RT-PCR Kit was chosen to perform real-time PCR, one of the advantages that SYBR Green over TaqMan, is SYBR do not need a specific probe to detect the PCR product. However, SYBR Green binds to any double-strand DNA generated during PCR. Therefore, it is important to make sure there is only a single PCR product produced, without any primer-dimer or non-specific amplification.

After 48 h post-transfection, total RNA was extracted by TRIzol reagent and converted to first-strand cDNA as described in section 3.7.1. Then the cDNA was diluted by 1:5 with water and 2  $\mu$ l of the diluted cDNA was used to carry out real-time PCR following manufacturer's instruction. Real-time PCR was carried out in 25  $\mu$ l volume containing SYBR green PCR buffer, MgCl<sub>2</sub>, dNTP blend, AmpliTaq Gold, AmpErase UNG, primers, water and template (diluted cDNA). Using the primers listed in table 3.3 to amplify part of the sbGHS-R1a and sbGHS-R1b, the PCR amplification of the epitope-tagged sbGHS-R1a and sbGHS-R1b was used the same primer as the non-tagged sbGHS-R. Before the PCR cycle started, the PCR mixture was incubated at 50°C for 2 min and then 95°C for 10 min, in order to activate AmpliTaq Gold, and the PCR condition is 94°C for 45 sec, 64°C for 45 sec (40 cycles). At the end of PCR, a dissociation curve was constructed to make sure there is no primer dimer. For the dissociation curve, the PCR product was first melted at 95°C, and then equilibrated at 60°C before being slowly dissociated back to 95°C. In addition, the PCR product was loaded and resolved by 1% agarose gel. DNA ladder was used as a marker.



### 3.7.3.1. Construction of standard curve

Plasmid DNAs (sbGHS-R1a, sbGHS-R1b, HA-sbGHS-R1a and HA-sbGHS-R1b) was serial diluted into different concentrations (10 ng/μl, 100 pg/μl, and from 10 pg/μl to 100 ag/μl by 10 fold dilutions) and real-time PCR was performed as described in section 3.7.3.

### 3.7.3.2. Data analysis

To calculate the number of molecules in each dilution of plasmid DNA in the standard curve, the following equations were used and then the standard curve was plotted by Ct value against log of number of molecules of the plasmid DNA. Ct value is the threshold cycle, at which a significant increase in the PCR product was measured by the real-time PCR machine (Applied Biosystems).

Equation 1: Calculation of pmol of ends of a double-strand DNA (dsDNA) molecules  
$$[2 \times 10^6 \times \mu\text{g (of dsDNA)}] / (N_{\text{bp}} \times 660 \text{ Da})$$

Key :  $N_{\text{bp}}$  : number of base pairs

Equation 2: Conversion of the unit of equation 1 from pmol to number of molecules  
$$\text{pmol} \times 6.02 \times 10^{23} / (1 \times 10^9)$$

From the standard curve, the amount of messenger RNA (mRNA) in the unknown samples was found using the following equations.

Equation 3: Calculation of the log mRNA amount in samples

$$(Ct \text{ value} - b) / m$$

Keys:  $b$  = y-intercept of standard curve line

$m$  = slope of standard curve line

Equation 4: Calculate the amount of mRNA in sample

$$10^{(\log \text{ mRNA amount})}$$

Equation 5: Calculate the mRNA amount per  $\mu\text{g}$  of total RNA

Amount of mRNA / amount of total RNA used

---

Gene Name	Primer	PCR product size (bps)
sbGHS-R1a	Forward: GTG GGA ATG AAT GGG ACT GG Reverse: GCC AAC ACC ACC ACC ACC AAC	275
sbGHS-R1b	Forward: GTG GGA ATG AAT GGG ACT GG Reverse: GGA TAA AGT TAT GCG TGT GCG	189

---

Table 3.3 Primers for PCR and the PCR product size



tgc

cctcttggcc aaatctctcg gagtgcctct cccttaactg cagctgggag gagacccgca  
 acgccacaag gaagtttgat cttggcctgc ctctctcaa ctactactca atccctcttc  
 ttacaggcat caccatcgcc tgcacgctgc tgtttctggt cggggtggcc ggtaatgtca  
 tgaccatitt ggtggtcagt aagtaccggg acatgcgcac aaccactaac ctttacctgt  
 gcagcatggc agtatccgac ctgctcatct tcctctgtat gccgctggac ctctaccgta  
 tgtggaggta caggccctgg cggtttgggg acgcgctctg caagctcttt cagttcgtgt  
 cagagtcatg cacctactcc accatcctca gcatcaccgc gctgtcagtg gagagatacc  
 tagcgatctg tttcccgtg cgtgccaaag ctttggttac caaaaggcgg gtacgcgccc  
 tcattcttct tctctggaca gtgtctctac tgagcgccgg tcccgtgtt gtcatggtgg  
 gagtggagcg tgacagcatg tggccaggaa atctcagttg ggtgggaatg aatgggactg  
 ▶ggttcttccc ggaggaagga gacacccggg agtgtaaaat gaccattac gcagtggagt  
 ccggcctgat gggggccatg gtgtggctga gctctgtgtt ctcttcatg ccggtgttct  
 gtctcacagt gctctacagc ctcatcggtc ggcggtgtg gcaaagacac agagaaacga  
acataaactc ccgtgtggcg catcgggaga aaagcaacag acagaccatc aagatgttgg  
 tggtggtggt gttggccttt gtctgtgct ggctgccgtt tcatgtagga cgctacctgc  
 agttccgttc tctggacgct ccatccccgc tgctgtctct gttgtccgag tactgcagct  
 tagtgtctgt ggttctcttc tacctgagcg ccgcatcaa ccccatctc tacaacatca  
 tgtcttgaa ataccggggc gcagcggcgc gtctcttcgg cctgatcgac agccagccgc  
 cccgaggccg cacagccagc accgtgaagg gagacggctc gaacggctgg acggaatcca  
 caatcagctt ctaa

Figure 3.5. Coding sequence for sbGHS-R1a (1157 bps, genebank no:AY151040)

Key: Arrows (→) above the coding sequence are the position of primers for amplification of 275 bps sbGHS-R1a real-time PCR product.

```

atgccctct
tggccaaatc tctcggagtg cctctccctt aactgcagct gggaggagac ccgcaacgcc
acaaggaagt ttgatcttgg cctgcctcct ctcaactact actcaatccc tcttcttaca
ggcatcacca tcgcctgcac gctgctgttt ctggtcgggg tggccggtaa tgtcatgacc
atfttgggtg tcagtaagta ccgggacatg cgcacaacca ctaaccttta cctgtgcagc
atggcagtat ccgacctgct catcttcctc tgfatgccgc tggacctcta ccgtatgtgg
aggtacaggc cctggcgggtt tggggacgcg ctctgcaagc tctttcagtt cgtgtcagag
tcatgcacct actccaccat cctcagcadc accgcgctgt cagtggagag atacctagcg
atctgtttcc cgctgcgtgc caaagctttg gttaccaaaa ggcgggtacg cgcctcatt
cttcttctct ggacagtgtc tctactgagc gccgggtcccg tgtttgtcat ggtgggagtg
gagcgtgaca gcatgtggcc aggaaatctc agttgggtgg gaatgaatgg gactgggttc
tccccggagg aaggagacac ccgggagtgt aaaatgacc attacgcagt ggagtccggc
ctgatggggg ccatgggtgt gctgagctct gtgttcttct tcatgccggt gttctgtctc
acagtgtctt acagcctcat cggtcggcgg ctgtggcaaa gacacagaga aacgaacata
aactcccgtg tggcgcatcg ggagaaaagc aacagacaga ccatcaagat gttgggtaag
ttacgcaaat tacgcacacg cataacttta tccatgtag

```

Figure 3.6. Coding sequence for sbGHS-R1b (887 bps genebank no:AY151041) Key: Arrows ( $\rightarrow$ ) above the coding sequence are the position of primers for amplification of 189 bps sbGHS-R1b real-time PCR product.



## **3.8. Measurement of caspase-3 activity**

### **3.8.1. Determination of caspase-3 activity using colorimetric assay**

#### **3.8.1.1. Introduction**

In this colorimetric assay, a caspase-3 substrate, which is composed of the caspase-3 recognition cleavage site (DEVD) and a coloured compound *p*-nitroaniline (*p*NA), was used. If caspase-3 is activated, it will cleave the substrate within the DEVD sequences, and the *p*NA will be released. Then, by monitoring the *p*NA absorbance at 405 nm, the caspase-3 activity can be studied.

#### **3.8.1.2. Induction of apoptosis**

Cells were seeded in 6-well plates. If there was transfection carried out, the procedures were as described in section 3.3, using 600  $\mu$ l transfection cocktail per well. After 48 h post-transfection, medium was aspirated. One and a half ml complete medium without antibiotic and 15  $\mu$ l of an apoptotic inducer or solvent control (DMSO) were added to each well and incubated for different time periods at 37°C.

#### **3.8.1.3. Preparation of cell lysates**

At the end of each incubation time, the medium was removed and the cells were washed with 1 ml PBSA. Next, another 1 ml PBSA was used to collect the cells from 6-well plate to a 1.5 ml eppendorf by pipetting up and down. Cells were collected by centrifugation at 2000 rpm (about 530 x g) for 5 min using micro-centrifuge (eppendorf) at 4°C. The cell pellets were resuspended in 40  $\mu$ l ice-cold lysis buffer



and incubated on ice for 5 min. The cell suspensions were centrifuged at 10,000 x g for 10 min at 4°C, and the supernatant (i.e. cell lysate) was collected and stored at -70 °C for not more than one week.

#### **3.8.1.4. Quantification of caspase-3 activity by measuring pNA absorbance**

The protein content in cell lysates was determined by a colorimetric method using Micro BCA™ Protein Assay Kit. Cell lysates were diluted 100-fold using 0.9% NaCl. Then 150 µl of each diluted cell lysates and BSA standards (0, 1, 2.5, 5, 7.5, 10, 15, 20, 40, 200 µg/ml) were mixed with 150 µl of BCA working reagent, which contained 25 parts of MA, 24 parts of MB and 1 part of MC. The resulting mixtures were incubated at 37°C for 2 h in 96-well plate. The absorbances of the protein samples at 562 nm were recorded. Samples were assayed in duplicate and the corresponding mean was fitted into the BSA standard curve by linear regression to estimate the protein concentration.

Determination of the microtiter-plate reader conversion factor. 100 µl of assay buffer and 50 µM pNA were added to a 96-well microtiter plate separately. Then the corresponding absorbances at 405 nm were recorded in duplicate. The conversion factor (CF) was calculated as follows:

$$\text{CF} = 50 \mu\text{M} / (\text{average absorbance at 405 nm of } 50 \mu\text{M pNA} - \text{average absorbance at } 405 \text{ nm of assay buffer})$$

The caspase-3 activity was measured by the absorbance of pNA. Appropriate volume

of assay buffer was added to each well of the microtiter plate and incubated at 37°C for 10 min. Then cells lysate containing 10 – 30 µg protein were added to each well, and incubated for another 10 min at 37°C. Finally, 10 µl of 2 mM caspase-3 substrate I was added to give a total reaction volume of 100 µl. The absorbances at 405 nm were measured immediately. Data were recorded at 5 min intervals for 2 h. Background absorbance was the absorbance of the mixture of assay buffer and caspase-3 substrate I.

#### **3.8.1.5. Data analysis**

The slopes (Vmax) from the plot of absorbances at 405 nm versus time of each sample were determined. Then the caspase-3 activity was calculated as follows:

$$\text{Caspase-3 activity (pmol/min/}\mu\text{g protein)} = \{(\text{Vmax} \times \text{CF} \times 100) / 1000\} / ([\text{protein}] \times \text{vol})$$

Keys:

[protein]: Cell lysate protein concentration (µg/µl)

vol: Volume of cell lysate (µl)

### **3.8.2. Determination of caspase-3 activity using bioluminescence resonance energy transfer (BRET<sup>2</sup>) assay**

#### **3.8.2.1. Introduction**

BRET<sup>2</sup> assay makes use of the caspase-3 biosensor (pGFP<sup>2</sup>-DEVD-Rluc(h)) to monitor the caspase-3 activity in living cells, which uptake and co-express the target



receptor and the caspase-3 biosensor. Caspase-3 biosensor made up of three components: green fluorescent protein (GFP<sup>2</sup>), a caspase-3 recognition cleavage site (DEVD) and humanized *Renilla* luciferase (Rluc(h)). The intact caspase-3 biosensor produces a strong BRET<sup>2</sup> signal in the presence of the Rluc coelenterazine substrate, DeepBlueC. If there is caspase-3 activity, the caspase-3 biosensor will be cleaved within the DEVD sequences, and then the BRET<sup>2</sup> signal between Rluc and GFP<sup>2</sup> will be disrupted, and the BRET<sup>2</sup> signal will decrease.

### 3.8.2.2. Quantification of caspase-3 activity using BRET<sup>2</sup> assay

Cells were transfected with caspase-3 biosensor (pGFP<sup>2</sup>-DEVD-Rluc(h)) or positive control vector (pGFP<sup>2</sup>-Rluc(h)) together with the targeted plasmid DNA. Transfection procedures were as described in section 3.3. The non-transfected cells were used to measure the background BRET<sup>2</sup> signal.

After 24 hours post-transfection, medium was removed and the cells were rinsed once with PBSA. The cells were incubated with trypsin/EDTA for 3 - 5 min. When the cells were completely detached from the culture plate or culture dish, complete medium without antibiotic was added to the cells, in order to inactivate the trypsin. The cells were collected by centrifugation at 1000 rpm for 5 min at room temperature using bench-top centrifuge (Jouan C412). The cell pellets were resuspended with a suitable volume of complete medium without antibiotic. Cells were counted using a hemocytometer, as described in section 3.1.1. Then, a working dilution of 300,000 cells/ml was prepared and 100  $\mu$ l of this working dilution (i.e. 30,000 cells) was added to each well of a 96-well white CulturPlate.



After the cells were incubated in 96-well white CulturPlate for 24 h, medium was removed and the cells in each well were rinsed with 100  $\mu$ l DMEM medium without serum, glutamine and phenol red. Then, 100  $\mu$ l of DMEM medium without serum, glutamine and phenol red were added to each well. Fifty  $\mu$ l of an apoptotic inducer or DMSO was added to each well and the cells were incubated at 37°C for a period of time as indicated in each graph.

At the end of each incubation time, 50  $\mu$ l of 20  $\mu$ M DeepBlueC was added to each well, and the plate was immediately read on the Fusion™ Universal Microplate Analyzer using the following settings: one second per well, PMT: 1100 volts and gain: 50. The 410 nm/515 nm filter pairs were used.

### 3.8.2.3. Data analysis

Assays were performed in duplicate or triplicate. The average counts obtained with non-transfected cells were subtracted from the counts of the transfected cells in individual wells, in order to obtain the corrected counts at 410 nm (Rluc(h) emission) or 515 nm (GFP<sup>2</sup> emission). The BRET<sup>2</sup> signal was then determined as the ratio between the corrected counts at 515 nm and 410 nm. When subtraction of the background counts yields negative values, a BRET<sup>2</sup> ratio of zero is assigned. The equation as follows:

$$\text{BRET}^2 \text{ signal} = \frac{(\text{GFP}^2 \text{ emission at 515 nm} - \text{GFP}^2 \text{ emission of non-transfected cells})}{(\text{Rluc(h) emission at 410 nm} - \text{Rluc(h) emission of non-transfected cells})}$$

### **3.8.3. Determination of caspase-3 activity using fluorescence resonance energy transfer (FRET) assay**

#### **3.8.3.1. Introduction**

FRET assay is a technique similar to BRET<sup>2</sup> assay, as FRET assay also makes use of the energy transfer between two different types of GFP. FRET caspase-3 biosensor made up of three components: cyan fluorescent protein (CFP), a caspase-3 recognition cleavage site (DEVD) and yellow fluorescent protein (YFP) (Luo *et al.*, 2001b). In this assay, when the donor (CFP) is excited, there is an energy transfer from the CFP to the acceptor (YFP). If there is activated caspase-3, then the caspase-3 will cleave the DEVD site, and then the energy transfer will be disrupted.

#### **3.8.3.2. Quantification of caspase-3 activity using FRET assay**

Cells were transfected with FRET caspase-3 biosensor (pCFP-DEVD-YFP) together with the target plasmid DNA. Transfection procedures were as described in section 3.3. The non-transfected cells were used to measure the background FRET signal.

After 24 h post-transfection, the cells were transferred into 96-well white CulturPlate, and incubated for another 24 h. Then the cells were incubated with apoptotic inducer or DMSO at 37°C for different period of time as described in section 3.8.2.2. At the end of the incubation, the cells in the plate were read on the Fusion<sup>TM</sup> Universal Microplate Analyzer using the following settings: one second per well, PMT: 1100 volts and gain: 50. The excitation filter is 440 nm, and the emission filter is 485 nm and 535 nm for CFP and YFP, respectively.

### 3.8.3.3. Data analysis

Assays were performed in duplicates. The calculations are similar to BRET<sup>2</sup> assay, the equation as follows:

FRET signal (YFP/CFP ratio) = (YFP emission at 526 nm - YFP emission of non-transfected cells) / (CFP emission at 480 nm - CFP emission of non-transfected cells)



## Chapter 4

### Results

In the following experiments, the cells were usually transfected with 0.25  $\mu\text{g/ml}$  target plasmid DNA plus 0.75  $\mu\text{g/ml}$  empty vector, as it gave an optimal basal and agonist-stimulated [ $^3\text{H}$ ]-IP production, as showed in figure 4.8. The epitope-tagged receptors were used, as through the epitope-tag, the receptor expression level can be quantified in protein level.

### 4.1 Characterization of GHS-R

#### 4.1.1 Properties of GHS-R1a

##### 4.1.1.1 Constitutively active receptor

hGHS-R1a has been demonstrated having a constitutive activity, when hGHS-R1a was transiently transfected in COS-7 cells (Holst *et al.*, 2004). To further examine the constitutive activity of hGHS-R1a and sbGHS-R1a, different concentrations of GHS-R1a plasmid DNA were transfected into HEK293 cells. After 48 hours post-transfection, [ $^3\text{H}$ ]-inositol phosphate ([ $^3\text{H}$ ]-IP) productions were measured as described in Chapter 3. If hGHS-R1a and sbGHS-R1a are constitutively active receptors, then in the absence of GHS-R agonists, there should still be an increase in [ $^3\text{H}$ ]-IP production with increasing concentration of DNA transfection. From figure 4.1, concentration-dependent increase in receptor expression was observed in basal [ $^3\text{H}$ ]-IP production in both hGHS-R1a and sbGHS-R1a. It implies that GHS-R1a of both species are constitutively active receptors, and this property will not be affected

by the epitope-tag.

Using SPa can also show hGHS-R1a is a constitutively active receptor. SPa has been shown to act as an inverse agonist of hGHS-R1a receptor in COS-7 cells with  $IC_{50}$  value of  $5.2 \pm 0.7$  nM (Holst *et al.*, 2003). In our study, HEK293 cells were transfected with 0.25  $\mu$ g/ml hGHS-R1a/2myc-hGHS-R1a/HA-hGHS-R1a plasmid DNA plus 0.75  $\mu$ g/ml empty vector, named pcDNA3.1(+). After 48 hours, the cells were incubated with 1  $\mu$ M SPa alone or together with different concentrations of ghrelin. If hGHS-R1a is a constitutively active receptor, in the presence of SPa, the basal activity will be decreased. From figure 4.2, the basal [ $^3$ H]-IP production among the non-tagged and epitope-tagged hGHS-R1a receptors were inhibited by incubation with SPa. There were  $86.53 \pm 0.98$ ,  $84.84 \pm 0.84$ ,  $85.27 \pm 1.04\%$  inhibition,  $n=3$ , in HEK293 cells transfected with hGHS-R1a, 2myc-hGHS-R1a or 3HA-hGHS-R1a, respectively. It showed epitope-tag did not affect hGHS-R1a constitutively active property. SPa not only affects GHS-R1a basal activity, but also the agonist-stimulated response. From figure 4.3, co-administration of ghrelin and SPa, the ghrelin-stimulated [ $^3$ H]-IP production was reduced, but the dose-response curve neither shift to the right nor left, it indicated that SPa acts as an inverse agonist of GHS-R1a.

#### 4.1.1.2 Characterization of epitope-tagged hGHS-R1a

hGHS-R1a transiently transfected in COS-7 cells showed an  $EC_{50}$  for ghrelin of  $0.19 \pm 0.06$  nM (Holst *et al.*, 2003). To show that hGHS-R1a transiently transfected in



HEK293 cells has a similar  $EC_{50}$  for ghrelin and to observe whether the epitope-tags (myc, HA) on the hGHS-R1a affect the affinity of hGHS-R1a for ghrelin, the following experiment was performed. HEK293 cells were transiently transfected with 0.25  $\mu\text{g}/\text{ml}$  hGHS-R1a/2myc-hGHS-R1a/3HA-hGHS-R1a plus 0.75  $\mu\text{g}/\text{ml}$  pcDNA3.1(+) and then the transfected cells were incubated with different concentrations of ghrelin and [ $^3\text{H}$ ]-IP production was measured as described in Chapter 3. From figure 4.4, the cells transfected with hGHS-R1a, 2myc-hGHS-R1a and 3HA-hGHS-R1a, the  $EC_{50}$  for ghrelin is  $0.56 \pm 0.04$  nM,  $0.85 \pm 0.50$  nM and  $1.34 \pm 0.36$  nM,  $n=3$ , respectively. It indicated that the potency of hGHS-R1a in our system is very similar to Holst et al, (2003). Among the hGHS-R1a, 2myc-hGHS-R1a and HA-hGHS-R1a, the  $EC_{50}$  were not statistical significantly different, indicating that the epitope-tag did not affect hGHS-R1a. In addition, the position of 3HA-hGHS-R1a log concentration-response curve is lower than that of hGHS-R1a and 2myc-hGHS-R1a, suggesting that the expression level of 3HA-hGHS-R1a is less than the other types of hGHS-R1a or 3HA-hGHS-R1a has lower constitutive activity.

Human and seabream GHS-R1a can respond to agonists in order to increase IP production. HEK293 cells stably expressed sbGHS-R1a showed a log concentration-dependent increase in GHRP-6-stimulated [ $^3\text{H}$ ]-IP production (Chan *et al.*, 2004b). From figure 4.5, in HEK293 cells transiently transfected with 1  $\mu\text{g}/\text{ml}$  hGHS-R1a or sbGHS-R1a and then incubated with 30  $\mu\text{M}$  GHRP-6, there was an increase in GHRP-6-stimulated [ $^3\text{H}$ ]-IP production. HEK293 cells transfected with 1



$\mu\text{g/ml}$  pcDNA3.1(+) was used to show the increase in the [ $^3\text{H}$ ]-IP production is due to the presence of GHS-R1a.

#### 4.1.2 Properties of GHS-R1b

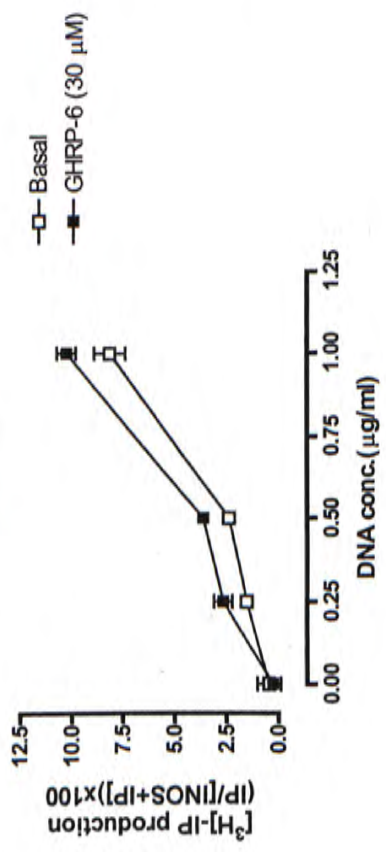
To determine whether hGHS-R1b responds to GHS-R agonists or not, HEK293 cells were transfected with 0.25  $\mu\text{g/ml}$  hGHS-R1b plasmid DNA plus 0.75  $\mu\text{g/ml}$  pcDNA3.1(+). Then the cells were incubated with agonist and the [ $^3\text{H}$ ]-IP production was measured. The basal and the agonist-stimulated [ $^3\text{H}$ ]-IP production in the cells transfected with hGHS-R1b were the same as the cells transfected with pcDNA3.1(+) (Fig. 4.6). It indicated that hGHS-R1b is not a constitutively active receptor and is unresponsive to agonists, under the assumption that hGHS-R1b is a  $G_q$ -coupled receptor. The epitope-tag did not alter hGHS-R1b property (Fig. 4.7).

#### 4.1.3 Conclusions

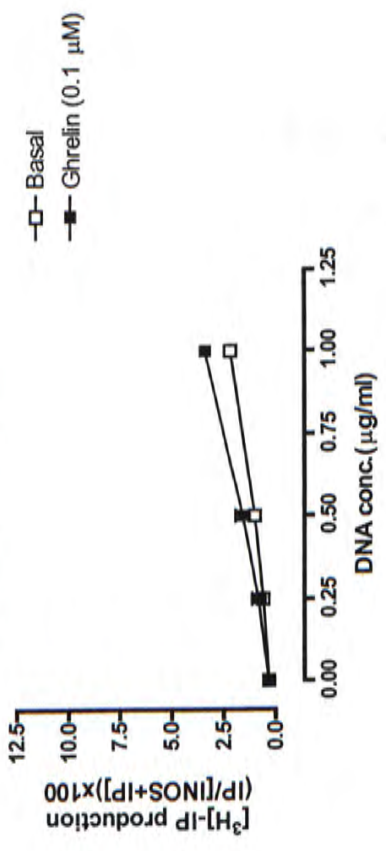
In HEK293 cells transiently transfected with different concentrations of hGHS-R1a or sbGHS-R1a, there was an increase in the basal [ $^3\text{H}$ ]-IP production, and there was an increase in GHRP-6 or ghrelin-stimulated [ $^3\text{H}$ ]-IP production. This shows that hGHS-R1a and sbGHS-R1a are constitutively active and responsive to agonists. The inverse agonist, SPa, inhibited the basal [ $^3\text{H}$ ]-IP production of hGHS-R1a and affected the ghrelin-stimulated [ $^3\text{H}$ ]-IP production, but without shifting the dose-response curve of ghrelin to the right. These data also indicated that hGHS-R1a is a constitutively active receptor. In HEK293 cells transfected with hGHS-R1b, there were no changes in the basal and the agonist-stimulated [ $^3\text{H}$ ]-IP production.

There was a similar  $EC_{50}$  among hGHS-R1a, 2myc-hGHS-R1a and HA-hGHS-R1a, indicating that the epitope-tags did not affect hGHS-R1a signaling. Also, the property of hGHS-R1b was not altered by the epitope-tag

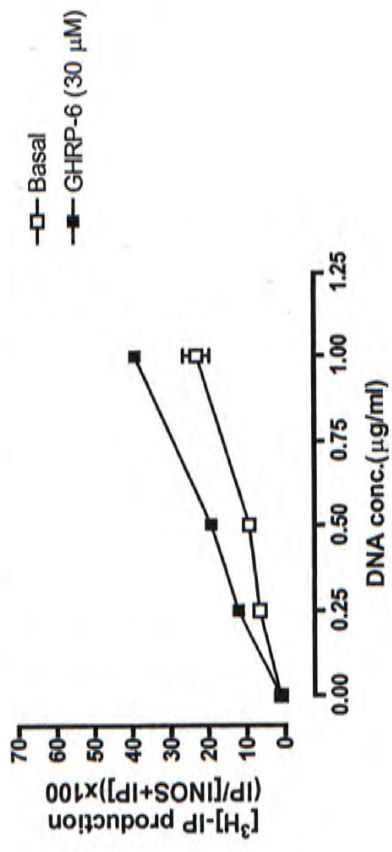
(A) hGHS-R1a



(B) 2myc-hGHS-R1a



(C) sbGHS-R1a



(D) HA-sbGHS-R1a

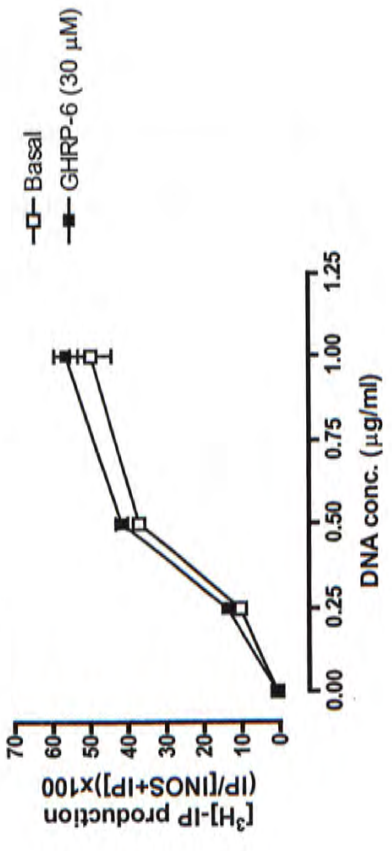




Figure 4.1 Basal and agonist-stimulated [<sup>3</sup>H]-IP production in HEK293 cells transiently transfected with different concentrations of GHS-R1a. (A) hGHS-R1a, (B) 2myc-hGHS-R1a, (C) sbGHS-R1a, and (D) HA-sbGHS-R1a. After 24 h post-transfection, the cells were labeled with 2  $\mu$ Ci/ml myo-[<sup>3</sup>H]-inositol and incubated overnight, and then [<sup>3</sup>H]-IP production was measured as described in Chapter 3. The cells were lysed following 1 h incubation with ghrelin or GHRP-6 or buffer. Results come from one experiment performed in duplicate, data shown are mean  $\pm$  S.D.

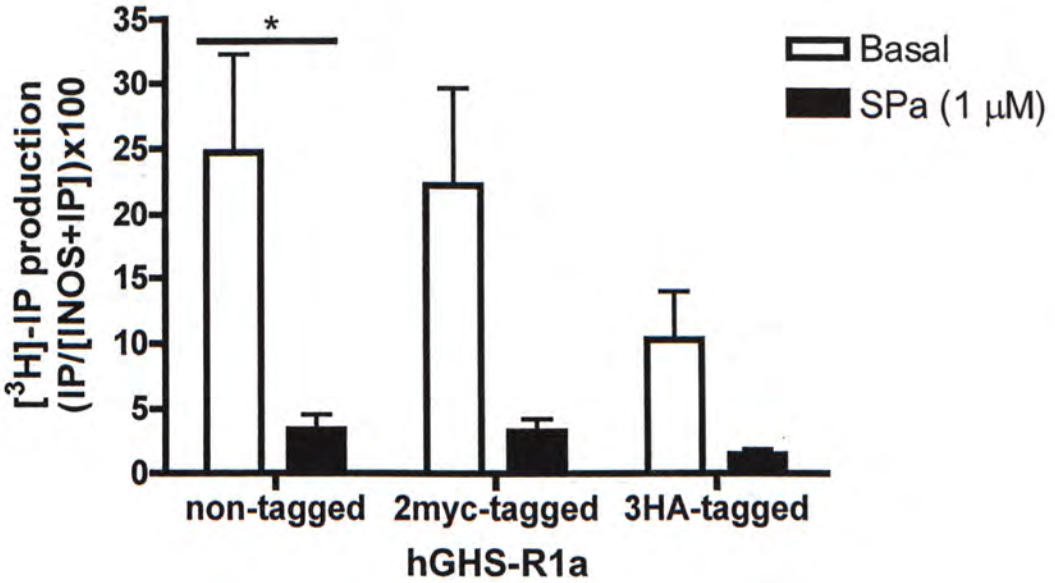


Figure 4.2 Effect of [D-Arg<sup>1</sup>,D-Phe<sup>5</sup>,D-Trp<sup>7,9</sup>,Leu<sup>11</sup>]-substance P (SPa) on the basal [<sup>3</sup>H]-IP production. HEK293 cells transiently transfected with 0.25 μg/ml hGHS-R1a/2myc-hGHS-R1a/3HA-hGHS-R1a plus 0.75 μg/ml pcDNA3.1(+). After 24 h post-transfection, the cells were labeled with 2 μCi/ml *myo*-[<sup>3</sup>H]-inositol and incubated overnight, and then [<sup>3</sup>H]-IP production was measured as described in Chapter 3. The cells were lysed following 1 h incubation with SPa or buffer. Results in figure represent mean ± S.E.M., n=3, of experiments performed in duplicate. (\* P<0.05, unpaired t-test)

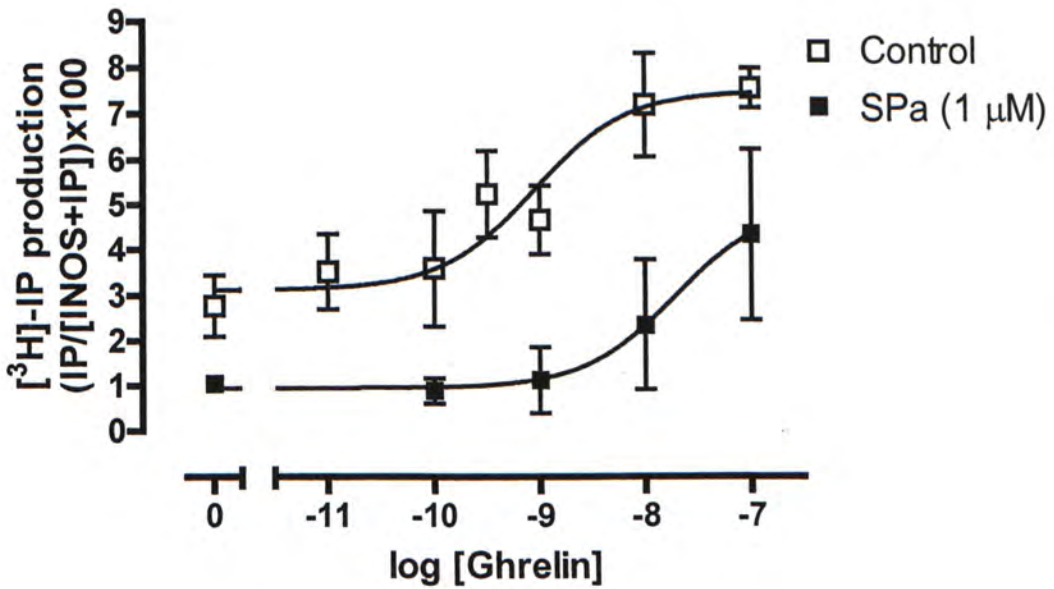


Figure 4.3 Effect of SPa on ghrelin-stimulated [ $^3\text{H}$ ]-IP production. HEK293 cells transfected with 0.25  $\mu\text{g}/\text{ml}$  hGHS-R1a plus 0.75  $\mu\text{g}/\text{ml}$  pcDNA3.1(+). After 24 h post-transfection, the cells were labeled with 2  $\mu\text{Ci}/\text{ml}$  *myo*-[ $^3\text{H}$ ]-inositol and incubated overnight, and then [ $^3\text{H}$ ]-IP production was measured as described in Chapter 3. The cells were lysed following 1 h incubation with ghrelin or together with SPa. Results come from one experiment performed in duplicate, data shown are mean  $\pm$  S.D.



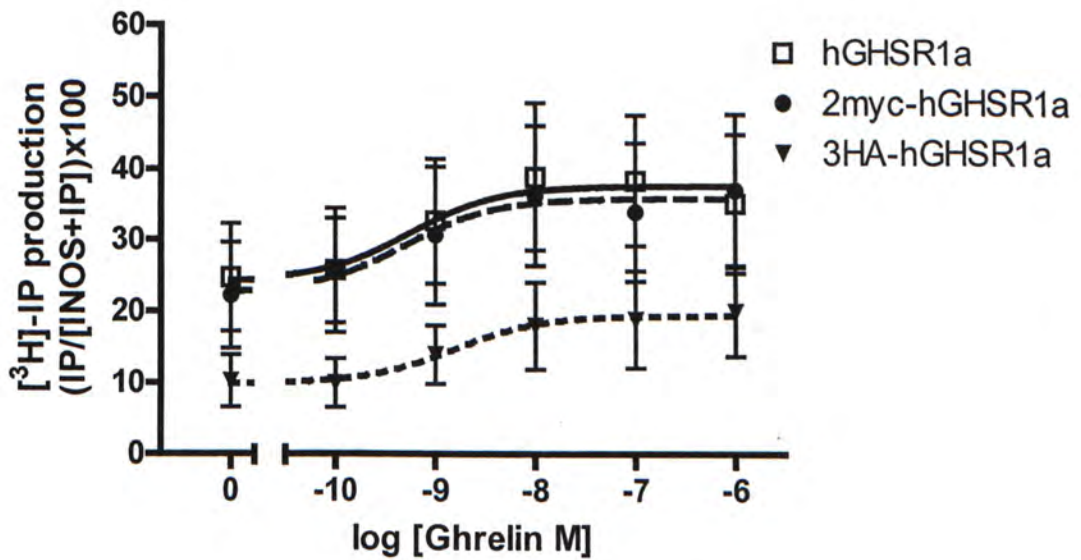


Figure 4.4 Characterization of epitope-tagged hGHS-R1a using ghrelin-stimulated  $[^3\text{H}]\text{-IP}$  production. HEK293 cells transiently transfected with 0.25  $\mu\text{g}/\text{ml}$  hGHS-R1a/2myc-hGHS-R1a/3HA-hGHS-R1a plus 0.75  $\mu\text{g}/\text{ml}$  pcDNA3.1(+). After 24 h post-transfection, the cells were labeled with 2  $\mu\text{Ci}/\text{ml}$  *myo*- $[^3\text{H}]\text{-inositol}$  and incubated overnight, and then  $[^3\text{H}]\text{-IP}$  production was measured as described in Chapter 3. The cells were lysed following 1 h incubation with ghrelin. Results in figure represent mean  $\pm$  S.E.M.,  $n=3$ , of experiments performed in duplicate.

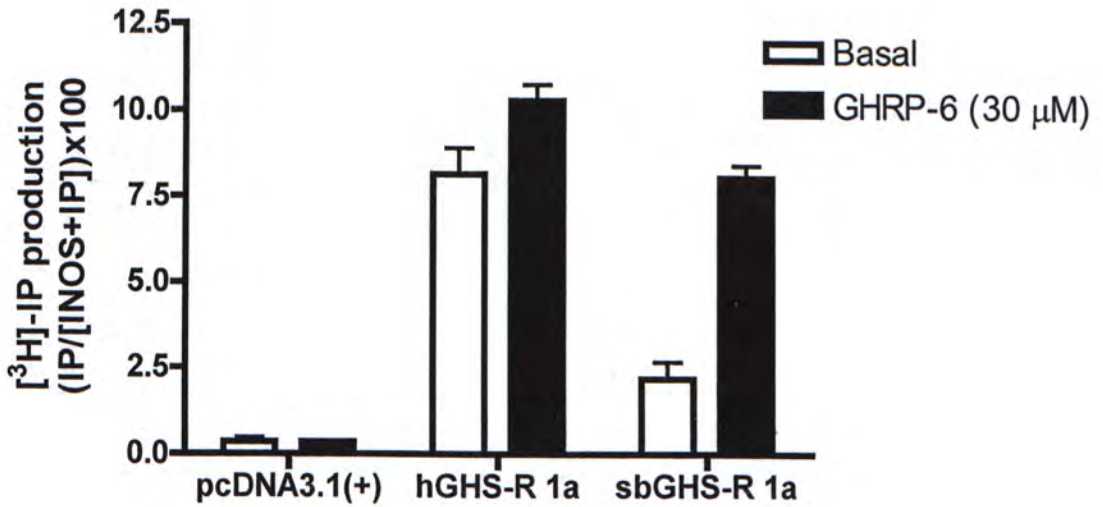


Figure 4.5 Comparison between hGHS-R1a and sbGHS-R1a on GHRP-6 stimulated [<sup>3</sup>H]-IP production. HEK293 cells transiently transfected with 1 μg/ml pcDNA3.1(+) as a control, or with 1 μg/ml hGHS-R1a or sbGHS-R1a. After 24 h post-transfection, the cells were labeled with 2 μCi/ml *myo*-[<sup>3</sup>H]-inositol and incubated overnight, and then [<sup>3</sup>H]-IP production was measured as described in Chapter 3. The cells were lysed following 1 h incubation with buffer or GHRP-6. Results come from one experiment performed in duplicate, data shown are mean ± S.D.

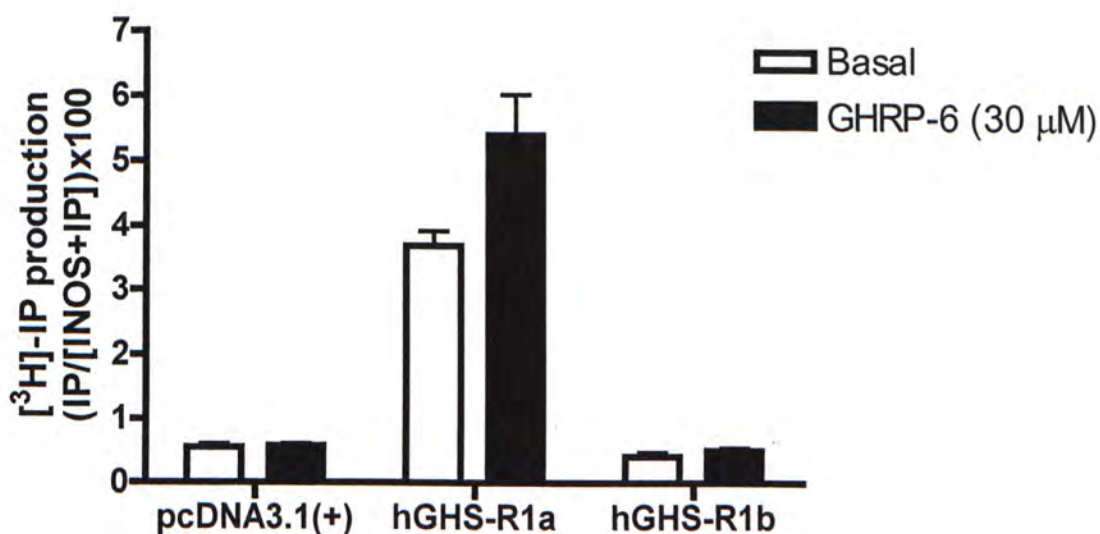


Figure 4.6 Comparison of hGHS-R1a and hGHS-R1b. HEK293 cells transiently transfected with 1 μg/ml pcDNA3.1(+) or 1 μg/ml hGHS-R1a was used as a negative and positive control, respectively. HEK293 cells were transiently transfected with 1 μg/ml hGHS-R1b were the test group. After 24 h post-transfection, the cells were labeled with 2 μCi/ml *myo*-[<sup>3</sup>H]-inositol and incubated overnight, and then [<sup>3</sup>H]-IP production was measured as described in Chapter 3. The cells were lysed following 1 h incubation with buffer or GHRP-6. Results come from one experiment performed in duplicate, data shown are mean ± S.D.



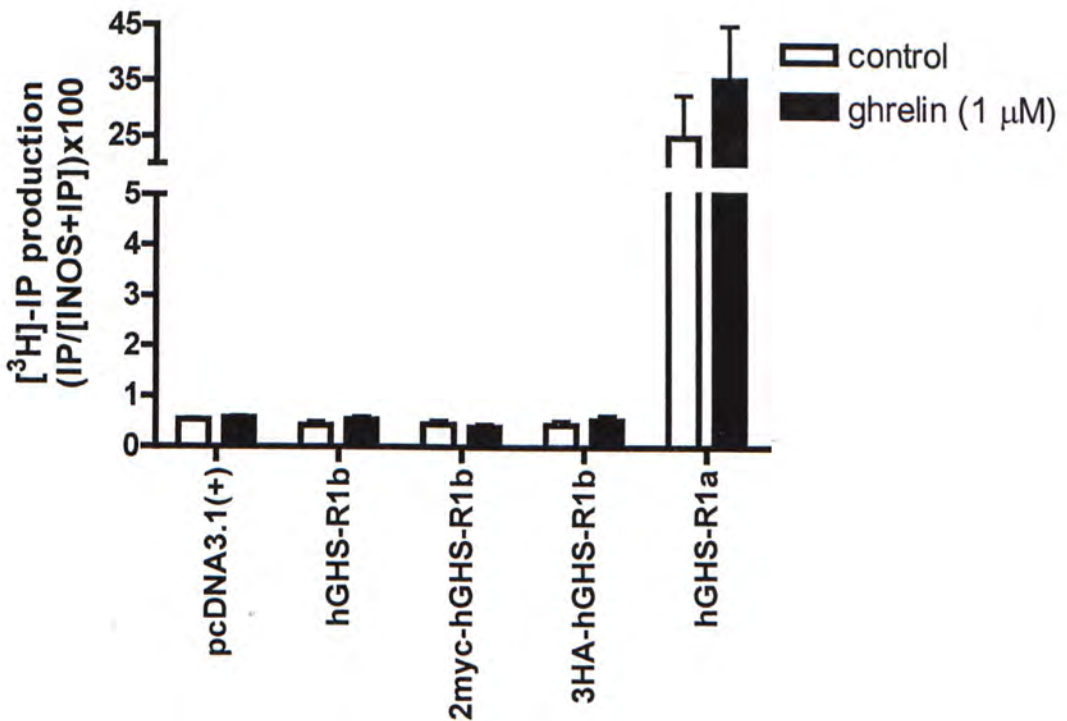


Figure 4.7 Characterization of epitope-tagged hGHS-R1b on the ability of the responsiveness to GHRP-6. HEK293 cells transiently transfected with 1  $\mu\text{g}/\text{ml}$  pcDNA3.1(+) or 1  $\mu\text{g}/\text{ml}$  hGHS-R1a was used as a negative and positive control, respectively. HEK293 cells were transiently transfected with 1  $\mu\text{g}/\text{ml}$  hGHS-R1b or epitope-tagged (2myc- or 3HA-) hGHS-R1b. After 24 h post-transfection, the cells were labeled with 2  $\mu\text{Ci}/\text{ml}$  *myo*- $^3\text{H}$ -inositol and incubated overnight, and then  $^3\text{H}$ -IP production was measured as described in Chapter 3. The cells were lysed following 1 h incubation with buffer or ghrelin. Results in figure represent mean  $\pm$  S.E.M.,  $n=3$ , of experiments performed in duplicate.

## 4.2 Effect of co-transfection of HEK293 cells

### 4.2.1 Effect of balancing DNA concentrations transfected into HEK293 cells

To investigate the interaction between GHS-R1a and GHS-R1b, one of the methods is to co-transfect GHS-R1a and GHS-R1b into HEK293 cells. Therefore, it is very important to look for artifactual results caused by the co-transfection of 2 different plasmids. To study the co-transfection effect, HEK293 cells were transfected with different concentrations of GHS-R1a plasmid DNA, and the total DNA concentration transfected was maintained at 1  $\mu\text{g}/\text{ml}$  by balancing with an empty vector.

For the cells transfected with hGHS-R1a or 2myc-hGHS-R1a alone, it showed a receptor concentration-dependent increase in both basal and agonist-stimulated [ $^3\text{H}$ ]-IP production, it also occurred in sbGHS-R1a and HA-sbGHS-R1a (Fig. 4.8). However, when the cells were co-transfected with hGHS-R1a or 2myc-hGHS-R1a and pcDNA3.1(+), then the effect of 0.25  $\mu\text{g}/\text{ml}$  and 0.5  $\mu\text{g}/\text{ml}$  hGHS-R1a or 2myc-hGHS-R1a in both basal and agonist-stimulated [ $^3\text{H}$ ]-IP production were greater than they were when transfected alone, and even greater than the effect of 1  $\mu\text{g}/\text{ml}$  hGHS-R1a or 2myc-hGHS-R1a (Fig. 4.8A and 4.8B). A similar effect was seen with HA-sbGHS-R1a. For example, in figure 4.8A, the basal [ $^3\text{H}$ ]-IP production for the cells transfected with 0.25  $\mu\text{g}/\text{ml}$  or 0.5  $\mu\text{g}/\text{ml}$  hGHS-R1a was 1.53 and 2.37, respectively, but when the cells co-transfected with 0.25  $\mu\text{g}/\text{ml}$  or 0.5  $\mu\text{g}/\text{ml}$  hGHS-R1a and pcDNA3.1(+) to 1  $\mu\text{g}/\text{ml}$ , the basal [ $^3\text{H}$ ]-IP production was 10.35 and 9.07, respectively. The 30  $\mu\text{M}$  GHRP-6-stimulated [ $^3\text{H}$ ]-IP production for the cells transfected with 0.25  $\mu\text{g}/\text{ml}$  or 0.5  $\mu\text{g}/\text{ml}$  hGHS-R1a was 2.65 and 3.62, respectively,



but when the cells co-transfected with 0.25  $\mu\text{g/ml}$  or 0.5  $\mu\text{g/ml}$  hGHS-R1a and pcDNA3.1(+) to 1  $\mu\text{g/ml}$ , the 30  $\mu\text{M}$  GHRP-6-stimulated [ $^3\text{H}$ ]-IP production was 19 and 21.2, respectively.

For the cells co-transfected with sbGHS-R1a and empty vector, the effect of 0.25  $\mu\text{g/ml}$  and 0.5  $\mu\text{g/ml}$  sbGHS-R1a in the 30  $\mu\text{M}$  GHRP-6 stimulated [ $^3\text{H}$ ]-IP production were greater than they were transfected alone, but they were not greater than 1  $\mu\text{g/ml}$  sbGHS-R1a. However, the basal [ $^3\text{H}$ ]-IP production was not affected by co-transfection (Fig. 4.8C). As the data variation at 0.5  $\mu\text{g/ml}$  was too large, so it needs more experiments to reach conclusion.

To determine whether the co-transfection potentiating effect on [ $^3\text{H}$ ]-IP production is specific to the additional empty vector, pcDNA3.1(+), HEK293 cells were co-transfected with 0.25  $\mu\text{g/ml}$  hGHS-R1a plasmid DNA plus 0.75  $\mu\text{g/ml}$  hGHS-R1b or a  $G_q$ -coupled receptor, human thromboxane  $A_2$  receptor (hTP $\alpha$ ). Then GHS-R agonist (1  $\mu\text{M}$  ghrelin) was used to stimulate the IP production through hGHS-R1a. When the cells were co-transfected with hGHS-R1a plus hGHS-R1b or hTP $\alpha$ , the 1  $\mu\text{M}$  ghrelin-stimulated [ $^3\text{H}$ ]-IP production was  $5.26 \pm 0.52$  and  $8.85 \pm 1.23$ ,  $n=2$ , respectively, which were greater than the cells transfected with hGHS-R1a alone ( $4.1 \pm 0.28$ ,  $n=2$ ) (Fig. 4.9). The cells co-transfected with hGHS-R1a plus hTP $\alpha$ , the basal [ $^3\text{H}$ ]-IP production was  $3.80 \pm 0.08$ ,  $n=2$ , which was slightly greater than the cells transfected with hGHS-R1a alone ( $2.73 \pm 0.04$ ,  $n=2$ ). However, the basal [ $^3\text{H}$ ]-IP production was not affected by co-transfecting hGHS-R1a with hGHS-R1b. All the



potentiating effects of the different addition plasmid DNA were smaller than the addition of empty vector.

In conclusion, there was a potentiating effect in both basal and agonist-stimulated [ $^3\text{H}$ ]-IP production, when HEK293 cells were co-transfected hGHSR-1a, 2myc-hGHS-R1a or HA-sbGHS-R1a with pcDNA3.1(+). This potentiation effect in sbGHS-R1a need more experiments to confirm. Also, this co-transfection potentiating effect was not specific for the additional empty vector, it also occur in the addition of other plasmid DNA, but the increase in the [ $^3\text{H}$ ]-IP production varies.

#### **4.2.2 Effect of balancing DNA concentration using another $G_q$ -coupled receptor**

To investigate the specificity of DNA concentration balancing effect in hGHS-R1a signaling, hTP $\alpha$  was used as a target receptor. Similar to hGHS-R1a, hTP $\alpha$  couples to  $G_q$  protein and leads to production of inositol phosphates and increase in intracellular calcium level (Foley *et al.*, 2001; Kinsella *et al.*, 1997). The experiment design was similar to that used to study the balancing effect in hGHS-R1a, just interchange the position of hGHS-R1a and hTP $\alpha$ , and using hTP $\alpha$  agonist, U46619. The cells co-transfected hTP $\alpha$  plus hGHS-R1b or hGHS-R1a, the U46619-stimulated [ $^3\text{H}$ ]-IP production was  $7.30 \pm 0.84$  and  $9.76 \pm 6.92$ ,  $n=2$ , respectively, which were greater than the cells transfected with hTP $\alpha$  alone ( $2.97 \pm 0.48$ ,  $n=2$ ) (Fig. 4.10). The basal [ $^3\text{H}$ ]-IP production was also increased when the cells were co-transfected with hTP $\alpha$  plus hGHS-R1a, it is due to the constitutive activity of hGHS-R1a, but not due to the

DNA concentration balancing effect in transfection. Taken together, the DNA concentration balancing effect in co-transfection was not specific to hGHS-R1a, but also occurred with another  $G_q$ -coupled receptor, hTP $\alpha$ .

### 4.2.3 Effect of $G_i$ - and $G_s$ -coupled receptor on GHS-R1a signaling

To determine if the variable potentiating effect of the balancing DNA concentration occurs using  $G_i$ - and  $G_s$ -coupled receptors, HEK293 cells were co-transfected with 0.25  $\mu\text{g/ml}$  hGHS-R1a plus 0.75  $\mu\text{g/ml}$   $G_i$ -coupled receptor,  $\mu$ -opioid receptor (MOR) or  $G_s$ -coupled receptor, mouse prostaglandin  $D_2$  receptor (mDP). Then the cells were incubated with buffer or 1  $\mu\text{M}$  ghrelin. For the cells co-transfected with hGHS-R1a mDP or MOR, both the basal and the ghrelin-stimulated [ $^3\text{H}$ ]-IP productions were greater than the cells transfected with hGHS-R1a alone (Fig. 4.11). The cells co-transfected with hGHS-R1a and mDP, the basal and ghrelin-stimulated [ $^3\text{H}$ ]-IP productions was 19.31 and 24.42, respectively, which were greater than the cells transfected with hGHS-R1a alone. The HEK293 cells co-transfected hGHS-R1a with MOR, the basal and ghrelin-stimulated [ $^3\text{H}$ ]-IP productions were 8.31 and 13.27, respectively, which were also greater than the cells transfected with hGHS-R1a alone. These data indicated that the co-transfection potentiating effect in [ $^3\text{H}$ ]-IP production was not only in response to  $G_q$ -coupled receptor, but also for  $G_i$ - and  $G_s$ -coupled receptors.

### 4.2.4 Potentiating effect of co-transfection appeared using different transfection reagents



The above experiments (section 4.2.1 to 4.2.3) used Lipofectamine2000 to carry out transient transfection of HEK293 cells. To determine the specificity of the DNA concentration balancing effect in transfection reagents, four different transfection reagents were used. The potentiating effect in co-transfection as also observed when different transfection reagents such as Lipofectamine, Lipofectamine2000, Fugene 6 and Genejuice were used. The GHRP-6-stimulated [ $^3\text{H}$ ]-IP production was greater in the cells co-transfected with hGHS-R1a plus pcDNA3.1(+) than the cells transfected with hGHS-R1a alone (Fig. 4.12), but using Fugene 6, the GHRP-6-stimulated [ $^3\text{H}$ ]-IP production was only slightly potentiated. The basal [ $^3\text{H}$ ]-IP productions were also potentiated, when Lipofectamine and Lipofectamine2000 were used, but not when using Fugene 6 or Genejuice. These data suggested that using different transfection reagents, the potentiating effect was also observed in agonist-stimulated [ $^3\text{H}$ ]-IP productions, but may not occur in the basal [ $^3\text{H}$ ]-IP production. It is unclear why some of the transfection reagents resulted in a potentiated basal [ $^3\text{H}$ ]-IP production but some of them did not.

#### 4.2.5 Co-transfection improves transfection efficiency

The transfection efficiency can be demonstrated using enhanced green fluorescent protein (EGFP) as a reporter gene (Zhang *et al.*, 1997). The transfection efficiency in HEK293 cells was quantified by EGFP expression using a counter (Victor-2 Multilabel) to measure the fluorescence intensity or fluorescence microscope to estimate the percentage of fluorescent cells (Jiang *et al.*, 2005). Using these techniques, the transfection efficiency difference between one type of plasmid DNA



transfection and co-transfection procedure was studied. HEK293 cells were transfected with 0.1  $\mu\text{g/ml}$  EGFP plasmid (pEGFP) DNA alone or plus other plasmid DNA, they were 0.25  $\mu\text{g/ml}$ , 0.5  $\mu\text{g/ml}$  and 1  $\mu\text{g/ml}$  2myc-hGHS-R1a alone or maintained the DNA concentration at 1  $\mu\text{g/ml}$  by balancing with pcDNA3.1(+). If the transfection efficiency increases, the fluorescent reading records from the counter (Victor-2 Multilabel) will increase, and under the fluorescent microscope, an increase in the number and the brightness of fluorescent cells will also be observed.

Transfection efficiency was not affected by transfecting different concentrations of 2myc-hGHS-R1a alone, as the fluorescence reading kept at around 9400 (Fig. 4.13). However, when co-transfecting 2myc-hGHS-R1a with pcDNA3.1(+) to a the final DNA concentration of 1.1  $\mu\text{g/ml}$ , the transfection efficiency of 0.25  $\mu\text{g/ml}$  and 0.5  $\mu\text{g/ml}$  2myc-hGHS-R1a were increased, as there were 2.02 and 1.58 fold-increase in the fluorescent readings, respectively. Also, reducing the amount of pcDNA3.1(+) used in maintaining the DNA concentration at 1.1  $\mu\text{g/ml}$ , the transfection efficiency also decreased. In addition, the HEK293 cells transfected with 0.1  $\mu\text{g/ml}$  pEGFP plus 1  $\mu\text{g/ml}$  pcDNA3.1(+), the fluorescent reading was higher than the HEK293 cells transfected with 0.1  $\mu\text{g/ml}$  pEGFP plus 1  $\mu\text{g/ml}$  2myc-hGHS-R1a. These observations indicated that the presence of the pcDNA3.1(+) increase the transfection efficiency in HEK293 cells. Under the fluorescence microscope, this phenomenon was also observed (Fig. 4.14).

#### 4.2.6 Conclusions

In conclusion, there was a potentiating effect in both basal and agonist-stimulated [ $^3\text{H}$ ]-IP production, when HEK293 cells were co-transfected hGHS-R-1a, 2myc-hGHS-R1a or HA-sbGHS-R1a with pcDNA3.1(+). It indicated that this potentiating effect was not affected by the epitope-tag. This potentiation effect in sbGHS-R1a need more experiments to confirm. One of the explanations for this phenomenon is the presence of pcDNA3.1(+) improves the transfection efficiency, as there was an gradually increase in the fluorescent signal came from the cells transfected with fixed amount of pEGFP plus increasing amount of pcDNA3.1(+).

Also, this co-transfection potentiating effect was not specific for the additional empty vector, it also occur in the addition of other plasmid DNA (hTP $\alpha$  and hGHS-R1b), but the increase in the [ $^3\text{H}$ ]-IP production varies and the basal [ $^3\text{H}$ ]-IP production may not be potentiated. The DNA concentration balancing effect in co-transfection was not specific to hGHS-R1a, but was seen with another G $_q$ -coupled receptor, hTP $\alpha$ . In addition, the co-transfection potentiating effect in [ $^3\text{H}$ ]-IP production not only occurred in balancing DNA with one type of GPCR, G $_q$ -coupled receptor, but also when using G $_i$ - or G $_s$ -coupled receptors, as in the HEK293 cells co-transfected with hGHS-R1a and MOR or mDP, the agonist-stimulated [ $^3\text{H}$ ]-IP production was greater than the HEK293 cells transfected with hGHS-R1a alone. Also, the potentiating effect was also observed in agonist-stimulated [ $^3\text{H}$ ]-IP productions using different transfection reagents, although this may not occur in the basal [ $^3\text{H}$ ]-IP production.



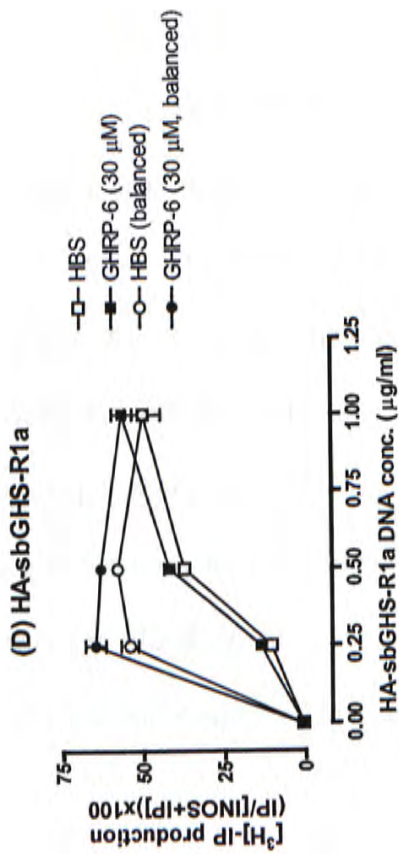
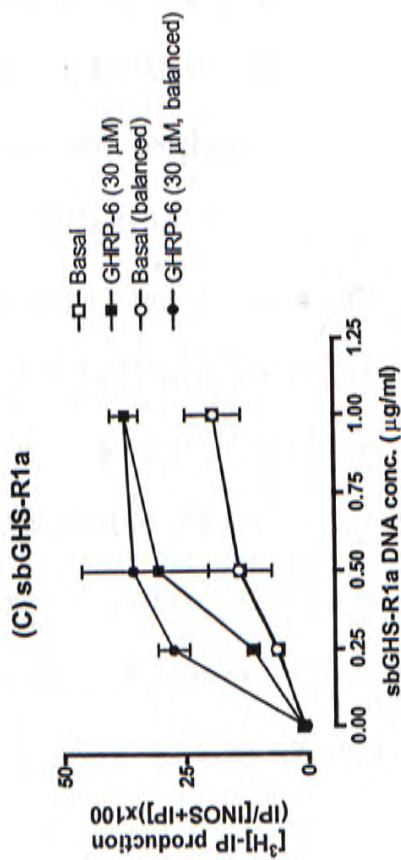
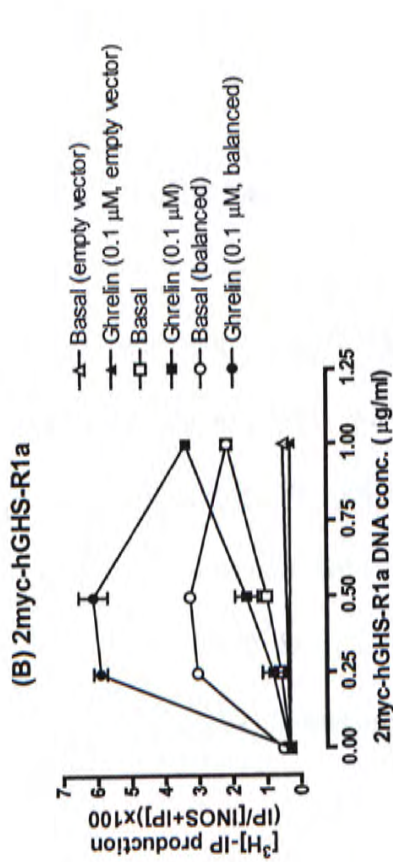
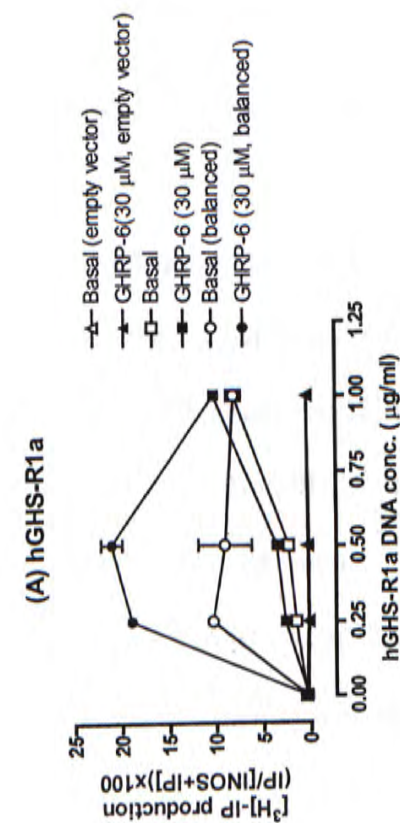




Figure 4.8 Effect of empty vector on co-transfection with hGHS-R1a or sbGHS-R1a in basal and agonist-stimulated [ $^3\text{H}$ ]-IP production. HEK293 cells were transfected (A) hGHS-R1a alone or balanced to 1  $\mu\text{g}/\text{ml}$  with pcDNA3.1(+), (B) 2myc-hGHS-R1a alone or balanced to 1  $\mu\text{g}/\text{ml}$  with pcDNA3.1(+), (C) sbGHS-R1a alone or balanced to 1  $\mu\text{g}/\text{ml}$  with pBK-CMV, (D) HA-sbGHS-R1a alone or balanced to with 1  $\mu\text{g}/\text{ml}$  pcDNA3.1(+)/Zeo. HEK293 cells transfected with pcDNA3.1(+) and pcDNA3.1(+)/Zeo were used as a control. After 24 h post-transfection, the cells were labeled with 2  $\mu\text{Ci}/\text{ml}$  *myo*-[ $^3\text{H}$ ]-inositol and incubated overnight, and then [ $^3\text{H}$ ]-IP production was measured as described in Chapter 3. The cells were lysed following 1 h incubation buffer or GHRP-6 or ghrelin. Results in figure (A), (B) and (D) come from one experiment performed in duplicate, data shown are mean  $\pm$  S.D. Results in figure (C) represent mean  $\pm$  S.D.,  $n=2$ , of experiments performed in duplicate.

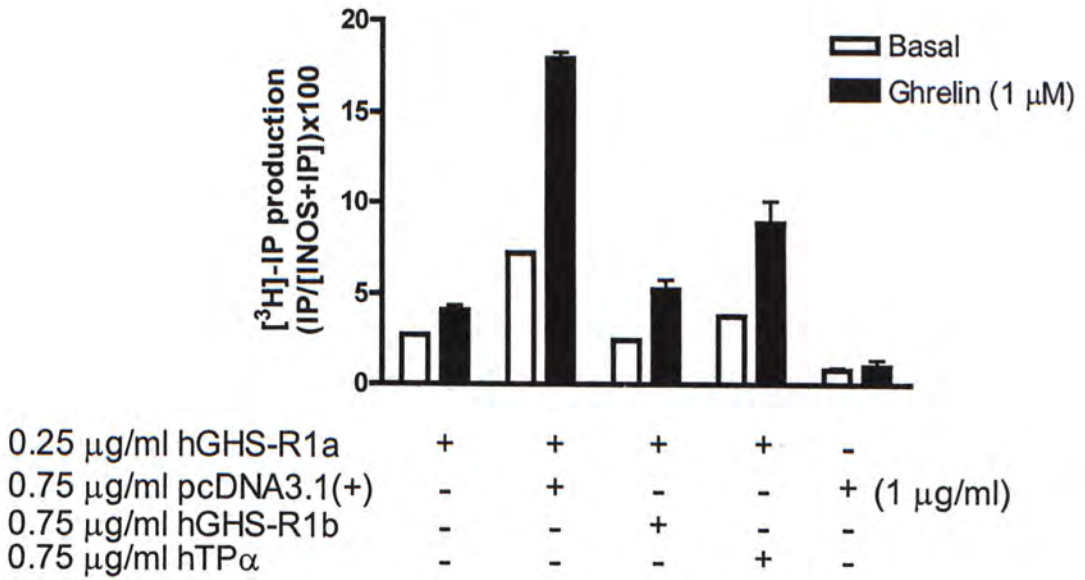
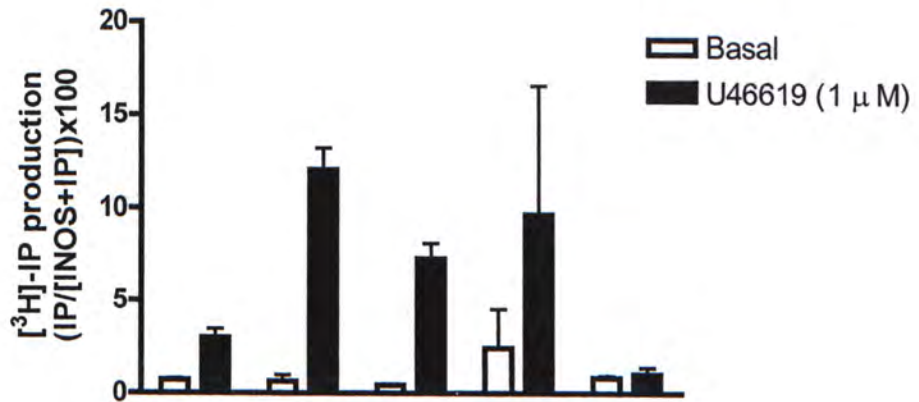


Figure 4.9 Effect of co-transfection on hGHS-R1a signaling. HEK293 cells transfected with 0.25 μg/ml hGHS-R1a or 1 μg/ml pcDNA3.1(+) were used as the controls. HEK293 cells were transfected with 0.25 μg/ml hGHS-R1a plus 0.75 μg/ml pcDNA3.1(+)/hGHS-R1b/G<sub>q</sub>-coupled receptor (hTPα). After 24 h post-transfection, the cells were labeled with 2 μCi/ml *myo*-[<sup>3</sup>H]-inositol and incubated overnight, and then [<sup>3</sup>H]-IP production was measured as described in Chapter 3. The cells were lysed following 1 h incubation with buffer or ghrelin. Results in figure represent mean ± S.D., n=2, of experiments performed in duplicate.



0.25 μg/ml hTPα	+	+	+	+	-
0.75 μg/ml pcDNA3.1(+)	-	+	-	-	+
0.75 μg/ml hGHS-R1b	-	-	+	-	-
0.75 μg/ml hGHS-R1a	-	-	-	+	-

Figure 4.10 Effect of co-transfection on hTP $\alpha$  signaling. HEK293 cells transfected with 0.25  $\mu$ g/ml hTP $\alpha$  or 1  $\mu$ g/ml pcDNA3.1(+) were used as the controls. HEK293 cells were transfected with 0.25  $\mu$ g/ml hTP $\alpha$  plus 0.75  $\mu$ g/ml pcDNA3.1(+)/hGHS-R1b/G $_q$ -coupled receptor (hGHS-R1a). After 24 h post-transfection, the cells were labeled with 2  $\mu$ Ci/ml *myo*-[ $^3$ H]-inositol and incubated overnight, and then [ $^3$ H]-IP production was measured as described in Chapter 3. The cells were lysed following 1 h incubation with buffer or U46619. Results in figure represent mean  $\pm$  S.D., n=2, of experiments performed in duplicate.



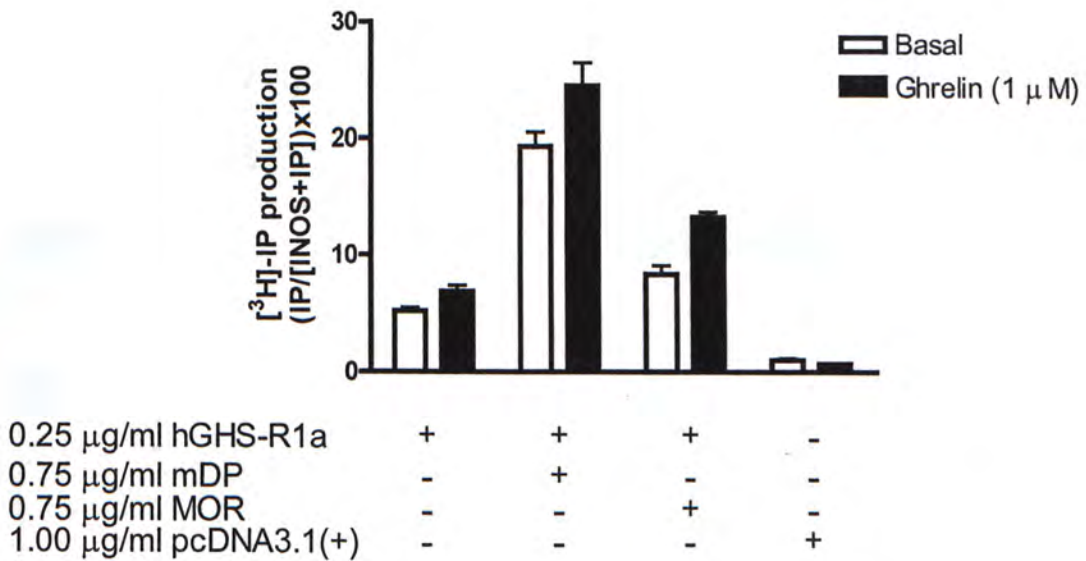
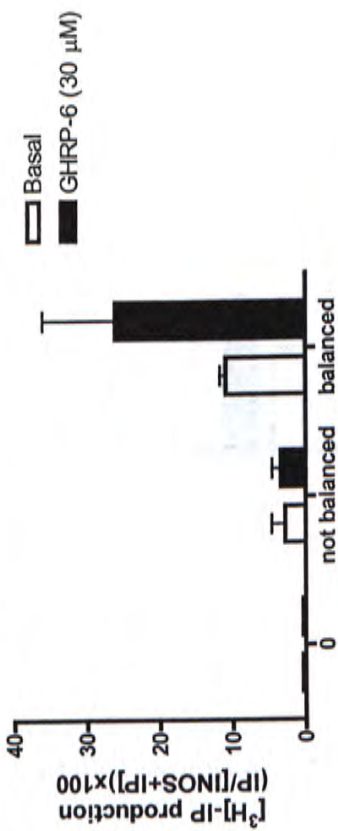


Figure 4.11 Effect of co-transfection on hGHS-R1a signaling with  $G_i$ - or  $G_s$ -coupled receptors. HEK293 cells transfected with 0.25 μg/ml hGHS-R1a or 1 μg/ml pcDNA3.1(+) were used as the controls. HEK293 cells were transfected with 0.25 μg/ml hGHS-R1a plus 0.75 μg/ml  $G_i$ -coupled receptor (MOR)/ $G_s$ -coupled receptor (mDP). After 24 h post-transfection, the cells were labeled with 2 μCi/ml *myo*-[ $^3$ H]-inositol and incubated overnight, and then [ $^3$ H]-IP production was measured as described in Chapter 3. The cells were lysed following 1 h incubation with buffer or ghrelin. Results come from one experiment performed in duplicate, data shown are mean  $\pm$  S.D.

(A) Lipofectamine



(B) Lipofectamine2000



(C) Fugene 6



(D) Genejuice

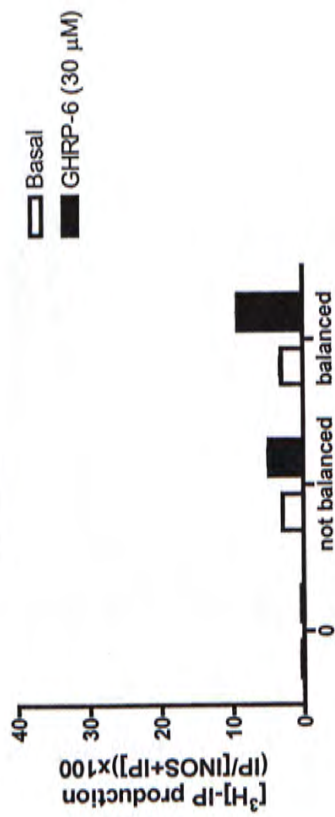
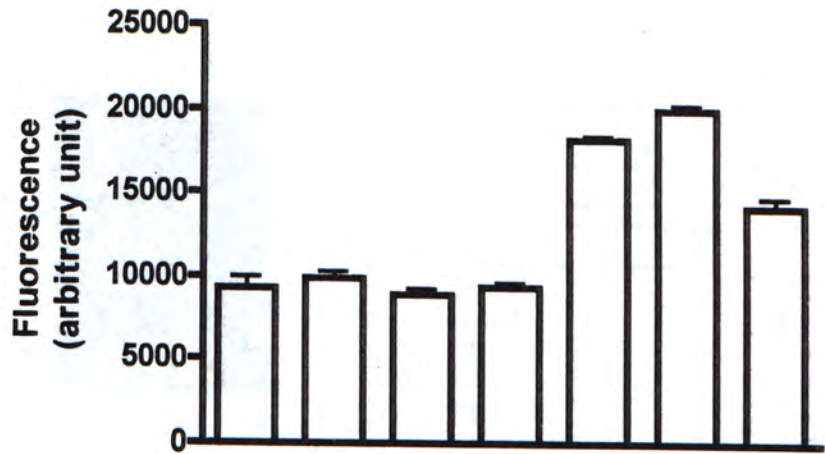


Figure 4.12 Co-transfection effect using different transfection reagents. HEK293 cells were transfected with 0.25  $\mu\text{g/ml}$  hGHS-R1a alone or with 0.75  $\mu\text{g/ml}$  pcDNA3.1(+) using (A) Lipofectamine, (B) Lipofectamine2000, (C) Fugene 6 or (D) Genejuice. After 24 h post-transfection, the cells were labeled with 2  $\mu\text{Ci/ml}$  *myo*-[ $^3\text{H}$ ]-inositol and incubated overnight, and then [ $^3\text{H}$ ]-IP production was measured as described in Chapter 3. The cells were lysed following 1 h incubation buffer or GHRP-6. Results in figure A, B, C represent mean  $\pm$  S.D., n=2, of experiments performed in duplicate. Results in figure D come from one experiment performed in duplicate, data shown are mean  $\pm$  S.D.





pEGFP ( $\mu\text{g/ml}$ )	0.1	0.1	0.1	0.1	0.1	0.1	0.1
2myc-hGHS-R1a ( $\mu\text{g/ml}$ )	-	0.25	0.5	1	-	0.25	0.5
pcDNA3.1(+) ( $\mu\text{g/ml}$ )	-	-	-	-	1	0.75	0.5

Figure 4.13 Effect of co-transfection on transfection efficiency. HEK293 cells transfected with 0.1  $\mu\text{g/ml}$  EGFP plasmid (pEGFP) DNA alone was used as a control. HEK293 cells transfected with 0.1  $\mu\text{g/ml}$  pEGFP plus increasing amounts of 2myc-hGHS-R1a alone or with pcDNA3.1(+) to maintained the DNA concentration at 1.1  $\mu\text{g/ml}$ . After 48 h post-transfection, the cells in the 24-well plate were washed with buffer and excited by 488 nm light and then the fluorescence produced by EGFP was measured by the counter (Victor-2 Multilabel). Results come from one experiment performed in duplicate, data shown are mean  $\pm$  S.D.

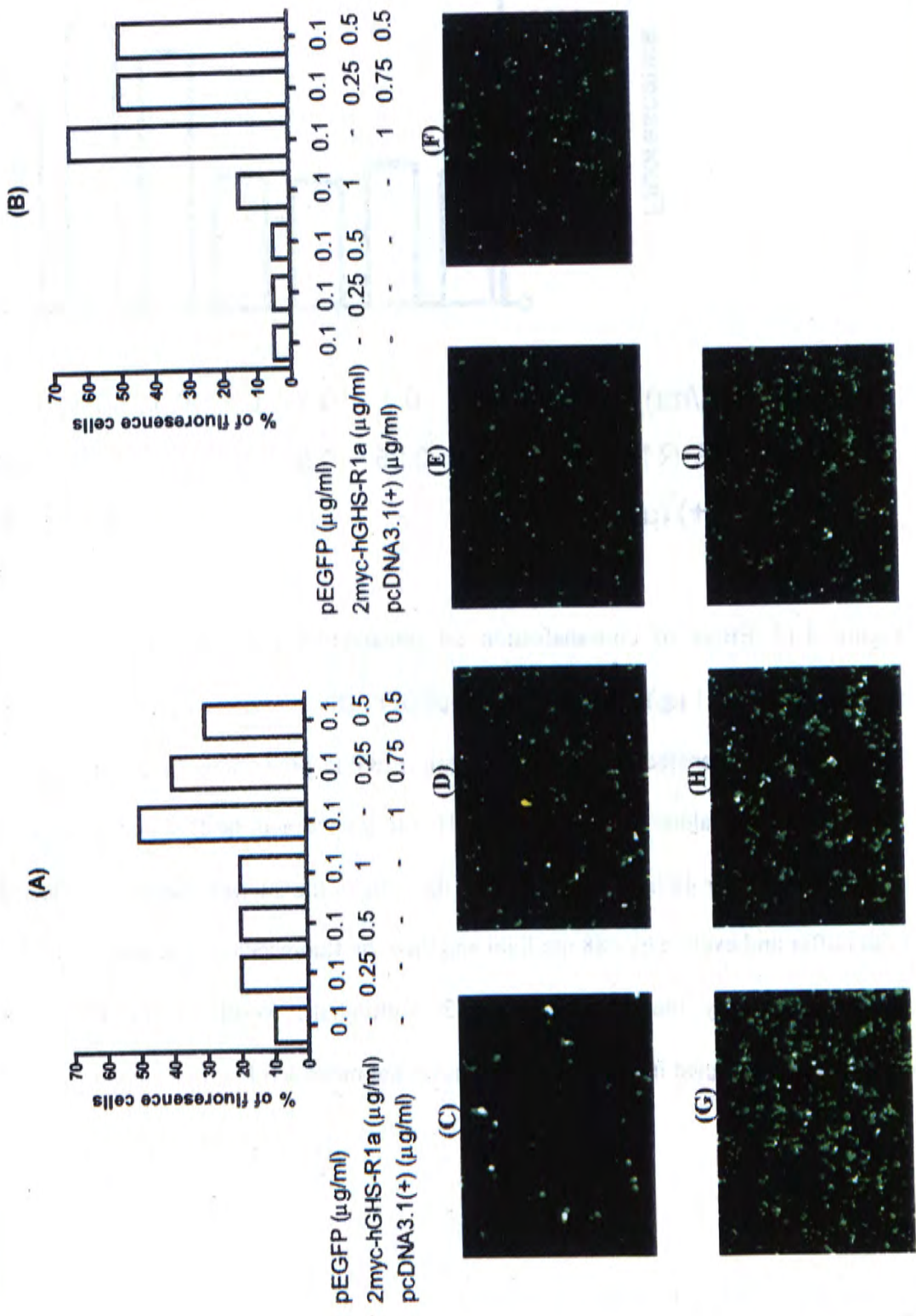


Figure 4.14 Effect of co-transfection on transfection efficiency. HEK293 cells transfected with 0.1  $\mu\text{g/ml}$  EGFP plasmid (pEGFP) DNA alone was used as a control. HEK293 cells transfected with 0.1  $\mu\text{g/ml}$  pEGFP plus increasing amounts of 2myc-hGHS-R1a alone or with pcDNA3.1(+) to maintain the DNA concentration at 1.1  $\mu\text{g/ml}$ . After 48 h post-transfection, the cells in the 24-well plate were washed with buffer and excited by 488 nm light and then estimated the cell confluency under fluorescence microscope. The figure A and B represent the estimation results from the two different observers, one of the observers (Figure A) is assayed blind to treatment. The figures C to I are images taken under fluorescence microscope, the cells were transfected with (C) 0.1  $\mu\text{g/ml}$  pEGFP, (D) 0.1  $\mu\text{g/ml}$  pEGFP plus 0.25  $\mu\text{g/ml}$  2myc-hGHS-R1a, (E) 0.1  $\mu\text{g/ml}$  pEGFP plus 0.5  $\mu\text{g/ml}$  2myc-hGHS-R1a, (F) 0.1  $\mu\text{g/ml}$  pEGFP plus 1  $\mu\text{g/ml}$  2myc-hGHS-R1a, (G) 0.1  $\mu\text{g/ml}$  pEGFP plus 1  $\mu\text{g/ml}$  pcDNA3.1(+), (H) 0.1  $\mu\text{g/ml}$  pEGFP plus 0.25  $\mu\text{g/ml}$  2myc-hGHS-R1a and 0.75  $\mu\text{g/ml}$  pcDNA3.1(+) and (I) 0.1  $\mu\text{g/ml}$  pEGFP plus 0.5  $\mu\text{g/ml}$  2myc-hGHS-R1a and 0.5  $\mu\text{g/ml}$  pcDNA3.1(+).



## **4.3 Development of cell lines stably expressing hGHS-R1a or hGHS-R1b**

### **4.3.1 Advantages of using a monoclonal cell line**

Monoclonal cell lines are derived from a single cell, so they are all identical to each other, the result between experiments will therefore be more consistent than using transient transfection methods to express the study target in a cell. Transfection efficiency varies from experiment to experiment, many factors can affect it, for example, cell density and cell culture health condition (Dalby *et al.*, 2004). Also, not all the cells can take up and express the target protein. In addition, as described in section 4.2, there is a variable potentiating effect resulting from co-transfection, so when studying the interaction between two proteins, using a monoclonal cell line which is already expressing one of the target proteins, will make the data easier to interpret.

### **4.3.2 Sensitivity of HEK293 cells to antibiotics**

To generate a stable cell line that expresses a target protein from an expression plasmid carrying an antibiotic resistance gene, it is necessary to determine the minimum antibiotic concentration required to kill the non-transfected cells. Mammalian cells exhibit a wide range of susceptibility to antibiotics, and many factors affect the stable cell line selection process, such as cell line, growth rate and cell density. Therefore, before the selection of the stable cell line, the susceptibility of HEK293 cells to G418 and Zeocin<sup>TM</sup> needed to be determined, as described in Chapter 3. 2myc-hGHS-R1a was inserted into pcDNA3.1(+) vector, which carries

the Neomycin resistance gene, therefore the cells expressing 2myc-hGHS-R1a are G418-resistant. From figure 4.15A, 600  $\mu\text{g/ml}$  G418 was sufficient to kill HEK293 cells, so this concentration was used to select the cells that stably expressed 2myc-hGHS-R1a. 2myc-hGHS-R1b was inserted into pcDNA3.1(+)/Zeo vector, which carries the Zeocin resistance gene, so the cells expressing 2myc-hGHS-R1b are Zeocin-resistant. From figure 4.15B, 300  $\mu\text{g/ml}$  Zeocin<sup>TM</sup> was sufficient to kill HEK293 cells, so 300  $\mu\text{g/ml}$  Zeocin<sup>TM</sup> was used to select the cells that stably expressed 2myc-hGHS-R1b.

#### **4.3.3 Production of polyclonal stable cell line**

Development of stable cell lines involves the uptake and the integration of transfected plasmid DNA into the chromosome at random sites, making the transfected plasmid DNA a permanent part of the genetics of the cell. Before the plasmid DNA integration, the plasmid DNA is cleaved by the endonucleases, which make random internal cuts in the DNA molecule (Snustad *et al.*, 1997), so it may result in a linearized DNA sequence, such as the cutting site in the middle of the target gene, which can not code for the target protein. Therefore, in the development of stable cell line, the 2myc-hGHS-R1a DNA plasmid and 2myc-hGHS-R1b DNA plasmid were linearized using *Sa*I and *Sca*I restriction enzymes, respectively, to make sure the circular plasmid DNAs were cleaved at the right position. In addition, the plasmid DNA integration is also a random process, if the integration occurred at the transcriptionally silent genomic locus, it will also result in no expression of the target protein.



To confirm if the establishment of the polyclonal 2myc-hGHS-R1a and 2myc-hGHS-R1b HEK293 stable cell lines were successful or not, IP assay and RT-PCR were used to confirm the presence of 2myc-hGHS-R1a and 2myc-hGHS-R1b, respectively, as described in Chapter 3. There was an increase in both basal and the ghrelin-stimulated [<sup>3</sup>H]-IP production in 2myc-hGHS-R1a HEK293 stable cell line, it indicating the presence of 2myc-hGHS-R1a (Fig. 4.16). For the RT-PCR, using primers named 2myc-hGHS-R1b as described in Chapter 3 Table 3.2, there was around 1000 base pairs (bps) PCR product which matched the expected size (983 bps), it therefore showed the presence of 2myc-hGHS-R1b in 2myc-hGHS-R1b HEK293 stable cell line (Fig. 4.17A). From Fig. 4.17B, it showed that there was absence of hGHS-R1a and hGHS-R1b in HEK293 cells.

#### **4.3.4 Monoclonal stable cell line selection**

There are two methods to develop a monoclonal cell line, one of the methods is to transfer cells into 96-well plates at 1 cell per well (Mounier *et al.*, 2004), as described in Chapter 3. This method is very convenient, the cells were left in the plate until single colonies were observed, then the single colony in each well was selected and bulked up. However, many wells contained more than one cell or had no cell. Although there were two discrete single colonies in the well, the colonies could not be selected. Also, cells are difficult to grow alone, it took very long time to develop a colony from a single cell. In addition, many cells transfected with 2myc-hGHS-R1b died at few cells per well, as floating cells were observed.



Therefore, another method was used, that is the use of the cloning ring (Russell, 1998), as described in Chapter 3, as it may overcome the previous problems. In this method, the cells grew in a 100 mm dish and had other cells in the surrounding environment during the development of the single colony. The single colony was bounded by cloning ring when the colony was large enough. Using this method, cells do not need to grow alone and one can select more single colonies, as long as the colonies are discrete and not too close to each other.

Although there were lots of improvements tried in the development of 2myc-hGHS-R1a and 2myc-hGHS-R1b HEK293 stable cell lines, it was still unsuccessful. After the screening of the 2myc-hGHS-R1a HEK293 stable cell lines by IP-assay, as described in Chapter 3, both the basal and the ghrelin-stimulated [<sup>3</sup>H]-IP production were as the same as the control, indicating that none of the monoclonal clones express 2myc-hGHS-R1a despite showing antibiotic resistance (data not shown). The clonal screening of 2myc-hGHS-R1b HEK293 stable cell lines by RT-PCR as described in Chapter 3, also indicated that none of the clones have the expression of 2myc-hGHS-R1b, as there was no band in the agarose gel (data not shown).

#### **4.3.5 Discussions**

Although many improvements had been made in order to increase the successfulness in the development of stable cell lines, including use of linearized circular plasmid DNA by specific restriction enzymes before transfection to prevent the random

cutting by endonucleases inside the cells and using cloning ring during selection of monoclonal cell line in order to prevent the cell to grow alone for a long time in 96-well plate, but i still could not obtain any monoclonal stable cell line. The unsuccessfulness might be due to the random integration of the linearized target plasmid DNA into the chromosome.

Recently, there is a new technique developed by a company (Invitrogen), called Flp-In™ system. This system eliminates the random integration of the plasmid DNA into chromosome during the development of the stable cell line. Briefly, a host cell line stably expressing a vector, called pFRT/*lacZeo* has been generated. This vector contains a Zeocin resistance gene for antibiotic selection and a FRT site which serves as the binding and cleavage site for the Flp recombinase. The pFRT/*lacZeo* stably expressed cell line can be developed on your own or obtained from the company. After this host cell line is ready, co-transfection of a vector called pcDNA5/FRT, which contains the gene of interest and FRT site, with another vector called pOG44, which constitutively expresses the Flp recombinase, into this stably expressed pFRT/*lacZeo* host cell. Upon co-transfection, the Flp recombinase expressed in pOG44 mediates homologues recombination between the FRT sites, such that pcDNA5/FRT inserts into the integrated FRT site in the chromosome (Craig, 1988; Sauer, 1994). This method makes sure the vector containing the target gene is inserted into the correct position of chromosome, at which the target gene is transcribed.

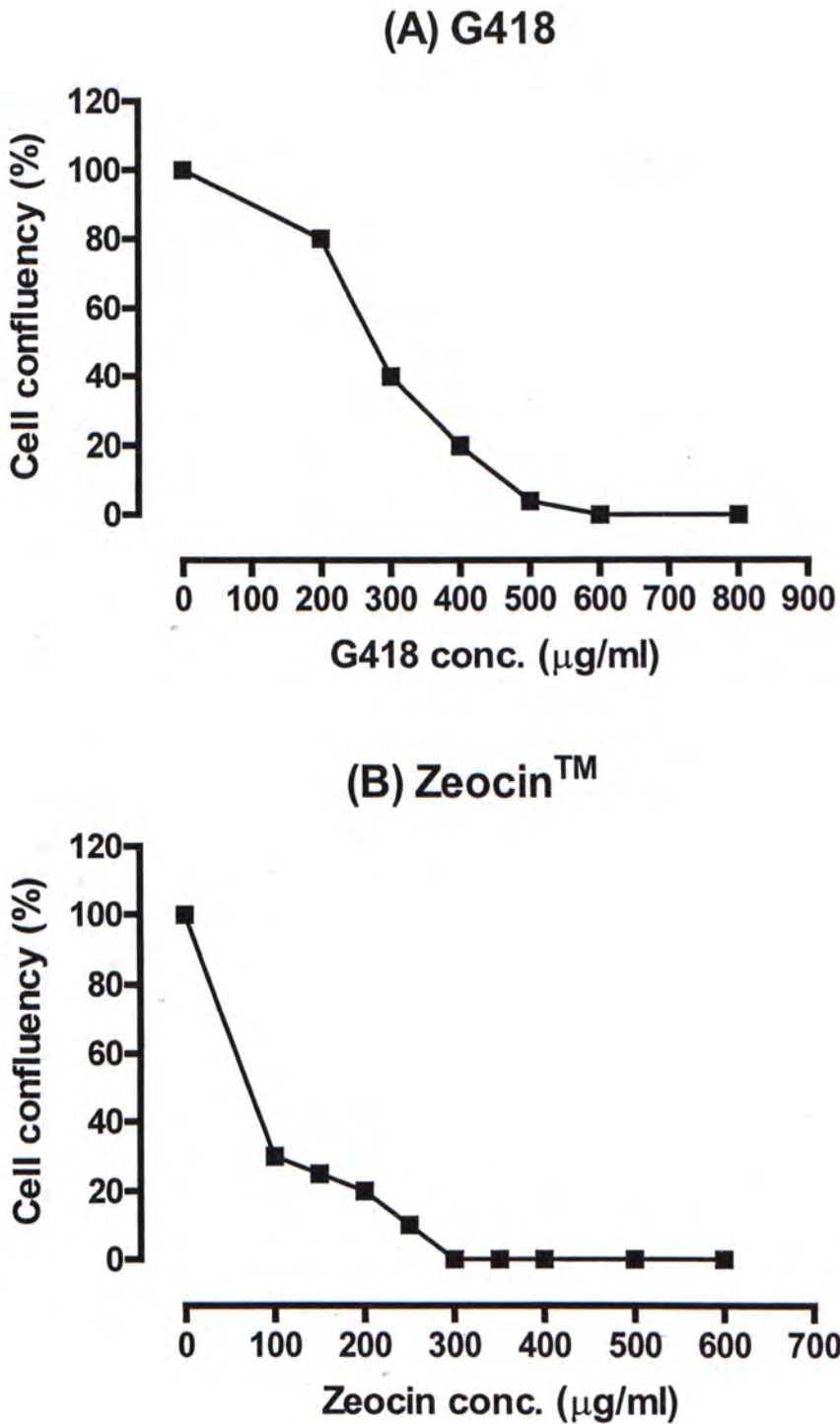


Figure 4.15 Antibiotic susceptibility curve of HEK293 cells to G418 and Zeocin<sup>TM</sup>.

The cell confluency was estimated after incubating the cells with antibiotic for 10 days.



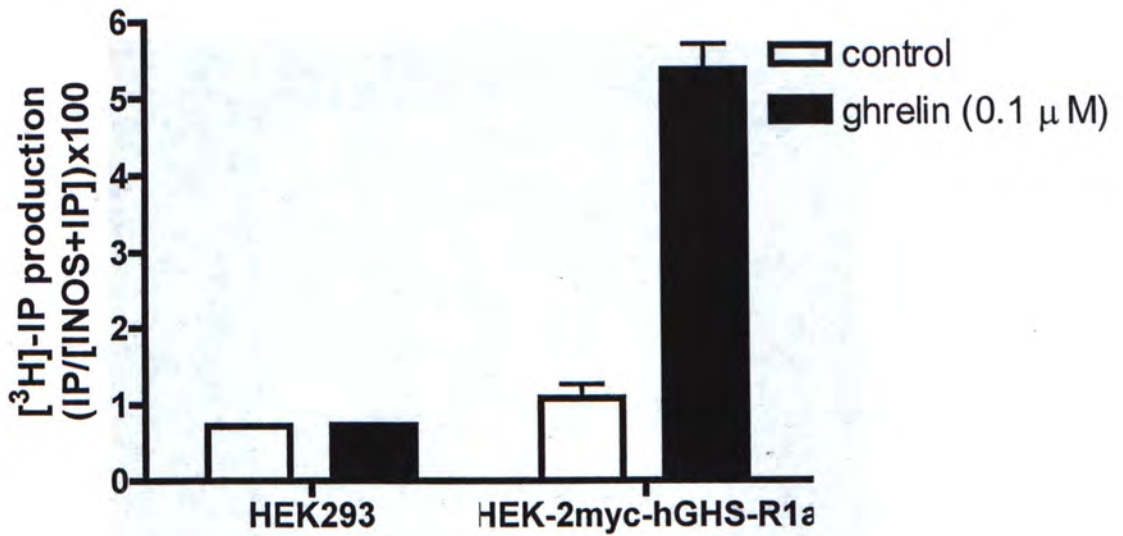
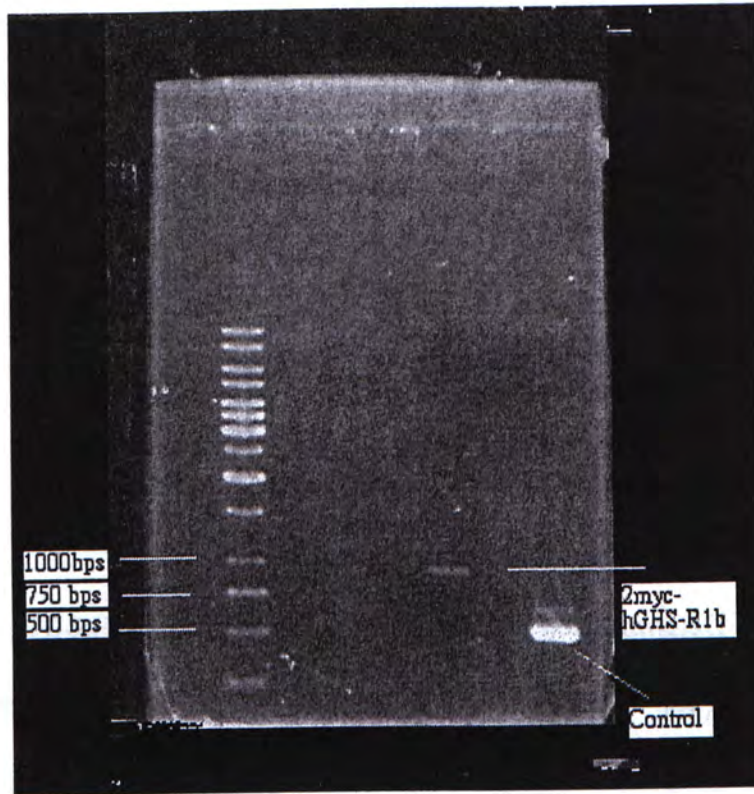
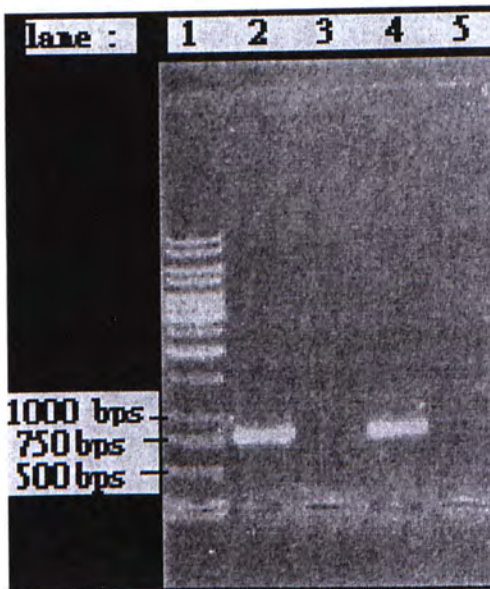


Figure 4.16 Determination of the presence of 2myc-hGHS-R1a in polyclonal HEK293 stable cell line. The HEK293 and polyclonal stable cells were labeled with 2  $\mu$ Ci/ml *myo*-[<sup>3</sup>H]-inositol and incubated overnight, and then [<sup>3</sup>H]-IP production was measured as described in Chapter 3. The cells were lysed following 1 h incubation with buffer or ghrelin. Results come from one experiment performed in triplicate, data shown are mean  $\pm$  S.E.M.

(A)



(B)



Lane	Cell types	PCR target gene
2	HEK293 cells transfected with hGHS-R1a	hGHS-R1a
3	Non-transfected HEK293 cells	
4	HEK293 cells transfected with hGHS-R1b	hGHS-R1b
5	Non-transfected HEK293 cells	

Figure 4.17 Ethidium bromide stained agarose gel showing (A) the presence of 2myc-hGHS-R1b in HEK-sbGHS-R1b cells and (B) the absence of hGHS-R1a and hGHS-R1b in HEK293 cells. The total RNA was extracted from (A) the polyclonal HEK-sbGHS-R1b stable cells line, (B) hGHS-R1a transfected HEK293 cells (lane 2), hGHS-R1b transfected HEK293 cells (lane 4) and HEK293 cells (lane 3 and 5), and then converted to first-strand cDNA and PCR was performed as described in Chapter 3. The PCR product was resolved in agarose gel. The expected size of control band, 2myc-hGHS-R1b, hGHS-R1a and hGHS-R1b are 500 bps, 983 bps, 806 bps and 807 bps, respectively. Control product was amplified by RT-PCR, using the cDNA provided in the SuperScript™ First-Strand Synthesis System (Invitrogen).



## 4.4 Effect of adenosine on GHS-R1a signaling

### 4.4.1 Adenosine acts as a partial agonist

To investigate the effect of adenosine on 2myc-hGHS-R1a, HEK293 cells were transiently transfected with 0.25  $\mu\text{g/ml}$  2myc-hGHS-R1a plus 0.75  $\mu\text{g/ml}$  pcDNA3.1(+), and then incubated with 0.1  $\mu\text{M}$  ghrelin and 0.1 mM adenosine alone or together. The concentration of ghrelin and adenosine used here, were expected to give a maximum activation of 2myc-GHS-R1a. As indicated in the figure 4.4, the ghrelin-stimulated [ $^3\text{H}$ ]-IP production reached plateau at 10 nM, and 0.1 mM adenosine stimulated maximum intracellular calcium increase in HEK293 cells expressing hGHS-R1a (Carreira *et al.*, 2004). From figure 4.18A, the adenosine-stimulated [ $^3\text{H}$ ]-IP production was  $37.54 \pm 1.47$ ,  $n=4$ , the response size of the basal and the ghrelin-stimulated [ $^3\text{H}$ ]-IP production was  $32.54 \pm 2.00$  and  $47.64 \pm 2.50$ ,  $n=4$ , respectively. It indicated that adenosine is a partial agonist of 2myc-hGHS-R1a, as adenosine increased the [ $^3\text{H}$ ]-IP production, but the response size is not as large as the ghrelin-stimulated [ $^3\text{H}$ ]-IP production. When the 2myc-hGHS-R1a expressed cells were incubated with ghrelin together with adenosine, there was a further increase in the ghrelin-stimulated [ $^3\text{H}$ ]-IP production (Fig. 4.18A). A further increase is not expected, as adenosine is a partial agonist of hGHS-R1a, the use of the maximum concentration of a partial agonist, the full agonist response should be reduced as many of the binding sites were also occupied by the partial agonist. In other paper, it demonstrated in HEK293 cells which stably expressed pig GHS-R1a, at the maximal concentration of adenosine, MK-0677 did

not cause a further activation of GHS-R1a (Smith *et al.*, 2000). Non-transfected HEK293 cells were not affected by 0.1  $\mu$ M ghrelin or 0.1 mM adenosine (Fig. 4.18B), indicating that the changes in the [ $^3$ H]-IP production were due to the expression of 2myc-hGHS-R1a.

#### 4.4.2 Effect of substance P analog on adenosine-mediated GHS-R1a signaling

SPa has been suggested to be an inverse agonist of GHS-R1a and it has also been shown in our system (Fig. 4.2). In addition, ghrelin-stimulated [ $^3$ H]-IP production was affected by SPa (Fig. 4.3). Adenosine was shown to increase [ $^3$ H]-IP production in our system, therefore it was interesting to investigate whether adenosine-stimulated [ $^3$ H]-IP production will also be affected by SPa. HEK293 cells were transfected with 2myc-hGHS-R1a as described in section 4.4.1, and then the cells were incubated with buffer, 0.1  $\mu$ M ghrelin, 0.1 mM adenosine alone or together with 1  $\mu$ M SPa. The basal [ $^3$ H]-IP production was significantly inhibited by  $68.86 \pm 9.11\%$ ,  $n=2$ , when the cells were incubated with SPa, indicating that SPa is an inverse agonist of 2myc-hGHS-R1a (Fig. 4.19). The adenosine-stimulated [ $^3$ H]-IP production was also significantly affected by SPa, it was inhibited by  $78.56 \pm 3.03\%$ ,  $n=2$ , the response size of SPa plus adenosine-stimulated [ $^3$ H]-IP production ( $7.79 \pm 1.85$ ,  $n=2$ ) was similar to the [ $^3$ H]-IP production ( $9.57 \pm 3.59$ ,  $n=2$ ) in HEK293 cells incubated with SPa only. However, the 0.1  $\mu$ M ghrelin-stimulated [ $^3$ H]-IP production was not affected by SPa, as the ghrelin concentration is too high that the effect of 1  $\mu$ M SPa cannot be observed. If using a lower concentration of ghrelin, the effect of SPa should be observed, as described in figure 4.3. Although in figure 4.3, the 0.1



$\mu\text{M}$  ghrelin-stimulated [ $^3\text{H}$ ]-IP production was still affected by the presence of 1  $\mu\text{M}$  SPa, it might be due to the low transfection efficiency, as indicated by the lower [ $^3\text{H}$ ]-IP production in figure 4.3 than in figure 4.19.

#### **4.4.3 Effect of adenosine deaminase (ADA) on adenosine- and ghrelin-stimulated GHS-R1a signaling**

In section 4.4.1, it showed that there was an adenosine-stimulated [ $^3\text{H}$ ]-IP production in the HEK293 cells transiently transfected with 2myc-hGHS-R1a. As there are many cells which endogenously produce adenosine, such as mast cells (Feoktistov *et al.*, 2003), so it is interesting to see if there was a component of the adenosine-stimulated [ $^3\text{H}$ ]-IP production in 2myc-hGHS-R1a transfected HEK293 cells due to any endogenous adenosine. In order to investigate this, ADA was used. ADA is an enzyme of the purine metabolism which catalyzes the irreversible deamination of adenosine to inosine (Cristalli *et al.*, 2001). HEK293 cells were transfected with 2myc-hGHS-R1a as described in section 4.4.1, and then the cells were preincubated with 1U/ml ADA or buffer for 30 min before incubating with 0.1  $\mu\text{M}$  ghrelin or 0.1 mM adenosine. In figure 4.20, pretreatment of cells with ADA caused a decrease in the basal, ghrelin- and adenosine-stimulated [ $^3\text{H}$ ]-IP production, it indicating that there may be an endogenous release of adenosine due to the expression of 2myc-hGHS-R1a, and then the endogenous adenosine will bind to the 2myc-hGHS-R1a and gives a further stimulation of basal and ligand-stimulated [ $^3\text{H}$ ]-IP production. If there were no endogenous release of adenosine, then only the adenosine-stimulated [ $^3\text{H}$ ]-IP production should be reduced, the basal and the



ghrelin-stimulated [ $^3\text{H}$ ]-IP production should remain unchanged. Another possible implication is that ADA produces a non-specific inhibition effect on [ $^3\text{H}$ ]-IP production.

To investigate whether the expression of 2myc-hGHS-R1a and other  $G_q$ -coupled receptors will cause the release of endogenous adenosine, HEK293 cells were transiently transfected with 0.25  $\mu\text{g/ml}$  hTP $\alpha$  plus 0.75  $\mu\text{g/ml}$  pcDNA3.1(+). In addition, HEK293 cells have an endogenously expressed muscarinic receptor, which when stimulated by 0.1 mM carbachol results in an increase in the intracellular calcium level (Luo *et al.*, 2001a). Both the hTP $\alpha$  and muscarinic receptor are  $G_q$ -coupled receptors. HEK293 cells were also transiently transfected with 0.25  $\mu\text{g/ml}$   $G_{\alpha q}\text{RC}$ , which is a constitutively active  $G_q$ -protein, plus 0.75  $\mu\text{g/ml}$  pcDNA3.1(+).  $G_{\alpha q}\text{RC}$  is used to show if the endogenous adenosine released is due to the receptor-dependent activation of  $G_q$ -protein or not. Cells were pre-incubated with 1U/ml ADA or buffer for 30 min and then the hTP $\alpha$ , endogenous muscarinic receptor and  $G_{\alpha q}\text{RC}$  transfected HEK293 cells were incubated with 1  $\mu\text{M}$  U46619, 0.1 mM carbachol and buffer, respectively. Pretreatment with ADA caused reductions in agonist-stimulated [ $^3\text{H}$ ]-IP production in the cells transiently transfected with hTP $\alpha$  and endogenously expressing muscarinic receptors (Fig. 4.21). There was also a decrease in ligand-independent [ $^3\text{H}$ ]-IP production in  $G_{\alpha q}\text{RC}$  transfected cells. Taken together, the endogenous adenosine release may not only be due to the expression of 2myc-hGHS-R1a, but also other  $G_q$ -coupled receptors. In addition, this endogenous adenosine release is not necessary to have a receptor-dependent activated  $G_q$  protein.

Alternatively, a non-specific effect of ADA still needs to be considered.

#### 4.4.4 Specificity of ADA

To investigate the specificity of ADA in the inhibition of [ $^3$ H]-IP production, the adenosine receptor antagonist theophylline was used. There is evidence to show that 10  $\mu$ M theophylline can block the pig GHS-R1a signaling induced by 2  $\mu$ M adenosine (Smith *et al.*, 2000). Also, theophylline can block the signaling activated by all the subtypes of adenosine receptor, as it is a non-selective adenosine receptor blocker (Germack *et al.*, 2004b). However, there has not been any evidence to show that theophylline can block the signaling mediated by hTP $\alpha$  receptor, G $_{\alpha q}$ RC, muscarinic receptors and purinergic (P $_2$ Y) receptors. Therefore, if the ADA inhibition effect on [ $^3$ H]-IP production was specific, then after the pretreatment with theophylline, only the cells expressing 2myc-hGHS-R1a and incubated with adenosine alone or together with ghrelin, will show the decrease in the agonist-stimulated [ $^3$ H]-IP production.

HEK293 cells were transiently co-transfected with 0.25  $\mu$ g/ml 2myc-hGHS-R1a, hTP $\alpha$  or G $_{\alpha q}$ RC with 0.75  $\mu$ g/ml pcDNA3.1(+). The transiently transfected and the non-transfected HEK293 cells were pre-incubated with 0.1 mM theophylline or buffer for 30 min, and then these cells were incubated with appropriate agonist alone for the receptor expressed in the cells or together with 0.1 mM adenosine. That means, the cells expressed 2myc-hGHS-R1a, hTP $\alpha$ , G $_{\alpha q}$ RC were incubated with 0.1  $\mu$ M ghrelin, 1  $\mu$ M U46619 and buffer, respectively. The non-transfected HEK293



cells, which endogenously express muscarinic receptors and purinergic P<sub>2</sub>Y receptors (P<sub>2</sub>Y), were incubated with 0.1 mM carbachol and 0.1 mM ATP, respectively. From figure 4.22, the pre-treatment of cells with theophylline did not cause any changes in any of the agonist-stimulated [<sup>3</sup>H]-IP production. It implicated that the ADA inhibition effect may not be specific and that the adenosine-sensitive site on hGHS-R1a is not recognized by theophylline. Tullin et al (2000) also showed that in BHK cells which stably expressed GHS-R1a, theophylline did not show any effect on adenosine- or MK-0677-induced calcium response.

#### 4.4.5 Conclusions

HEK293 cells transfected with 2myc-hGHS-R1a and incubated with a high concentration adenosine, which expect to show a maximum activation of hGHS-R1a, showed that there was an increase in the [<sup>3</sup>H]-IP production and the response size is not as large as ghrelin, suggesting that adenosine is a partial agonist of hGHS-R1a. When adenosine was co-administrated with ghrelin, there was an additive increase in the ghrelin-stimulated [<sup>3</sup>H]-IP production, this result is not expected as adenosine is a partial agonist, as activation of a receptor by the high concentration of partial agonist plus the full agonist, the full agonist-stimulated response should be decreased. In Smith *et al.* (2000), it demonstrated in HEK293 cells which stably expressed pig GHS-R1a, at the maximal concentration of adenosine, MK-0677 did not cause a further activation of GHS-R1a. Besides ghrelin-stimulated [<sup>3</sup>H]-IP production, the adenosine-stimulated [<sup>3</sup>H]-IP production was affected by SPa, but this could just be affect on the basal activity, as there was only a slight increase in the [<sup>3</sup>H]-IP



production by adenosine.

There is not enough evidence here to show that part of the ghrelin-stimulated [ $^3\text{H}$ ]-IP production is due to the endogenous release of adenosine, as there was a decrease in basal, ghrelin- and adenosine-stimulated [ $^3\text{H}$ ]-IP production in 2myc-hGHS-R1a transfected cells after pretreatment with ADA. Also, muscarinic receptor-, hTP $\alpha$ - and G $_{\alpha q}$ RC-activated [ $^3\text{H}$ ]-IP production were also decreased. In addition, pretreatment of cells with theophylline did not inhibit any agonist-stimulated [ $^3\text{H}$ ]-IP production in 2myc-hGHS-R1a, hTP $\alpha$  and G $_{\alpha q}$ RC transfected HEK293 cells and non-transfected HEK293 cells which endogenously express muscarinic receptor and P $_2$ Y receptors. In Tullin et al (2000) it was also shown that in BHK cells which stably expressed GHS-R1a, theophylline did not show any effect on adenosine- or MK-0677-induced calcium response.

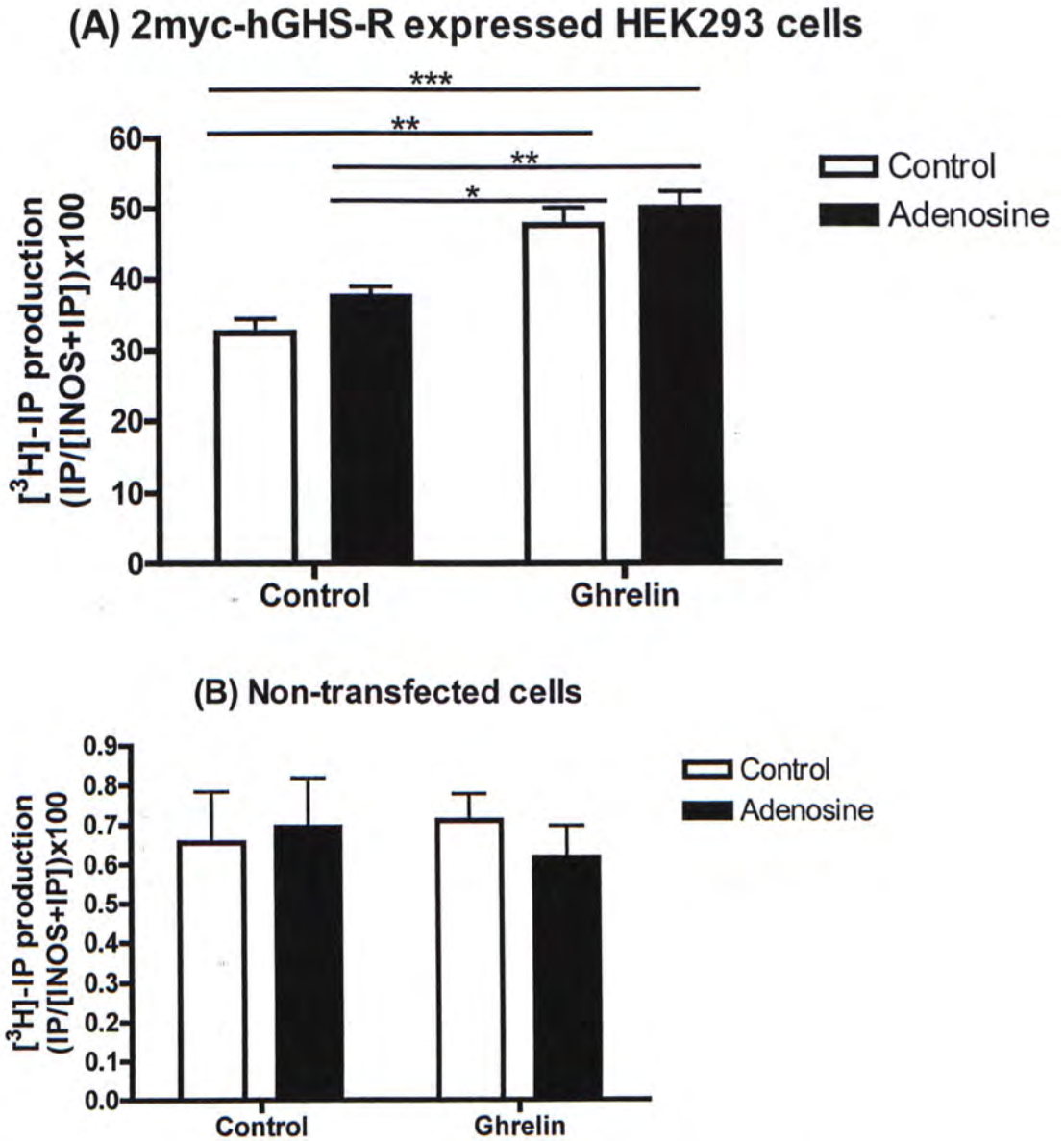


Figure 4.18 Effect of 0.1 mM adenosine alone or on 0.1  $\mu$ M ghrelin-stimulated  $[^3\text{H}]$ -IP production in (A) HEK293 cells transiently transfected 0.25  $\mu\text{g}/\text{ml}$  2myc-hGHS-R1a plus 0.75  $\mu\text{g}/\text{ml}$  pcDNA3.1(+). After 24 h post-transfection, the cells were labeled with 2  $\mu\text{Ci}/\text{ml}$  *myo*- $[^3\text{H}]$ -inositol and incubated overnight, and then  $[^3\text{H}]$ -IP production was measured as described in Chapter 3. The cells were lysed following 1 h incubation with buffer, adenosine, ghrelin or adenosine plus ghrelin. (B) Non-transfected HEK293 cells were used to show ghrelin and adenosine did not affect the cells. Results in figure represent mean  $\pm$  S.E.M.,  $n=4$ , of experiments performed in duplicate. (\* $p<0.05$ , \*\* $<0.01$ , \*\*\* $<0.001$ , one-way ANOVA was used.)

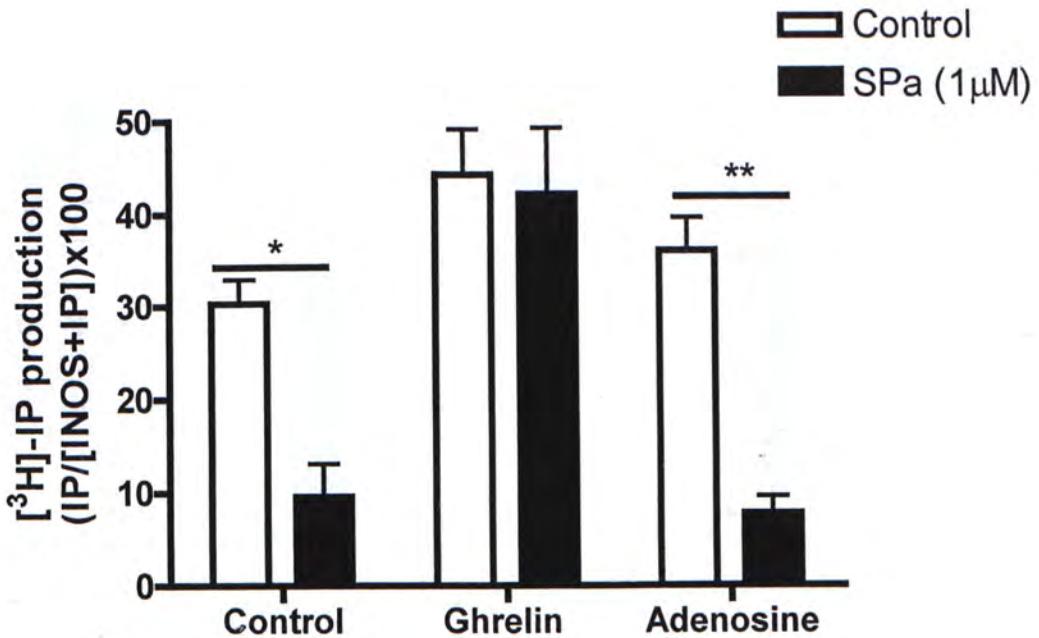


Figure 4.19 Effect of 1  $\mu$ M SPa on basal, 0.1  $\mu$ M ghrelin- and 0.1 mM adenosine-stimulated [ $^3$ H]-IP production. HEK293 cells were transiently transfected with 0.25  $\mu$ g/ml 2myc-hGHS-R1a plus 0.75  $\mu$ g/ml pcDNA3.1(+). After 24 h post-transfection, the cells were labeled with 2  $\mu$ Ci/ml *myo*-[ $^3$ H]-inositol and incubated overnight, and then [ $^3$ H]-IP production was measured as described in Chapter 3. The cells were lysed following 1 h incubation with buffer, ghrelin, adenosine alone or together with SPa. Results in figure represent mean  $\pm$  S.D., n=2, of experiments performed in duplicate. (\*P<0.05, \*\*P<0.01, one-way ANOVA was used.)



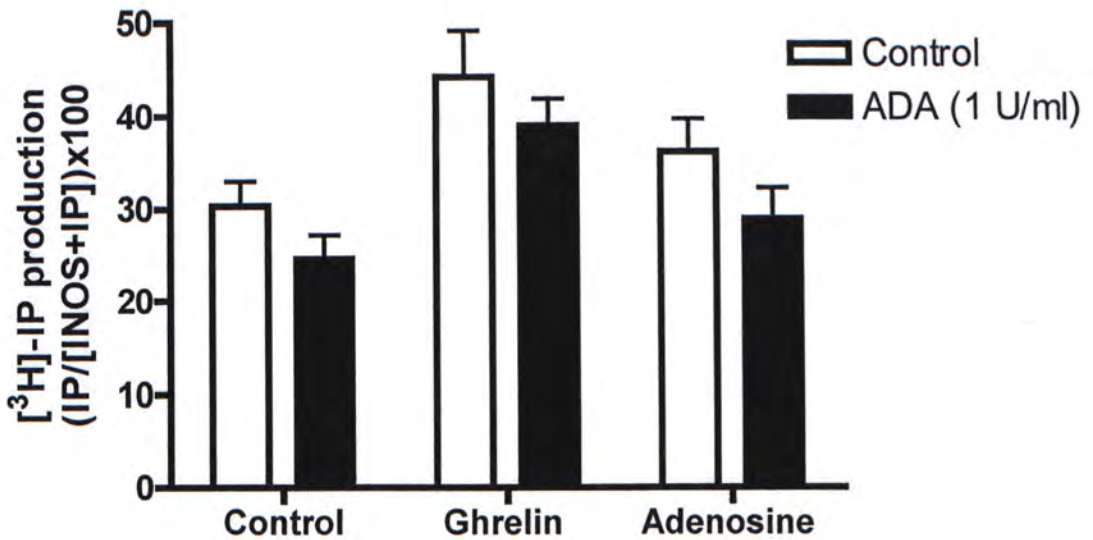


Figure 4.20 Effect of 1 U/ml ADA on basal, 0.1  $\mu$ M ghrelin- and 0.1 mM adenosine-stimulated [ $^3$ H]-IP production. HEK293 cells were transiently transfected with 0.25  $\mu$ g/ml 2myc-hGHS-R1a plus 0.75  $\mu$ g/ml pcDNA3.1(+). After 24 h post-transfection, the cells were labeled with 2  $\mu$ Ci/ml *myo*-[ $^3$ H]-inositol and incubated overnight, and then [ $^3$ H]-IP production was measured as described in Chapter 3. The cells were lysed following pre-incubated with ADA or buffer for 30 min and then 1 h incubation with buffer, ghrelin, adenosine alone. Results in figure represent mean  $\pm$  S.D., n=2, of experiments performed in duplicate.

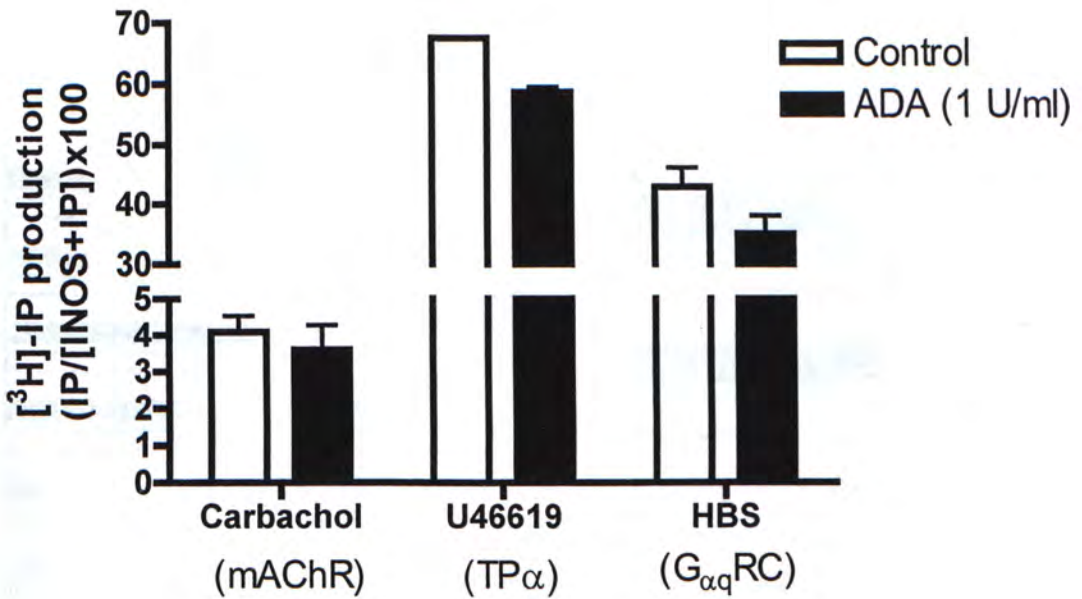
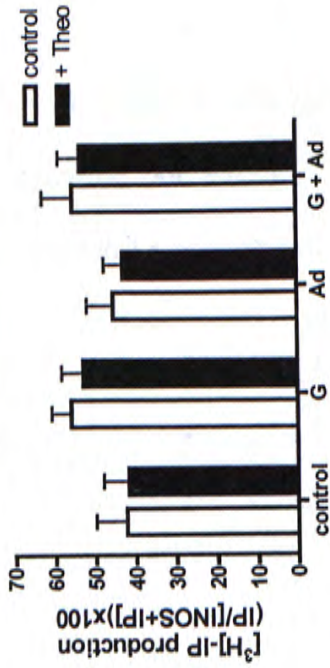
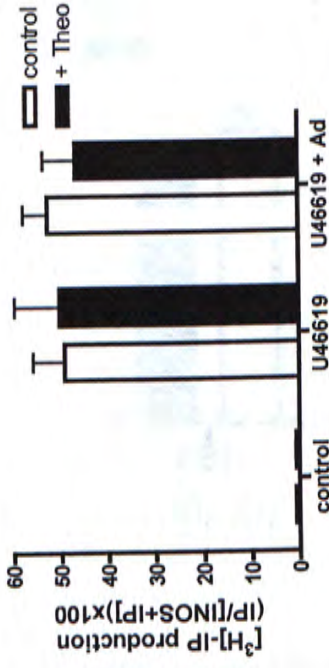


Figure 4.21 Effect of 1 U/ml ADA on [ $^3$ H]-IP production activated by G $_q$ -coupled receptors (muscarinic receptor, mAChR and TP $\alpha$ ) and constitutively active G $_q$  protein (G $\alpha_q$ RC). HEK293 cells were endogenously expressed muscarinic receptor. HEK293 cells were transiently co-transfected 0.25  $\mu$ g/ml TP $\alpha$  or G $\alpha_q$ RC with 0.75  $\mu$ g/ml pcDNA3.1(+). All the cells were pre-incubated with buffer or 1 U/ml ADA for 30 min then the HEK293 cells expressing endogenous mAChR, TP $\alpha$  and G $\alpha_q$ RC were incubated with 0.1 mM carbachol, 1  $\mu$ M U46619 and buffer, respectively. [ $^3$ H]-IP production was determined as chapter 3. Results come from one experiment performed in duplicate, data shown are mean  $\pm$  S.D.

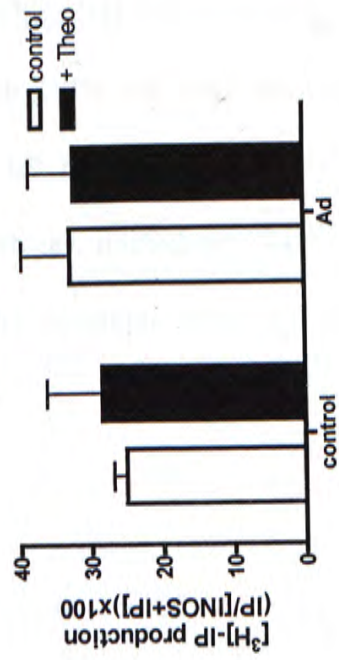
(A) 2myc-hGHS-R1a



(B) hTP $\alpha$



(C) G $\alpha_q$  RC



(D) HEK293 cells

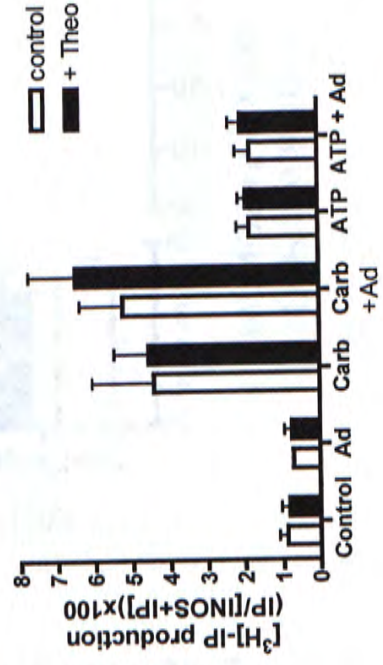




Figure 4.22 Effect of 0.1 mM theophylline (Theo) on basal, agonist and agonist plus adenosine-stimulated [ $^3$ H]-IP production. HEK293 cells transfected with (A) 0.25  $\mu$ g/ml 2myc-hGHS-R.1a plus 0.75  $\mu$ g/ml pcDNA3.1(+) (B) 0.25  $\mu$ g/ml hTP $\alpha$  plus 0.75  $\mu$ g/ml pcDNA3.1(+) (C) 0.25  $\mu$ g/ml G $_{\alpha_q}$ RC plus 0.75  $\mu$ g/ml pcDNA3.1(+) (D) non-transfected HEK293 cells endogenously expressed muscarinic receptor and purinergic (P2Y) receptor. All the cells were pre-incubated with buffer or theophylline for 30 min and then incubated with buffer or agonist or agonist plus adenosine as stated in the graphs. After 24 h post-transfection, the cells were labeled with 2  $\mu$ Ci/ml *myo*-[ $^3$ H]-inositol and incubated overnight, and then [ $^3$ H]-IP production was measured as described in Chapter 3. Results in figure A represents mean  $\pm$  S.E.M., n=3, of experiments performed in duplicate. Results in figure B, C, D represents mean  $\pm$  S.D., n=2, of experiments performed in duplicate.

Key: Ghrelin (G), Adenosine (Ad), Carbachol (Carb).

## **4.5 Role of GHS-R in apoptosis**

Preliminary result in our laboratory showed that sbGHS-R1a and HA-sbGHS-R1b may be involved in the regulation of apoptosis (Fig. 4.23). The staurosporine-induced caspase-3 activity in HEK293 cells was higher than that in HEK-sbGHS-R1a cells, regardless of the transfected plasmid DNA (Fig. 4.23). It suggested that stably expressed sbGHS-R1a protected the cells against staurosporine-induced apoptosis and that sbGHS-R1a has anti-apoptotic properties. HEK293 cells transfected with HA-sbGHS-R1b had a higher basal and staurosporine-induced caspase-3 activity than that in HEK293 cells, suggesting that HA-sbGHS-R1b is pro-apoptotic. In addition, the pro-apoptotic effect of HA-sbGHS-R1b was masked by the anti-apoptotic effect of sbGHS-R1a, as the caspase-3 activity did not change much when HEK-sbGHS-R1a cells were transfected with HA-sbGHS-R1b. In conclusion, these results suggested that sbGHS-R1a is anti-apoptotic, while HA-sbGHS-R1b is pro-apoptotic. The following experiments were performed to optimize the conditions for further study of the role of hGHS-R subtypes in the regulation of apoptosis.

### **4.5.1 Different methods to measure caspase-3 activity**

#### **4.5.1.1 Colorimetric assay**

In the following colorimetric assay experiments, the caspase-3 activities were measured as described in Chapter 3. The cells were incubated with apoptotic inducer in the presence of FBS. DMSO treatment group showed the caspase-3 activity was



not affected by the solvent of apoptotic inducers, as the caspase-3 activity remain unchanged after DMSO incubation.

#### **4.5.1.1.1 Time course for staurosporine and etoposide in HEK293 cells**

The optimal incubation time for each apoptotic inducer was determined so that the apoptotic inducer will induce a measurable caspase-3 activity in HEK293 cells. HEK293 cells were incubated with 10  $\mu$ M staurosporine or 100  $\mu$ M etoposide in the presence of FBS for different incubation times as stated in figure 4.24A and 4.24B.

A time-dependent increase in caspase-3 activity was observed for both staurosporine and etoposide treatment of HEK293 cells (Fig. 4.24). For the staurosporine-induced caspase-3 activity, it reached maximum at 8 h, there was  $9.77 \pm 1.94$  fold increase,  $n=2$ , in caspase-3 activity (Fig. 4.24A) compared to the caspase-3 activity at 0 h staurosporine incubation and 0.1% DMSO used in dissolving the staurosporine did not affect the caspase-3 activity in HEK293 cells. For the etoposide-induced caspase-3 activity, 48 h incubation induced 8.10-fold increase,  $n=1$ , when compared to the caspase-3 activity at 0 h etoposide incubation, it was better than 24 h treatment which induced 2.51-fold increase,  $n=1$  (Fig. 4.24B). Although 24 h etoposide treatment did not induce a highest caspase-3 activity, the size of the etoposide-induced caspase-3 activity is clearly measurable. In addition, 48 h treatment may not be ideal to use, as it may need the etoposide replacement after 24 hours. Therefore, in the following experiments, HEK293 cells were incubated with 10  $\mu$ M staurosporine or 100  $\mu$ M etoposide for 8 h and 24 h respectively, in order to



have an optimal measurement of caspase-3 activity. The staurosporine-induced caspase-3 activity was very small in this experiment because a small amount of caspase-3 substrate (4  $\mu\text{M}$ ) was used. In the experiment using etoposide, 200  $\mu\text{M}$  caspase-3 substrate was used, and the absolute level of etoposide-induced caspase-3 activities was larger than that in staurosporine experiment. Therefore, 200  $\mu\text{M}$  caspase-3 substrate was used in the following experiments.

When HEK293 cells were incubated with 100  $\mu\text{M}$  etoposide for 24 h, there was only 2.51-fold increase in caspase-3 activity, however, in 8 h staurosporine-induced caspase-3 activity, there was  $9.77 \pm 1.94$  fold increase. Therefore, higher concentrations of etoposide were used, to see whether it gives a greater caspase-3 activity. In this experiment, HEK293 cells were incubated with 100  $\mu\text{M}$ , 150  $\mu\text{M}$  and 200  $\mu\text{M}$  etoposide for 24 h in the presence of serum. The etoposide-induced caspase-3 activity did not increase further by using higher etoposide concentrations (Fig. 4.25), and the DMSO concentrations used in dissolving the staurosporine did not affect the caspase-3 activity in HEK293 cells. Therefore, in the following experiments, HEK293 cells were incubated with 100  $\mu\text{M}$  etoposide for 24 h to have an optimal caspase-3 activity.

Serum starvation was also used to induced caspase-3 activity in HEK293 cells, however incubated the cells in the medium without serum for 24 h, there was still no increase in the caspase-3 activity (Fig. 4.26).

#### 4.5.1.1.2 Effect of 2myc-hGHS-R1a on staurosporine- and etoposide-induced caspase-3 activity

To investigate the role of 2myc-hGHS-R1a in the regulation of apoptosis, HEK-2myc-hGHS-R1a polyclonal cells were used. The cells were incubated with 10  $\mu$ M staurosporine for 4 h and 100  $\mu$ M etoposide for 24 and 48 h in the presence of serum. Wild type HEK293 cells were used as a reference. The caspase-3 activity in all the DMSO treated groups of HEK-2myc-hGHS-R1a polyclonal cells was as the same as the HEK293 cells, were around 0.02 pmol/min/ $\mu$ g protein (Fig. 4.27). In HEK-2myc-hGHS-R1a cells, the staurosporine-induced caspase-3 activity was lower than that in HEK293 cells (Fig. 4.27A). It suggested that the expression of 2myc-hGHS-R1a might protect the HEK293 cells to undergo staurosporine-induced apoptosis by 25.1% inhibition. It is expected, as from the preliminary results described in section 4.5, it suggested that the stably expressing sbGHS-R1a in the HEK293 cells, the staurosporine-induced caspase-3 activity was lower than that in HEK293 cells, that is stably expression of sbGHS-R1a induced an anti-apoptotic effect to HEK293 cells. In addition, as demonstrated in section 4.1, the properties of hGHS-R1a and sbGHS-R1a were the same.

In contrast to staurosporine, etoposide-induced caspase-3 activity was higher in the HEK-2myc-hGHS-R1a (Fig. 4.27B). It suggested that 2myc-hGHS-R1a might enhance etoposide-induced apoptosis in HEK293 cells by  $0.34 \pm 0.38$  fold,  $n=2$ , and 0.68 fold for 24 and 48 h, respectively. However, there was a large variation in 24 h etoposide incubation data, and the other two treatment groups were only tested once,



so it needs more experiments to conclude the role of 2myc-hGHS-R1a in staurosporine- and etoposide-induced caspase-3 activity.

#### **4.5.1.1.3 Time course for staurosporine and etoposide in sbGHS-R monoclonal stable cell line**

There was the failure of the development of monoclonal HEK-2myc-hGHS-R1a and HEK-2myc-hGHS-R1b cells lines and the variable potentiating effect in co-transfection. In addition, the properties between human and seabream GHS-R are similar as described in section 4.1. Therefore, HEK-sbGHS-R1a and HEK-sbGHS-R1b monoclonal stable cell lines were used to study the role of GHS-R in apoptosis regulation. To optimize the colorimetric assay conditions used in the sbGHS-R monoclonal stable cell lines, the apoptotic inducers incubation time was determined. The experimental design is similar to section 4.5.1.1.1, in these experiments not only HEK293 cells were used, but also HEK-sbGHS-R1a and HEK-sbGHS-R1b.

Among these three cell lines, in order to have an optimized 10  $\mu$ M staurosporine- and 100  $\mu$ M etoposide-induced caspase-3 activity, the cells were incubated for 8 h and 24 h respectively (Fig. 4.28 and Fig. 4.29). Compared to the caspase-3 activity in 0 h staurosporine incubation, for 8 h staurosporine-induced caspase-3 activity, there were 14.57-fold increase and 13.30-fold increase,  $n=1$ , for HEK-sbGHS-R1a and HEK-sbGHS-R1b cells, respectively. Compared to the caspase-3 activity at 0 h etoposide incubation, for 24 h etoposide-induced caspase-3 activity, there were



0.91-fold increase and 0.45-fold increase,  $n=1$ , for HEK-sbGHS-R1a and HEK-sbGHS-R1b cells, respectively.

The staurosporine-induced caspase-3 activity in HEK293 cells was greater than that in the HEK-sbGHS-R1a and HEK-sbGHS-R1b cell lines (Fig. 4.28), the similar pattern was also observed in 24 h etoposide-induced caspase-3 activity (Fig. 4.29). That suggests that the stably expressed sbGHS-R1a and sbGHS-R1b caused an anti-apoptotic effect to HEK293 cells. This phenomenon was also observed in later experiments, such as figure 4.31. By comparing the two stable cell lines, HEK-sbGHS-R1a has a greater staurosporine-induced caspase-3 activity than the HEK-sbGHS-R1b (Fig. 4.28); This was also observed in etoposide-induced caspase-3 activity at 24 h (Fig. 4.29). It suggested that the anti-apoptotic effect raised by sbGHS-R1b may be greater than sbGHS-R1a, or it is just due to the difference in the receptor expression level. In general, the staurosporine-induced caspase-3 activity was greater than the one induced by etoposide.

#### **4.5.1.1.4 Effect of sbGHS-Rs on staurosporine- and etoposide-induced caspase-3 activity in HEK293 cells**

To determine the role of sbGHS-R1a and sbGHS-R1b on apoptosis, HEK293 cells were transfected with 1  $\mu\text{g/ml}$  sbGHS-R1a and sbGHS-R1b, and then the cells were incubated with 10  $\mu\text{M}$  staurosporine for 8 h or 100  $\mu\text{M}$  etoposide for 48 h in the presence of serum. HEK293 cells transfected with 1  $\mu\text{g/ml}$  empty vector, namely pBK-CMV, was used as the control.

The expression of sbGHS-R1a or sbGHS-R1b did not make any marked changes on the staurosporine-induced caspase-3 activity (Fig. 4.30A). It indicated that sbGHS-R does not affect the staurosporine-induced caspase-3 activity, but it might be because the transiently expressed receptor level is not high enough to cause an observable effect on caspase-3 activity. For the etoposide-induced caspase-3 activity, sbGHS-R1a and sbGHS-R1b expressed in the cells slightly increased the caspase-3 activity (Fig. 4.30B). In this experiment, the fold increase in etoposide-induced caspase-3 activity is much smaller than the previous experiments, so it needs further experiments to conclude the role of sbGHS-R in etoposide-induced caspase-3 activity.

#### **4.5.1.1.5 Effect of sbGHS-Rs on staurosporine-induced caspase-3 activity in sbGHS-R monoclonal stable cell line**

To investigate the role of sbGHS-R1a and sbGHS-R1b on the staurosporine-induced apoptosis in HEK293, HEK-sbGHS-R1a and HEK-sbGHS-R1b cells, these cells were transfected with 1  $\mu\text{g}/\text{ml}$  sbGHS-R1a or sbGHS-R1b, and then the cells were incubated with 10  $\mu\text{M}$  staurosporine for 8 h in the presence of serum. Cells were transfected with 1  $\mu\text{g}/\text{ml}$  empty vector, namely pBK-CMV, was used as a control.

The staurosporine-induced caspase-3 activity was less in the HEK-sbGHS-R1a and HEK-sbGHS-R1b cells than that in HEK293 cells, this pattern did not alter by the transiently expressed pBK-CMV, sbGHS-R1a and sbGHS-R1b (Fig. 4.31). The



transiently expression of pBK-CMV (Fig. 4.31A), sbGHS-R1a (Fig. 4.31B) and sbGHS-R1b (Fig. 4.31C) did not make any changes on the staurosporine-induced caspase-3 activity in HEK293, HEK-sbGHS-R1a and HEK-sbGHS-R1b cells. It indicated that sbGHS-R did not affect the staurosporine-induced caspase-3 activity. From the preliminary results described in section 4.5, HA-sbGHS-R1b is pro-apoptotic and stably expressed sbGHS-R1a is anti-apoptotic, therefore, part of the expected results is the HEK293 transfected with sbGHS-R1b results in an increase in staurosporine-induced caspase-3 activity in HEK293 cells and the caspase-3 activity in the HEK-sbGHS-R1a transfected with sbGHS-R1b is lower than that in the HEK293 cells transfected with sbGHS-R1b.

#### **4.5.1.1.6 Differences between epitope-tagged and non-tagged sbGHS-Rs in staurosporine-induced caspase-3 activity**

To investigate whether the presence of the epitope-tag will alter the function of sbGHS-R in apoptosis, HEK293 and HEK-sbGHS-R1a were transfected with 1  $\mu\text{g/ml}$  HA-tagged or non-tagged sbGHS-R1a and sbGHS-R1b, and then the cells were incubated with 10  $\mu\text{M}$  staurosporine for 8 h in the absence of serum. HEK293 cells transfected with 1  $\mu\text{g/ml}$  empty vector, namely pBK-CMV or pcDNA3.1(+)/Zeo, were used as controls.

In general, the caspase-3 activities were higher than the previous experiments, it is because the cells incubated with apoptotic inducers in the absence of serum. The expression of HA-sbGHS-R1a or HA-sbGHS-R1b in both HEK293 and



HEK-sbGHS-R1a cells caused a slight increase in staurosporine-induced caspase-3 activity (Figs. 4.32A and 4.32C). In contrast to epitope-tagged sbGHS-R, the expression of sbGHS-R1a and sbGHS-R1b did not affect the staurosporine-induced caspase-3 activity (Figs. 4.32B and 4.32D). It indicated that the epitope-tag may alter the properties of sbGHS-R in the regulation of apoptosis.

#### **4.5.1.1.7 The role of epitope-tagged sbGHS-R1b in staurosporine-induced caspase-3 activity**

The epitope-tagged sbGHS-R seems involved in regulating the staurosporine-induced caspase-3 activity, as described in section 4.5.1.1.6. The role of HA-sbGHS-R1b in regulating apoptosis was studied and tried to repeat the preliminary result stated in section 4.5. HEK293 and HEK-sbGHS-R1a cells were transfected with 1  $\mu$ g/ml HA-sbGHS-R1b, and then the cells were incubated with 10  $\mu$ M staurosporine for 8 h in the absence of serum. Cells transfected with 1  $\mu$ g/ml pcDNA3.1(+)/Zeo were used as controls.

When HEK293 cells were transfected with HA-sbGHS-R1b, the staurosporine-induced caspase-3 activity increased by 15.29-fold compared to basal caspase-3 activity, but there was just 10.49-fold increase in the HEK293 cells transfected with empty vector (Fig. 4.33). It suggested that the expression of HA-sbGHS-R1b enhances the HEK293 cells to undergo apoptosis. The transient expression of HA-sbGHS-R1b in HEK-sbGHS-R1a cells caused a slight increase in the staurosporine-induced caspase-3 activity. In addition, the staurosporine-induced

caspase-3 activity was less in the HEK-sbGHS-R1a than HEK293 cells. It indicated that sbGHS-R1a stably expressed in HEK293 cells protects against apoptosis as seen in figure 4.23.

These results were as the same as the preliminary data described in section 4.5, except the basal caspase-3 activity in the HEK293 cells transfected with HA-sbGHS-R1b did not increase when compared to HEK293 cells transfected with empty vector, it is still unknown why it is the case. In addition, it indicated that using HA-tagged GHS-R, rather than the non-tagged GHS-R and induced caspase-3 activity by apoptotic inducer in the absence of serum, the same conclusion can be obtained as the preliminary data described in section 4.5.

#### **4.5.1.1.8 Effect of staurosporine and etoposide on GHS-R1a signaling**

It is useful to choose an apoptotic inducer which does not affect the signaling response to 2myc-hGHS-R1a. HEK-2myc-hGHS-R1a polyclonal cells were incubated with the 10  $\mu$ M staurosporine or 100  $\mu$ M etoposide alone and together with 0.1  $\mu$ M ghrelin. The cells just incubated with or without ghrelin were used to show the basal and the ghrelin-stimulated [ $^3$ H]-IP production in the 2myc-hGHS-R1a signaling in the absence of apoptotic inducer. The DMSO treatment groups were used to show that any changes in the apoptotic inducer treatment groups are due to inducer itself, and are not due to the solvent. Then the [ $^3$ H]-IP production was measured, as described in chapter 3. A similar experiment was carried out to determine the effect of apoptotic inducers on sbGHS-R1a signaling, just using



HEK-sbGHS-R1a cells and 3.6  $\mu\text{M}$  GHRP-6, instead of HEK-2myc-hGHS-R1a and ghrelin, respectively. 3.6  $\mu\text{M}$  GHRP-6 is the  $\text{EC}_{50}$  concentration in [ $^3\text{H}$ ]-IP production in HEK-sbGHS-R1a cells (Chan *et al.*, 2004b).

The basal [ $^3\text{H}$ ]-IP production in the HEK-2myc-hGHS-R1a polyclonal cells was as the same as the cells incubated with 10  $\mu\text{M}$  staurosporine or 100  $\mu\text{M}$  etoposide (Fig. 4.34A). The ghrelin-stimulated [ $^3\text{H}$ ]-IP production was as the same as the cells incubated with 10  $\mu\text{M}$  staurosporine plus ghrelin or 100  $\mu\text{M}$  etoposide with ghrelin. These indicated that neither the basal nor the ghrelin-stimulated [ $^3\text{H}$ ]-IP production were affected by 10  $\mu\text{M}$  staurosporine or 100  $\mu\text{M}$  etoposide.

The effect of staurosporine and etoposide on sbGHS-R1a activated [ $^3\text{H}$ ]-IP production were similar to that in HEK-2myc-hGHS-R1a polyclonal cells, except the effect of staurosporine on the basal [ $^3\text{H}$ ]-IP production. When HEK-sbGHS-R1a cells were incubated with 10  $\mu\text{M}$  staurosporine, the basal [ $^3\text{H}$ ]-IP production was increased by 0.44 fold (Fig. 4.34B). This difference may be due to the low basal activity in the HEK-2myc-hGHS-R1a polyclonal cells, so the effect of staurosporine on the basal [ $^3\text{H}$ ]-IP production cannot be observed. To confirm it, instead of using HEK-2myc-hGHS-R1a polyclonal cells, the effect of staurosporine on basal [ $^3\text{H}$ ]-IP production should be studied in the HEK293 cells which transiently expressed 2myc-hGHS-R1a, which shows a better constitutive activity (Figs. 4.8, 4.18, 4.19 and 4.22). Although there is a clue to suggest that staurosporine may affect the basal [ $^3\text{H}$ ]-IP production in sbGHS-R1a signaling, but since staurosporine always can



induce caspase-3 activity, it is still used in the later experiment as an internal positive control.

#### 4.5.1.2 BRET<sup>2</sup> assay

Besides colorimetric assay, BRET<sup>2</sup> assay was used to monitor the caspase-3 activity in living HEK293 cells, which uptake and express the caspase-3 biosensor and the target receptor. HEK293 cells were transfected with 1 µg/ml caspase-3 biosensor or positive vector in 60 mm dish. After 24 h post-transfection, the transfected cells were transferred into white 96-well plate and left in the incubator overnight. The cells were incubated with 10 µM staurosporine or 0.1% DMSO for different time periods, and then the caspase-3 activity was measured as described in Chapter 3. The positive vector transfected cells were used to show that the decrease in the BRET<sup>2</sup> signal of the caspase-3 biosensor expressed cells, it is because of the activation of the caspase-3 and the cleavage of the biosensor.

After incubation with staurosporine, the BRET<sup>2</sup> signal in the caspase-3 biosensor transfected cells had a slight decrease at 4 h, and there was 28.57% decrease at 8 h, in which the BRET<sup>2</sup> signal in the cells incubated with DMSO remains unchanged (Fig. 4.35). At 24 h, all the caspase-3 biosensor in the transfected cells was cleaved, as the BRET<sup>2</sup> signal was decreased to zero. In the positive vector expressed cells, the BRET<sup>2</sup> signal did not decrease in the staurosporine treatment groups, except at 24 h staurosporine treatment. There were decrease in the BRET<sup>2</sup> signal in the caspase-3 biosensor expressed cells after staurosporine treatment, it means staurosporine can

induce caspase-3 activity in HEK293 cells. However, the size of BRET<sup>2</sup> signal reduction is small even incubated the cells with staurosporine for 8 h. This project is to study the role of GHS-R in apoptosis, within this small change in the BRET<sup>2</sup> signal, it is very difficult to observe the effect of GHS-R in caspase-3 activity. In contrast to BRET<sup>2</sup> assay, in the colorimetric assay, HEK293 cells incubated with staurosporine for 8 h, there was larger fold increase in caspase-3 activity.

#### **4.5.1.3 FRET assay**

One of the methods which is similar to BRET<sup>2</sup> assay was also used to study the caspase-3 activity, it is FRET assay. From other previous studies, there should be a very sharp decrease in the FRET signals, when there is an increase in the caspase-3 activity (Luo *et al.*, 2001b). HEK293 cells were transfected with 0.5 µg/ml FRET biosensor plus 0.5 µg/ml target plasmid DNA or 1 µg/ml target plasmid DNA, and then on the assay day, the cells were incubated with 0.25% DMSO, 10 µM staurosporine or 100 µM etoposide for different incubation times. The caspase-3 assay was measured as described in Chapter 3. The cells transfected with 1 µg/ml target plasmid DNA were used as a control, the FRET signal should remain unchanged for any treatments. From the preliminary data, the results were not reproducible, as the biosensor was cleaved at different time points for the same treatment between different independent experiments.

#### **4.5.1.4 Conclusions**

Before further examining the role of GHS-Rs in the regulation of apoptosis using



hGHS-Rs, it is necessary to optimize the conditions used in the colorimetric assay, in order to measure the caspase-3 activity effectively. In HEK293 cells, the optimal incubation time for staurosporine and etoposide is 8 and 24 h, respectively. In HEK-2myc-hGHS-R1a polyclonal stable cell line, it seems stably expressed 2myc-hGHS-R1a protected the cells against staurosporine-induced caspase-3 activity, but enhanced the cells undergo etoposide-induced caspase-3 activity. However, the effect of staurosporine- and etoposide-induced caspase-3 activity between HEK293 and HEK-2myc-hGHS-R1a is small, it might due to the use of polyclonal stable cell line.

Since the use of polyclonal stable cell line may result in small difference in staurosporine- and etoposide-induced caspase-3 activity between HEK293 and HEK-2myc-hGHS-R1a cells, so instead of using HEK-2myc-hGHS-R1a polyclonal stable cell line, HEK-sbGHS-R1a and HEK-sbGHS-R1b monoclonal stable cell lines were used. In HEK-sbGHS-R1a and HEK-sbGHS-R1b cells, in order to have an optimal staurosporine- and etoposide-induced caspase-3 activity, it was necessary to incubate these cells with staurosporine and etoposide for 8 and 24 h. The staurosporine- or etoposide-induced caspase-3 activity was lower in these stable cell lines than in the non-transfected HEK293 cells, it showed that the stably expressed sbGHS-R1a and sbGHS-R1b induced anti-apoptotic effect to the cells. However, in transiently transfected sbGHS-R1a or sbGHS-R1b into HEK293, HEK-sbGHS-R1a and HEK-sbGHS-R1b cells, there was no effect on the staurosporine-induced caspase-3 activity. These results are not expected, as in the preliminary study



described in section 4.5, transiently transfected HA-sbGHS-R1b into HEK293 cells, the staurosporine-induced caspase-3 activity was higher than that in HEK293 cells.

The difference between the epitope-tagged and non-tagged sbGHS-R in apoptosis regulation and the presence of serum in staurosporine-induced caspase-3 activity was investigated. The staurosporine-induced caspase-3 activity was larger in the absence of serum and the staurosporine-induced caspase-3 activity was larger in the HEK293 cells transfected with HA-sbGHS-R1a or HA-sbGHS-R1b than in the non-transfected HEK293 cells. When HEK293 and HEK-sbGHS-R1a cells were transfected with HA-sbGHS-R1b and incubated with staurosporine in the absence of serum, it showed that the HA-sbGHS-R1b caused an increase in the staurosporine-induced caspase-3 activity and this pro-apoptotic effect of HA-sbGHS-R1b was inhibited by stably expressed sbGHS-R1a. It indicated that sbGHS-R1a is anti-apoptotic. These results matched the preliminary results described in section 4.5, except there was no increase in the basal caspase-3 activity in the HA-sbGHS-R1b transfected cells.

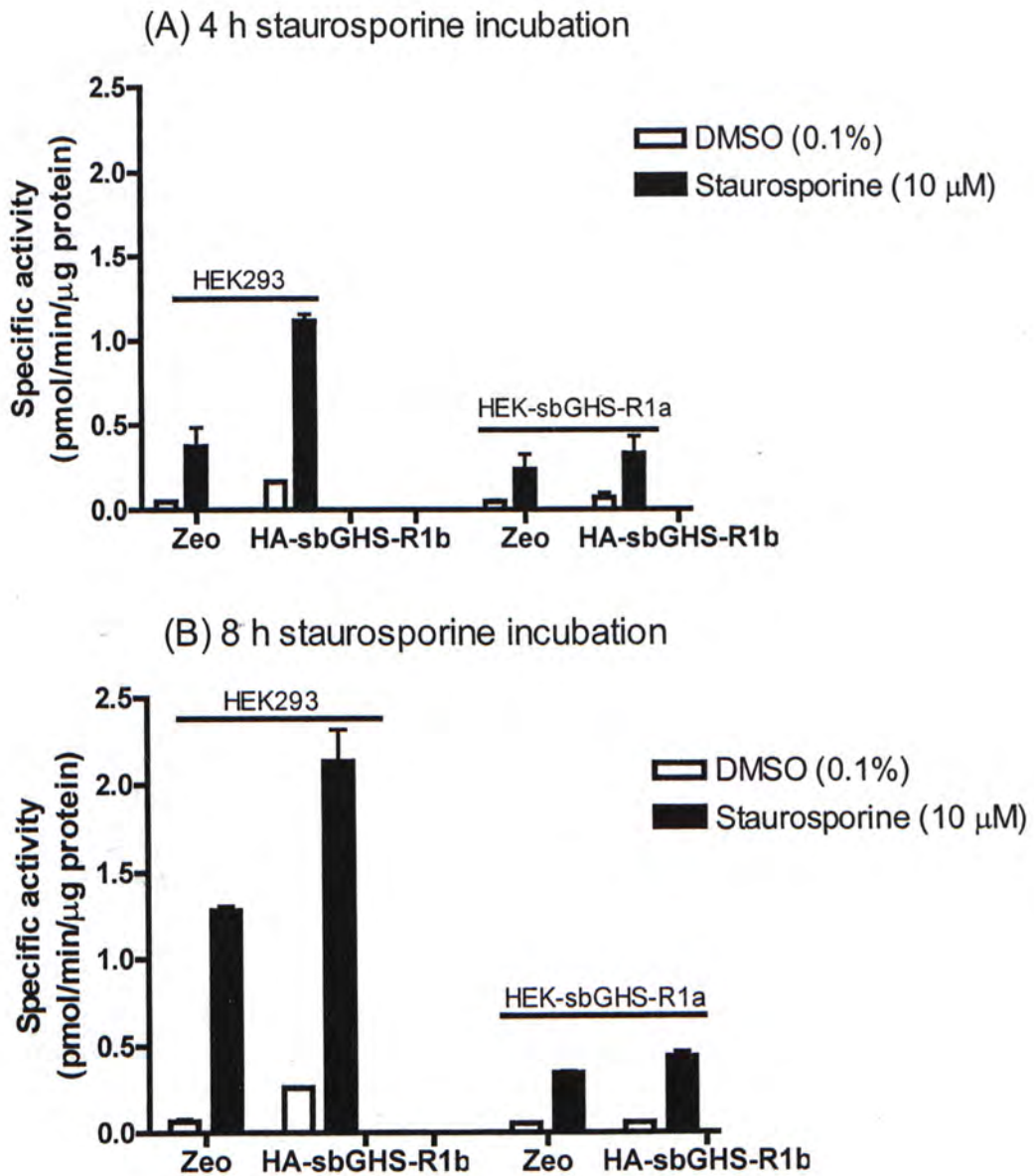


Figure 4.23 Effect of sbGHS-R on staurosporine-induced caspase-3 activity. HEK293 and HEK-sbGHS-R1a cells were transfected with 1  $\mu\text{g/ml}$  pcDNA3.1(+)/Zeo (Zeo) or HA-sbGHS-R1b, and then the cells were incubated with 10  $\mu\text{M}$  staurosporine or 0.1% DMSO for 4 h or 8 h. At the end of the incubation time, the cells were lysed and the protein was collected for caspase-3 activity measurement as described in Chapter 3. Results in figure A represents mean  $\pm$  S.D.,  $n=2$ , of experiments performed in duplicate. Results in figure B come from one experiment performed in duplicate, data shown are mean  $\pm$  S.D. (These experiments were performed by Chris Leung.)

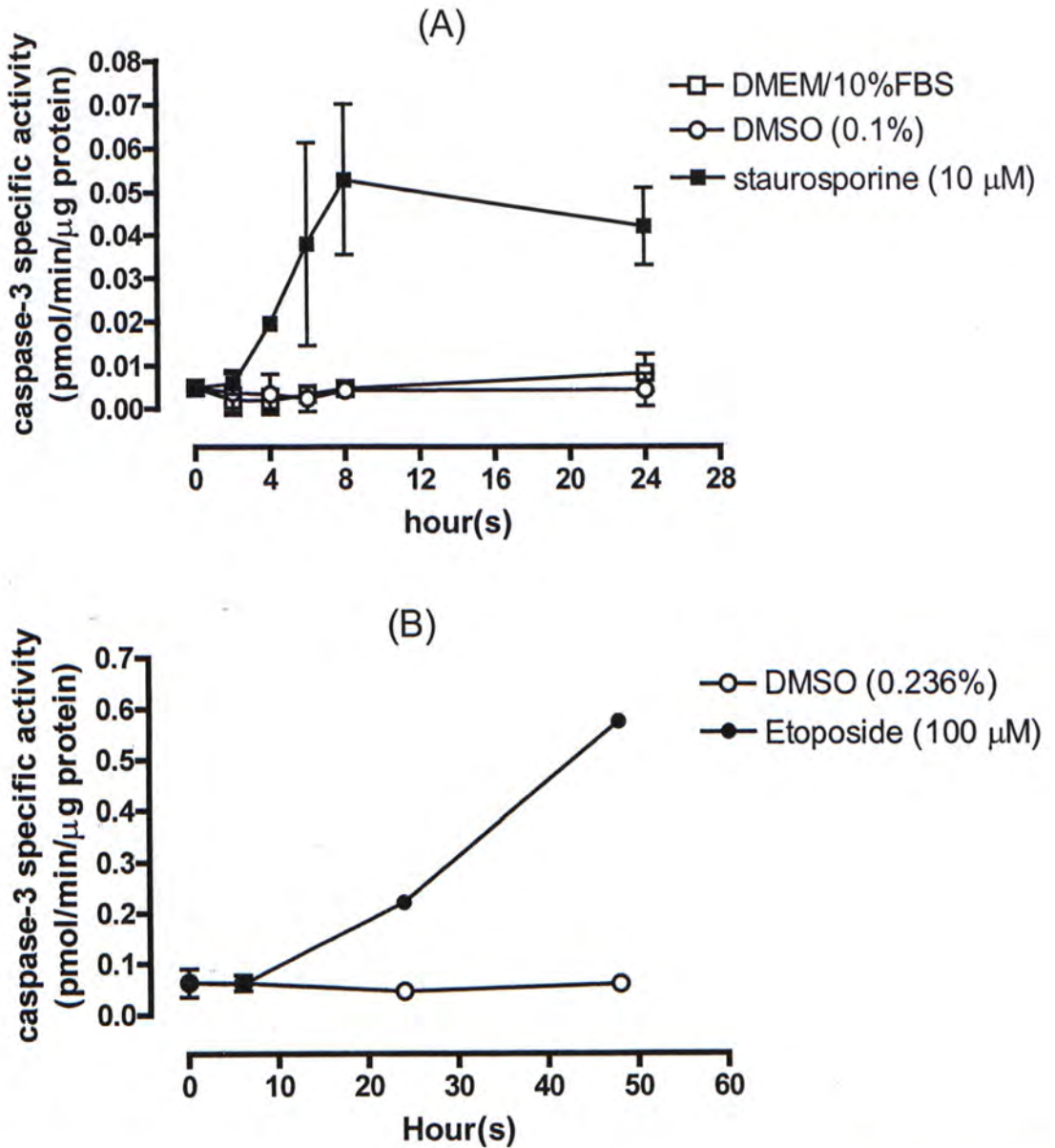


Figure 4.24 Activation of caspase-3 activity by (A) 10  $\mu\text{M}$  staurosporine and (B) 100  $\mu\text{M}$  etoposide with different incubation time in HEK293 cells. At the end of each incubation time, the cells were lysed and the protein was collected for caspase-3 activity measurement as described in Chapter 3. (A) 4  $\mu\text{M}$  caspase-3 substrate was used and results in figure represent mean  $\pm$  S.D.,  $n=2$ , of experiments performed in duplicate. (B) 200  $\mu\text{M}$  caspase-3 substrate was used and results come from one experiment performed in duplicate, data shown are mean  $\pm$  S.D.



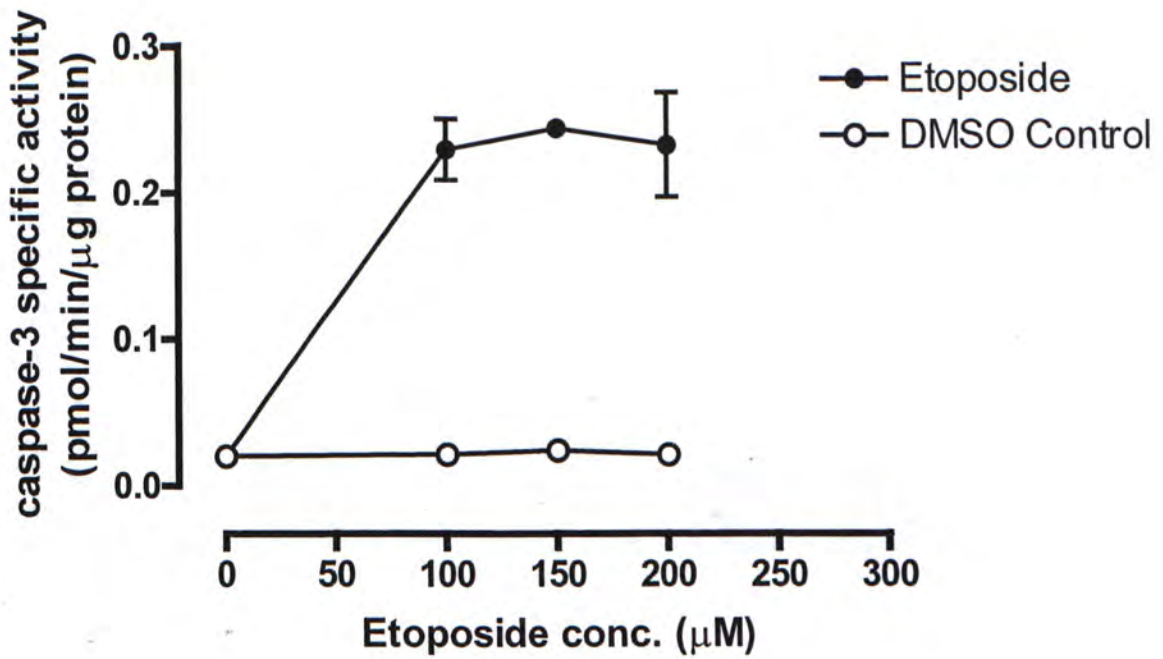


Figure 4.25 Activation of caspase-3 activity by different concentrations of etoposide in HEK293 cells. HEK293 cells incubated with different DMSO concentrations, to match each etoposide concentration for 24 h. At the end of each incubation time, the cells were lysed and the protein was collected for caspase-3 activity measurement as described in Chapter 3. Results come from one experiment performed in duplicate, data shown are mean  $\pm$  S.D.

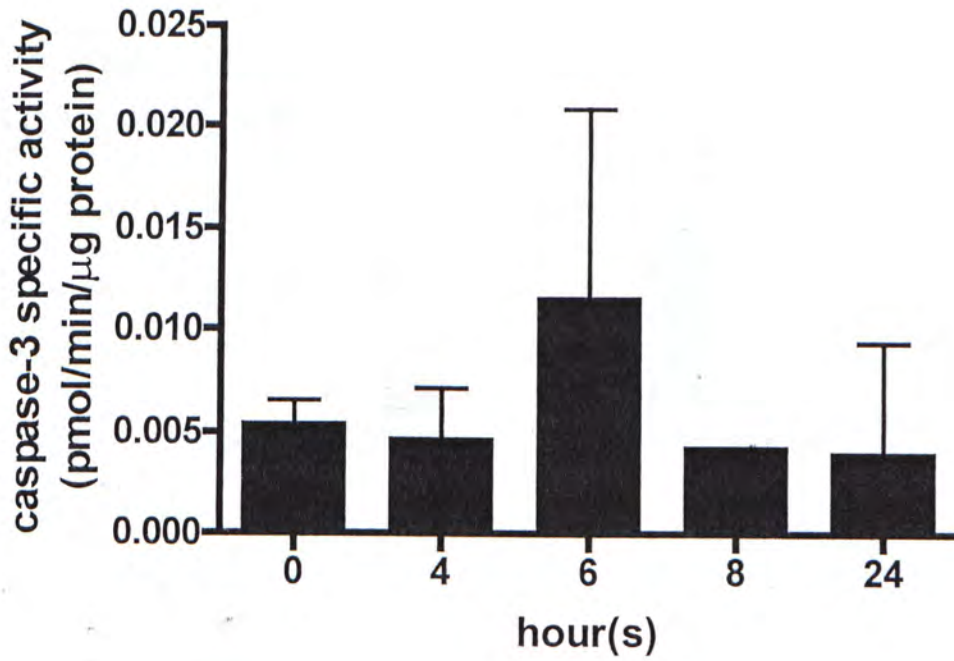


Figure 4.26 Lack of serum starvation induced caspase-3 activity in HEK293 cells. HEK293 cells were incubated in plain DMEM for different time periods as stated in the graph. At the end of each incubation time, the cells were lysed and the protein was collected for caspase-3 activity measurement as described in Chapter 3. Results come from one experiment performed in duplicate, data shown are mean  $\pm$  S.D.

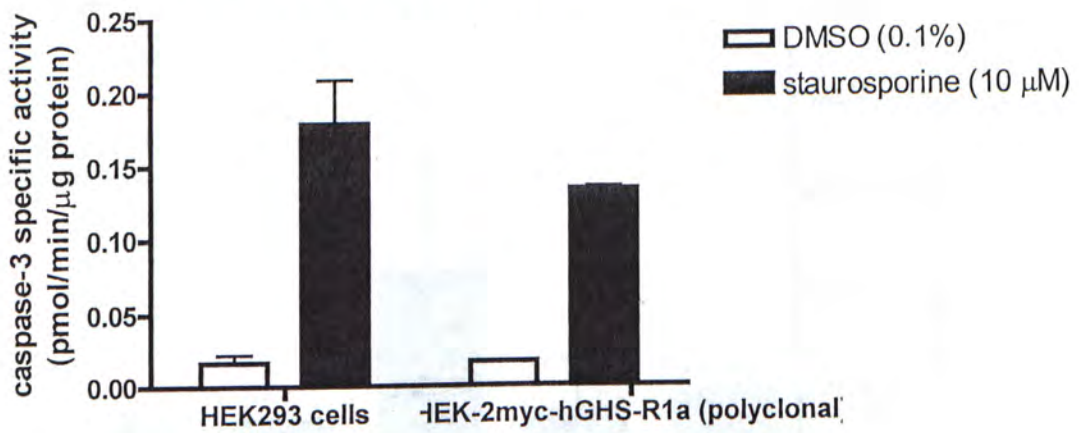
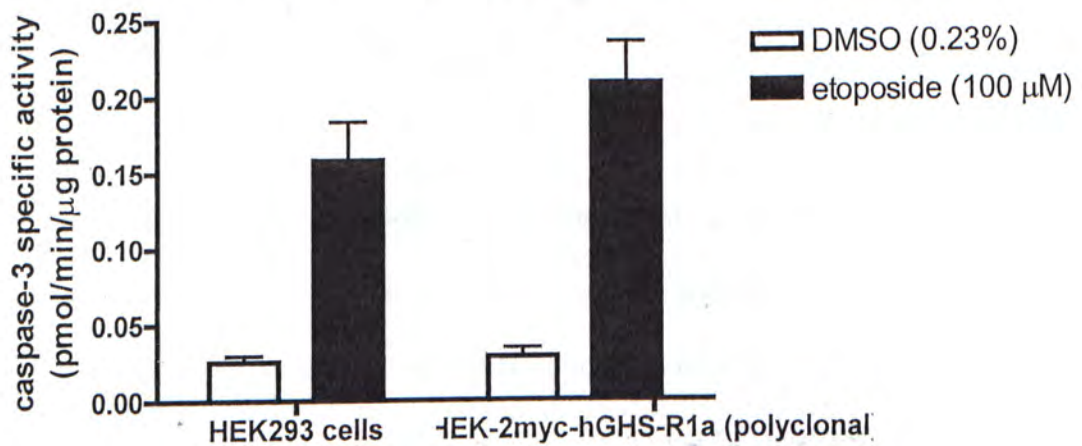
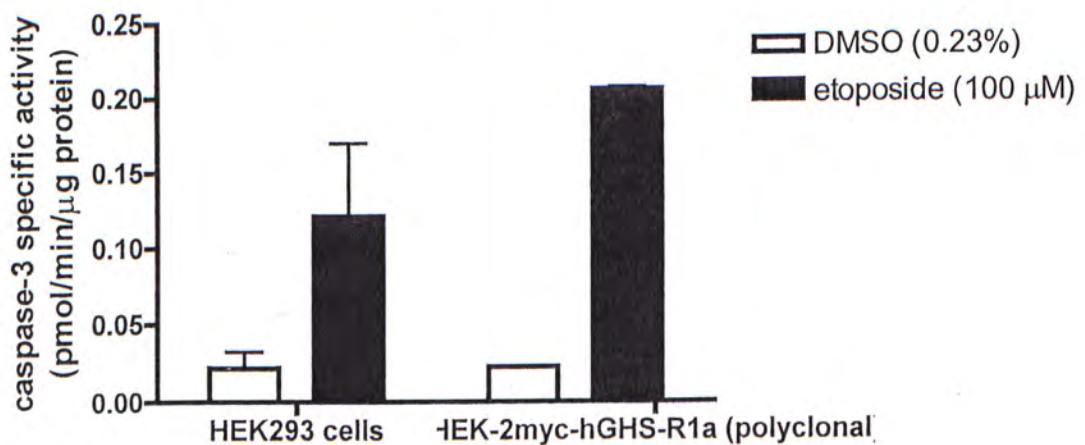
**(A) 4 hours staurosporine incubation****(B) 24 hours etoposide incubation****(C) 48 hours etoposide incubation**



Figure 4.27 Effect of 2myc-hGHS-R1a on (A) 10  $\mu$ M staurosporine- and (B) 100  $\mu$ M etoposide-induce caspase-3 activity in HEK293 cells. HEK293 cells incubated with different DMSO concentrations, which respected for staurosporine or etoposide concentration, act as a control. HEK293 cells and HEK-2myc-hGHS-R1a polyclonal stable cell line were incubated with (A) staurosporine for 24 h or (B) etoposide for 24 h and (C) 48 h. At the end of each incubation time, the cells were lysed and the protein was collected for caspase-3 activity measurement as described in Chapter 3. Results in figure A and C come from one experiment performed in duplicate, data showed are mean  $\pm$  S.D. Results in figure B represent mean  $\pm$  S.D., n=2, of experiments performed in duplicate.

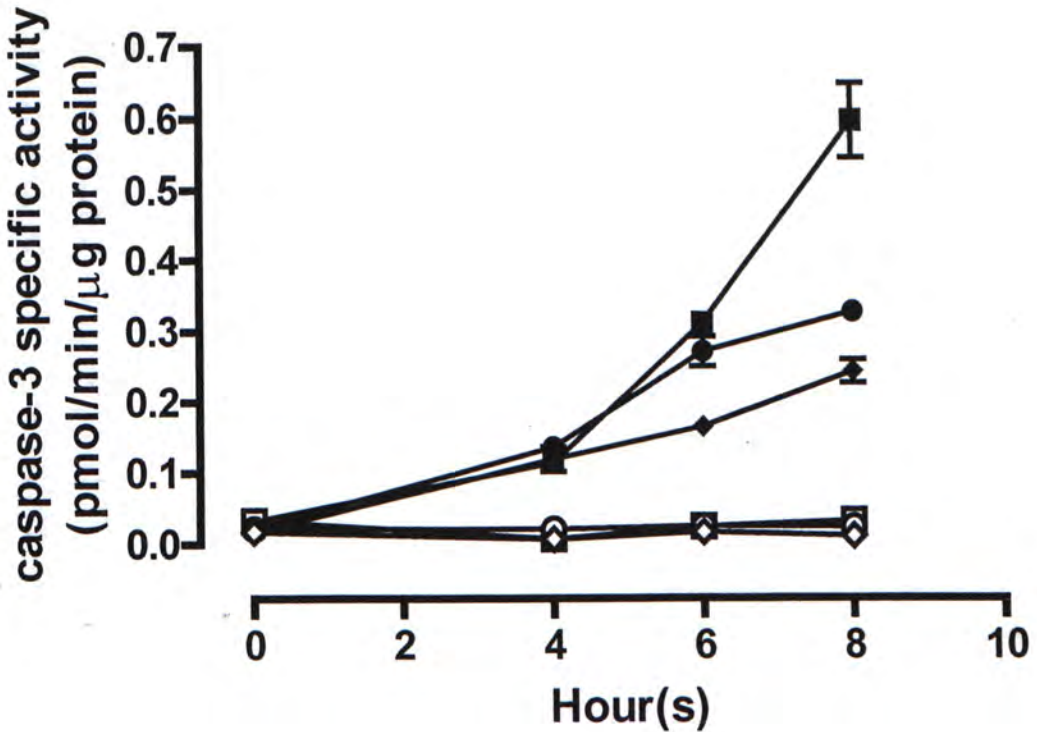


Figure 4.28 Activation of caspase-3 activity by 10  $\mu$ M staurosporine with different incubation time in (■) HEK293 cells, (●) HEK-sbGHS-R1a monoclonal stable cell line and (◆) HEK-sbGHS-R1b monoclonal stable cell line. The open symbols represent the cells incubated with 0.1% DMSO as the control for staurosporine. At the end of each incubation time, the cells were lysed and the protein was collected for caspase-3 activity measurement as described in Chapter 3. Results in figure come from one experiment performed in duplicate, data showed are mean  $\pm$  S.D.

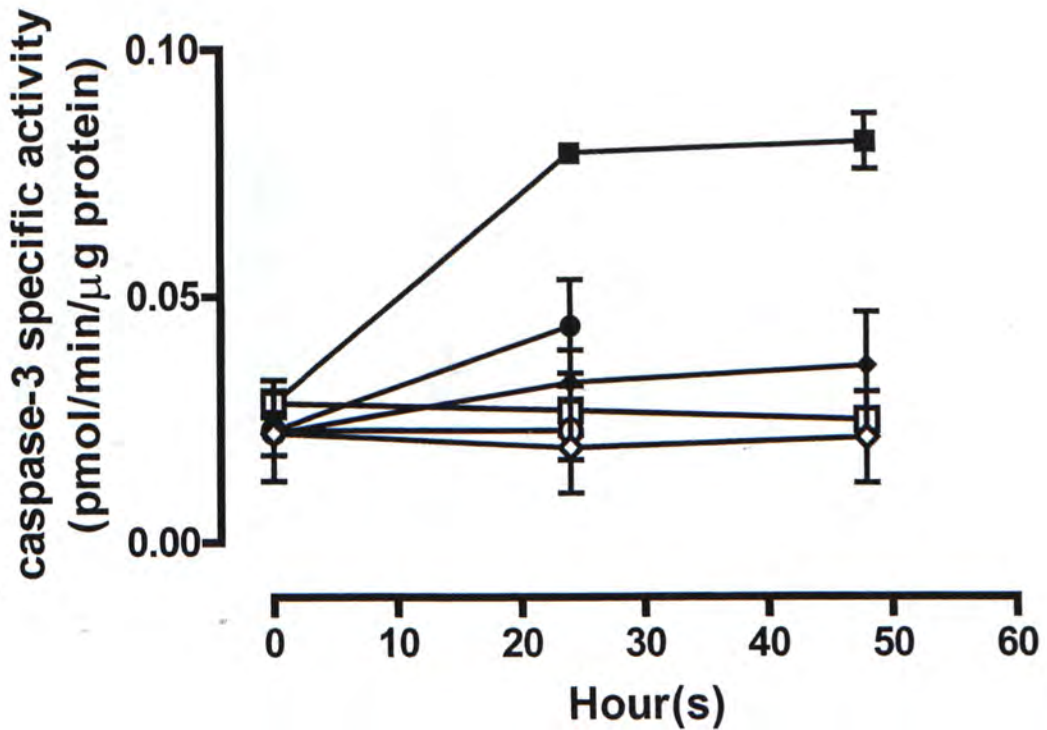


Figure 4.29 Activation of caspase-3 activity by 100  $\mu\text{M}$  etoposide with different incubation time in (■) HEK293 cells, (●) HEK-sbGHS-R1a monoclonal stable cell line and (◆) HEK-sbGHS-R1b monoclonal stable cell line. The open symbols represent the cells incubated with 0.23% DMSO as the control for etoposide. At the end of each incubation time, the cells were lysed and the protein was collected for caspase-3 activity measurement as described in Chapter 3. Results in figure come from one experiment performed in duplicate, data shown are mean  $\pm$  S.D.



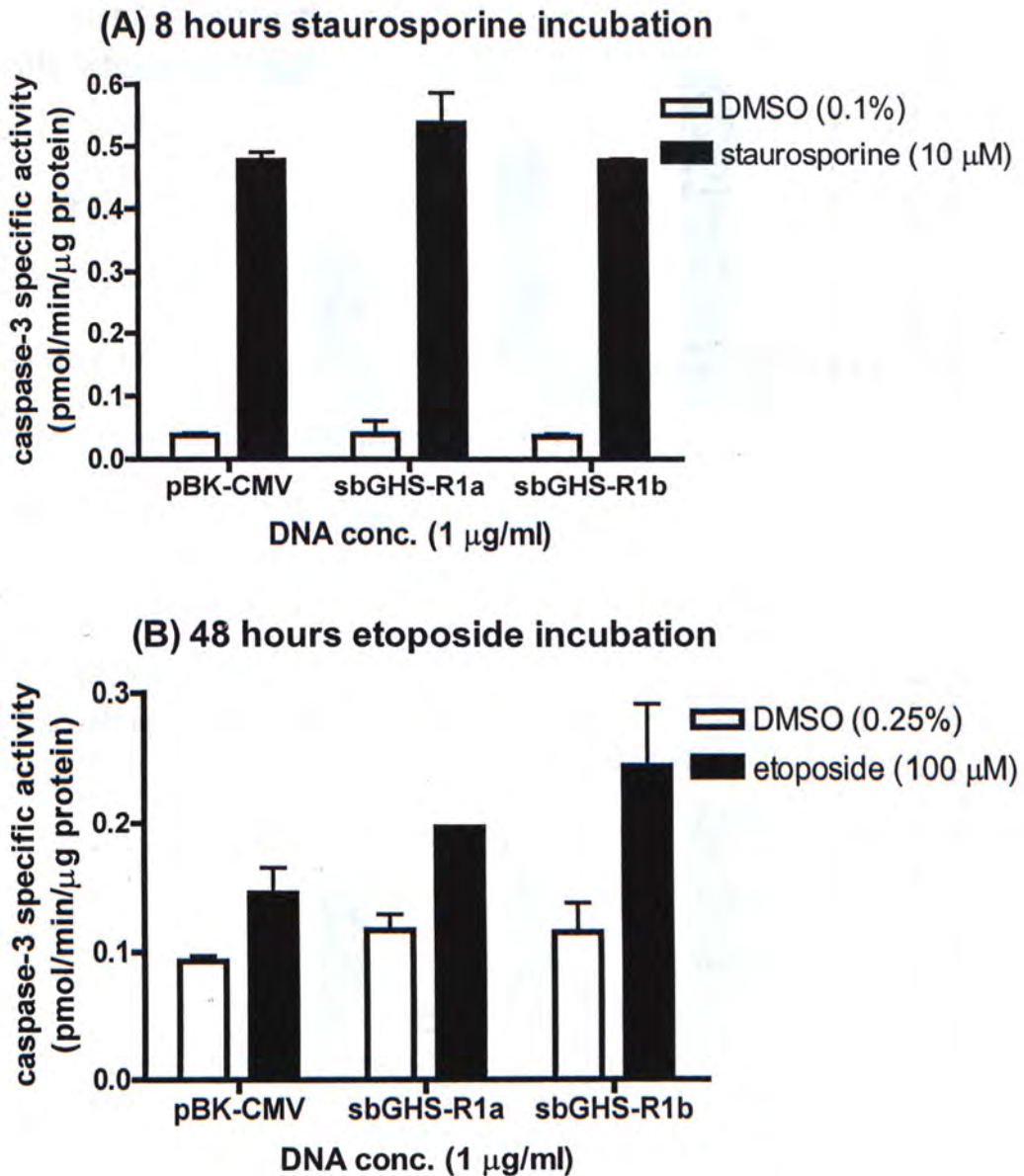


Figure 4.30 Effect of sbGHS-R1a and sbGHS-R1b on (A) staurosporine- and (B) etoposide-induced caspase-3 activity. HEK293 cells were transiently transfected with 1 μg/ml pBK-CMV, sbGHS-R1a or sbGHS-R1b and incubated with 10 μM staurosporine or 100 μM etoposide for 8 h and 48 h, respectively. At the end of incubation time, the cells were lysed and the protein was collected for caspase-3 activity measurement as described in Chapter 3. Results in figure come from one experiment performed in duplicate, data shown are mean ± S.D. In figure A, two experiments were performed and one set of data is shown.

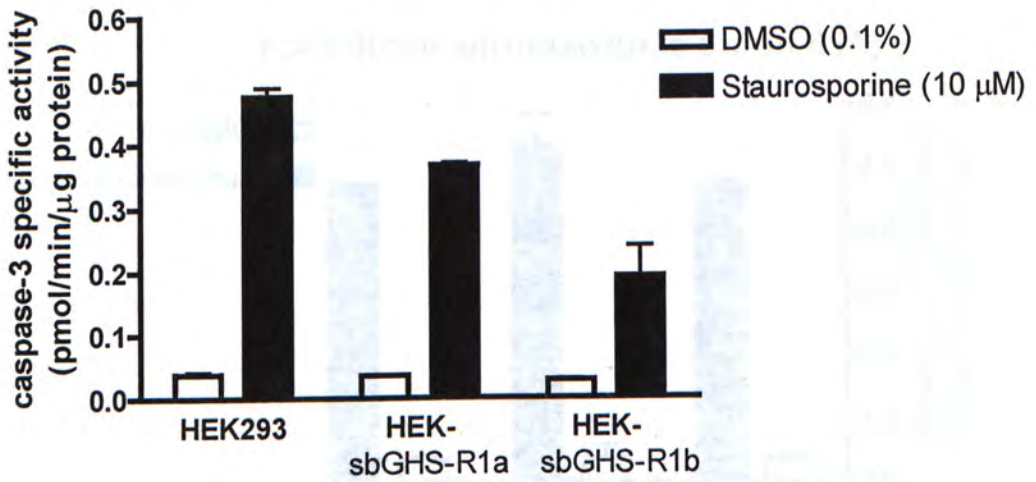
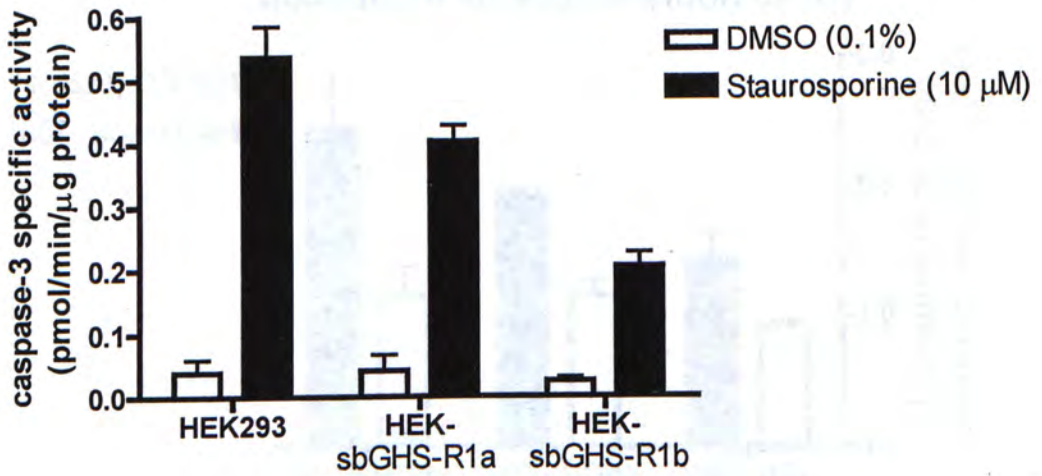
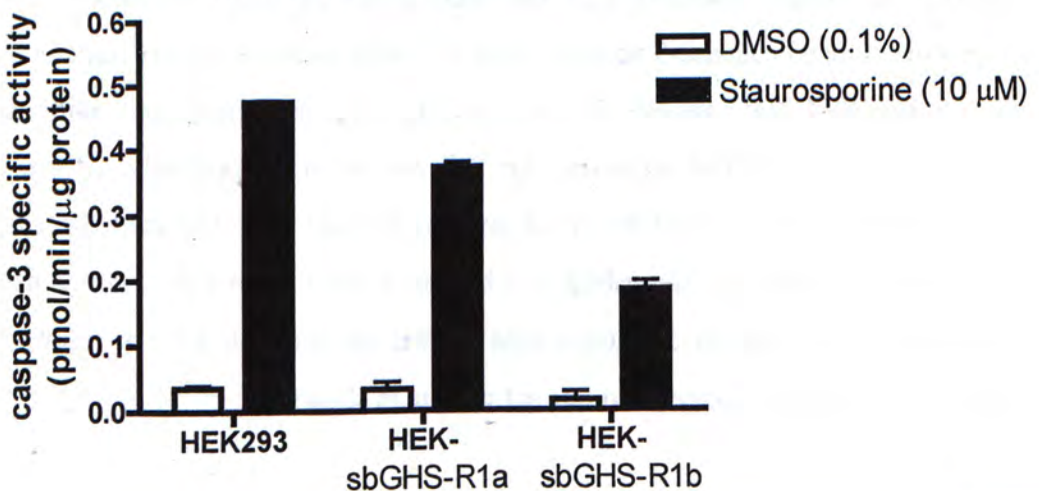
**(A) 1  $\mu$ g/ml pBK-CMV****(B) 1  $\mu$ g/ml sbGHS-R1a****(C) 1  $\mu$ g/ml sbGHS-R1b**

Figure 4.31 Effect of sbGHS-R1a and sbGHS-R1b on staurosporine-induced caspase-3 activity in HEK293, HEK-sbGHS-R1a and HEK-sbGHS-R1b cells. These three types of cells were transfected with (A) 1  $\mu\text{g/ml}$  pBK-CMV or (B) 1  $\mu\text{g/ml}$  sbGHS-R1a or (C) 1  $\mu\text{g/ml}$  sbGHS-R1b. After 48 h post-transfection, these cells were incubated with 10  $\mu\text{M}$  staurosporine or 0.1% DMSO for 8 h. At the end of the incubation time, the cells were lysed and the protein was collected for caspase-3 activity measurement as described in Chapter 3. Results in figure come from one experiment performed in duplicate, data shown are mean  $\pm$  S.D.



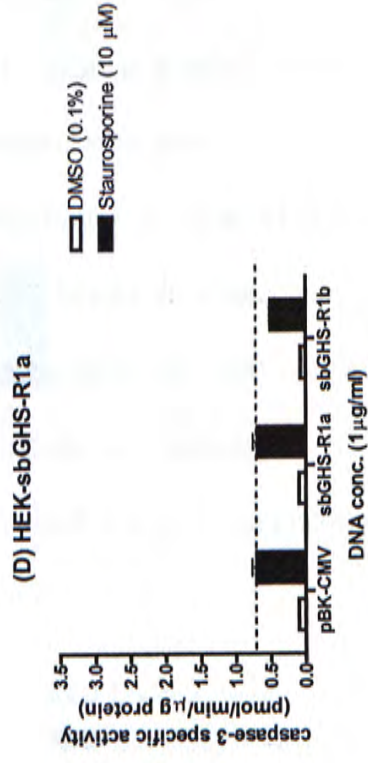
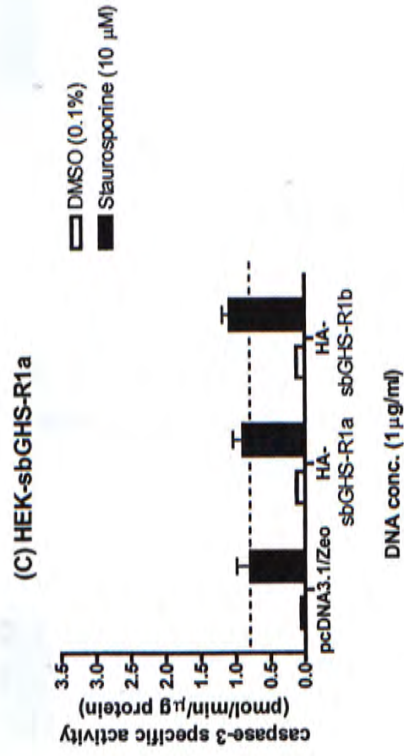
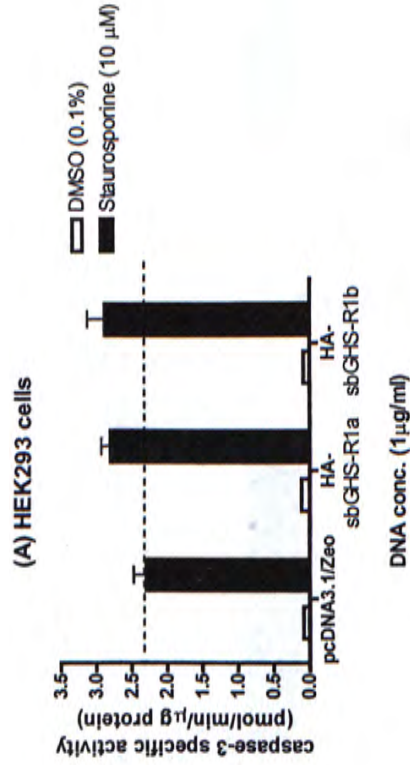


Figure 4.32 Effect of epitope tag (HA) on the function of sbGHS-R in caspase-3 activity regulation. 1  $\mu\text{g/ml}$  HA-sbGHS-R1a or HA-sbGHS-R1b was transfected into (A) HEK293 cells or (C) HEK-sbGHS-R1a cells. 1  $\mu\text{g/ml}$  sbGHS-R1a or sbGHS-R1b was transfected into (B) HEK293 cells or (D) HEK-sbGHS-R1a cells. Cells transfected with pcDNA3.1(+)/Zeo or pBK-CMV were used as a reference. After 48 h post-transfection, cells were incubated for 8 h with 10  $\mu\text{M}$  staurosporine or 0.1% DMSO, which is respected for the 10  $\mu\text{M}$  staurosporine and act as a control. At the end of the incubation time, the cells were lysed and the protein was collected for caspase-3 activity measurement as described in Chapter 3. Results come from one experiment performed in duplicate, data shown are mean  $\pm$  S.D.

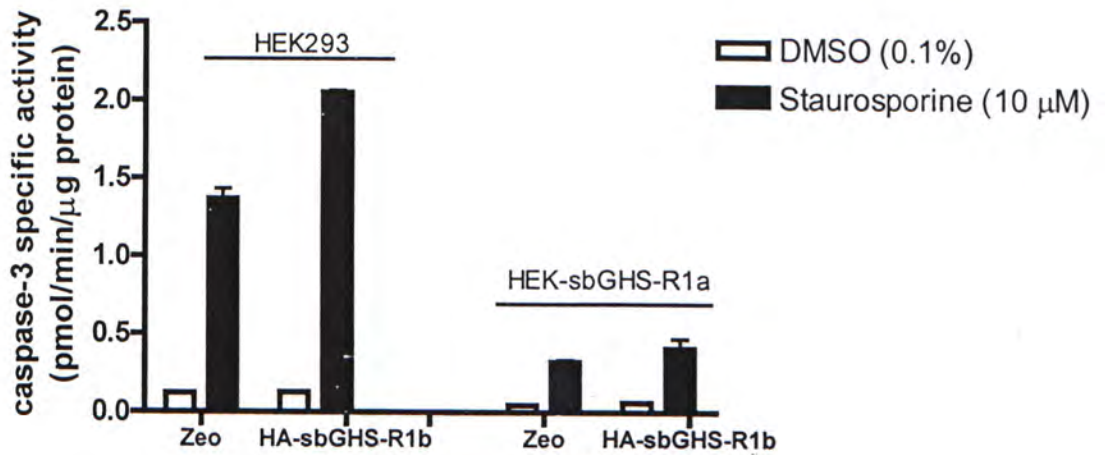


Figure 4.33 Effect of sbGHS-R on staurosporine-induced caspase-3 activity. HEK293 and HEK-sbGHS-R1a cells were transfected with 1 μg/ml pcDNA3.1(+)/Zeo (Zeo) or HA-sbGHS-R1b, and then the cells were incubated with 10 μM staurosporine or 0.1% DMSO for 8 hours. At the end of the incubation time, the cells were lysed and the protein was collected for caspase-3 activity measurement as described in Chapter 3. Results in figure come from one experiment performed in duplicate, data shown are mean ± S.D.



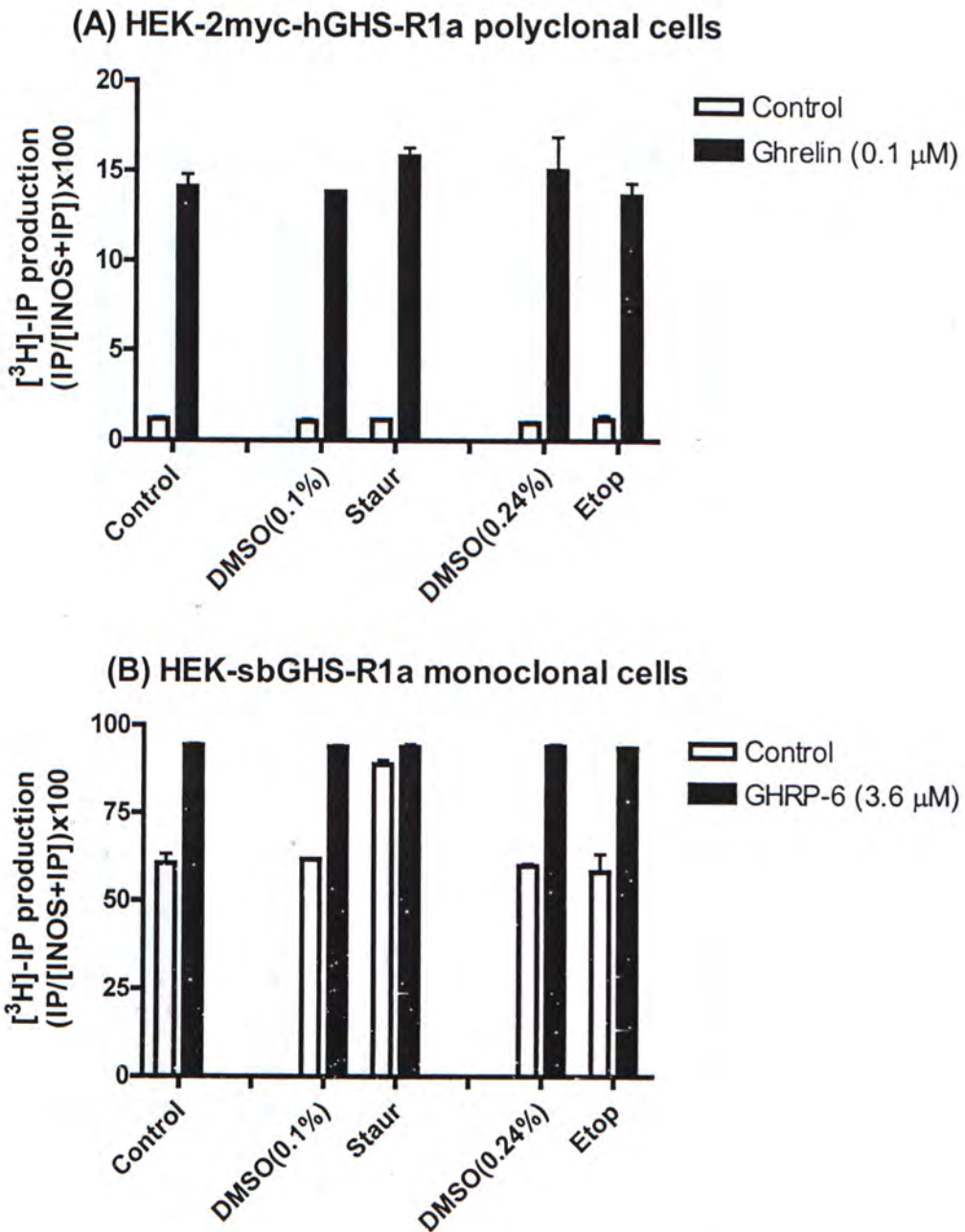


Figure 4.34 Effect of 10  $\mu\text{M}$  staurosporine and 100  $\mu\text{M}$  etoposide on agonist stimulated [ $^3\text{H}$ ]-IP production in (A) HEK-2myc-hGHS-R1a polyclonal cells and (B) HEK-sbGHS-R1a monoclonal cells. The cells were labeled with 2  $\mu\text{Ci/ml}$  *myo*-[ $^3\text{H}$ ]-inositol and incubated overnight, and then [ $^3\text{H}$ ]-IP production was measured as described in Chapter 3. The cells were lysed following 1 h incubation with staurosporine or etoposide alone or together with ghrelin or GHRP-6. Results come from one experiment performed in duplicate, data shown are mean  $\pm$  S.D.

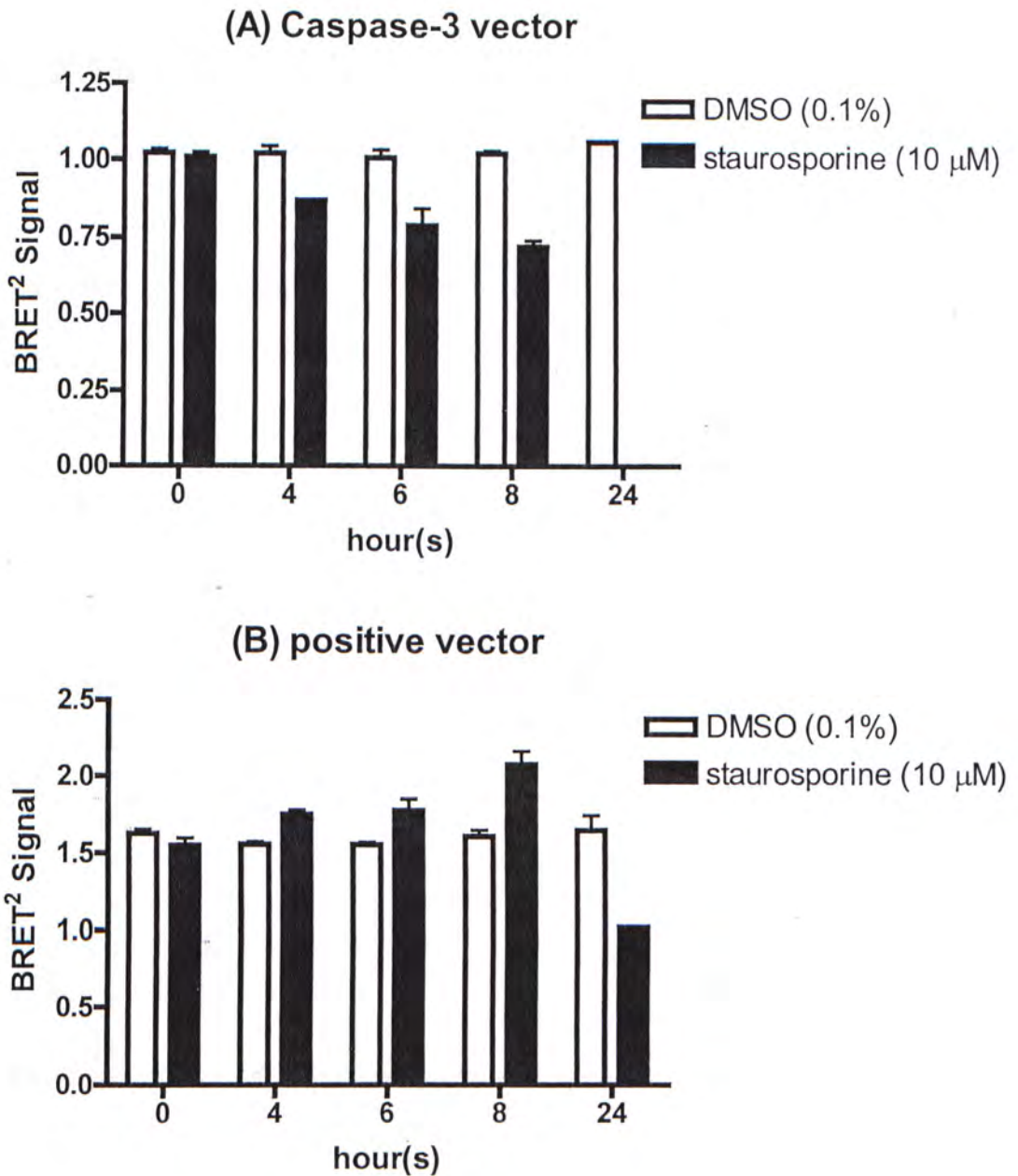


Figure 4.35 Determination of the sensitivity of BRET<sup>2</sup> assay for staurosporine in HEK293 cells. HEK293 cells were transfected with (A) 1 µg/ml caspase-3 biosensor or (B) 1 µg/ml positive vector, and then the cells were incubated with 10 µM staurosporine or 0.1% DMSO for different incubation times. The BRET<sup>2</sup> signal was measured as described in chapter 3. The positive vector transfected cells were used as a negative control. Results in figure come from one experiment performed in duplicate, data shown are mean ± S.D.

## 4.6 Determination of GHS-R amount in terms of mRNA

### 4.6.1 Determination of GHS-R amount in stable cell lines

To determine the amount of sbGHS-R1a and sbGHS-R1b expressed in the HEK-sbGHS-R1a and HEK-sbGHS-R1b cells respectively, real-time RT-PCR was performed. Total RNA was extracted from HEK-sbGHS-R1a and HEK-sbGHS-R1b cells and the first-strand were produced from them, and then real-time PCR was performed as described in Chapter 3. The standard curve using sbGHS-R1a and sbGHSR-1b plasmid DNA was constructed (Fig. 4.36), to determine the amount of sbGHS-R1a and sbGHS-1b in the stable cell lines respectively, as described in Chapter 3. From the corresponding standard curve, it was determined that there are  $4.38 \times 10^8 \pm 1.83 \times 10^8$  mRNA copy/ $\mu\text{g}$  total RNA sbGHS-R1a and  $7.78 \times 10^9 \pm 3.83 \times 10^9$  mRNA copy/ $\mu\text{g}$  total RNA sbGHS-R1b,  $n=3$ , in HEK-sbGHS-R1a and HEK-sbGHS-R1b, respectively.

### 4.6.2 Transfected DNA amount match with stable cell lines

In order to have a fair comparison, we need to have the same expression level of sbGHS-R in both transiently transfected cells and the stable cell lines. Therefore, it is necessary to determine how much of the sbGHS-R needs to be transfected into the HEK293 cells, hence, there is an equal amount of sbGHS-R between the transfected cells and the stable cell lines. The experimental design was similar to section 4.6.1, except there involved transfection, which is 48 h before the total RNA extraction. HEK293 cells were transfected with 0.25  $\mu\text{g}/\text{ml}$ , 0.5  $\mu\text{g}/\text{ml}$ , 0.75  $\mu\text{g}/\text{ml}$  and 1  $\mu\text{g}/\text{ml}$



concentrations of HA-sbGHS-R1a or HA-sbGHS-R1b and the plasmid DNA concentrations was balanced to 1  $\mu\text{g/ml}$  with empty vector. The amount of HA-sbGHS-R in the transiently transfected cells were much higher than in the stable cell lines. HEK293 cells transfected with only 0.75  $\mu\text{g/ml}$  empty vector plus 0.25  $\mu\text{g/ml}$  HA-sbGHS-R1a or 0.25  $\mu\text{g/ml}$  HA-sbGHS-R1b, the amount of the transiently expressed sbGHS-R1a or sbGHS-R1b was already similar to that in the HEK-sbGHS-R1a and HEK-sbGHS-R1b, respectively (Fig. 4.37).

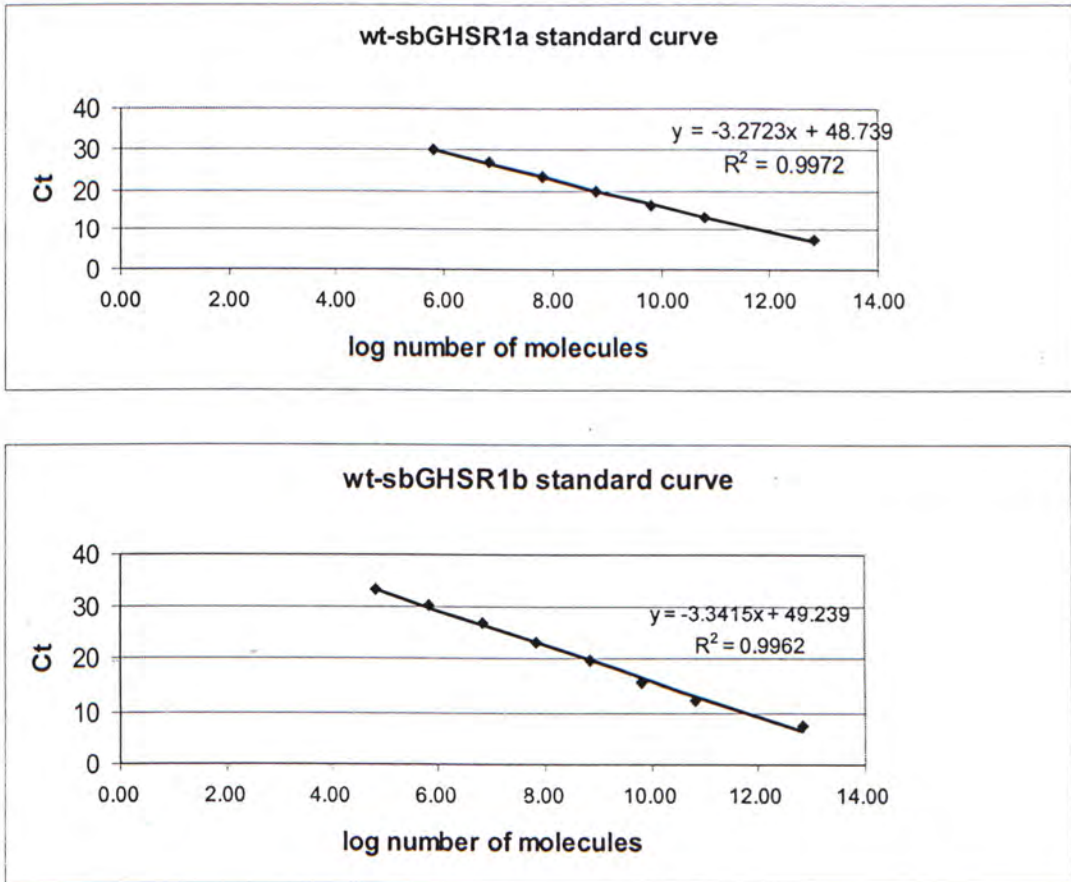


Figure 4.36 Real-time PCR standard curves for (A) sbGHS-R1a and (B) sbGHS-R1b. The standard curves were constructed by sbGHS-R1a and sbGHS-R1b plasmid DNA using real-time PCR as described in chapter 3. The amount of mRNA was reflected by the Ct value, which was recorded by the PCR machine. Ct value means the threshold cycle at which a significantly increase in PCR products was detected. Three independent standard curves were constructed, one set of data is shown. Results in figure come from one experiment performed in duplicate, data shown are mean  $\pm$  S.D.

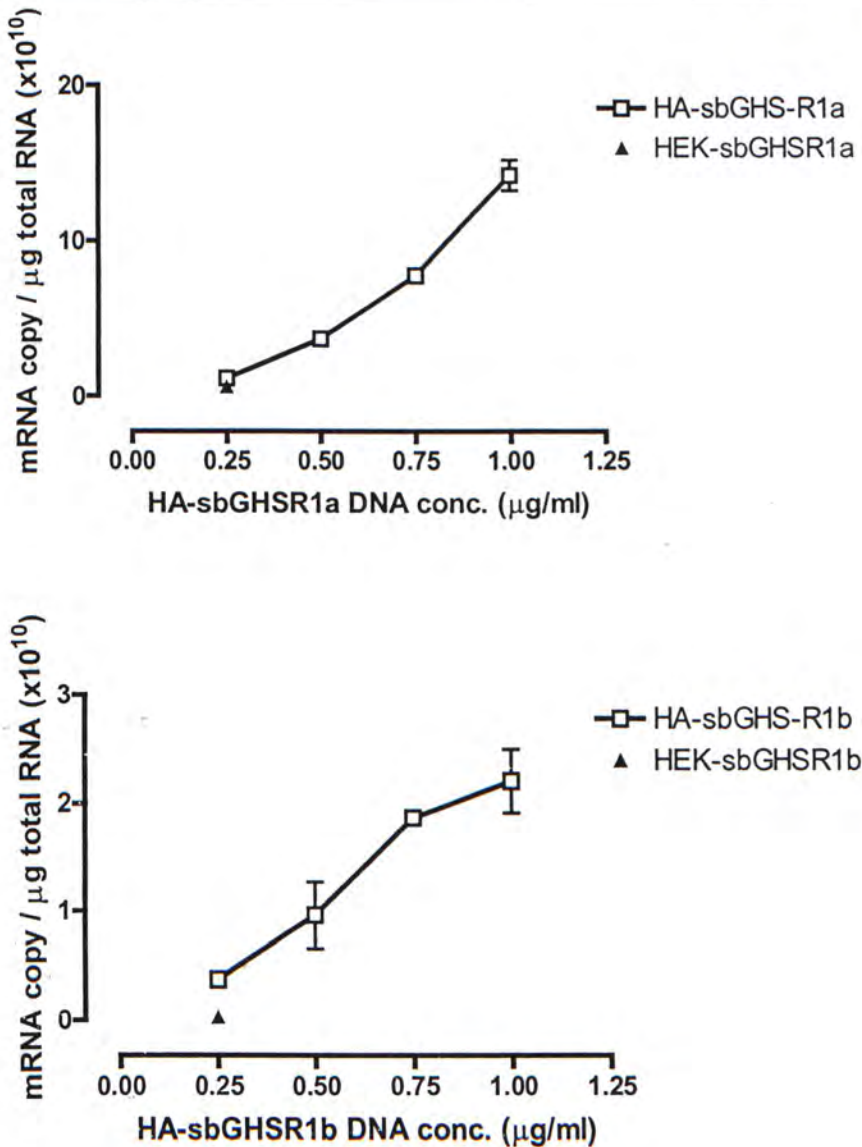


Figure 4.37 Determination of HA-sbGHS-R1a and HA-sbGHS-R1b plasmid DNA amount in transfection, to match with the mRNA amount present in HEK-sbGHS-R1a and HEK-sbGHS-R1b, respectively. HEK293 cells were transfected with 0.25, 0.5, 0.75 and 1 μg/ml HA-sbGHS-R1a or HA-sbGHS-R1b plasmid DNA and the total DNA concentration was balanced to 1 μg/ml by pcDNA3.1(+)/Zeo. After 48 hours post-transfection, the total RNA in these transfected cells, HEK-sbGHS-R1a and HEK-sbGHS-R1b cells were extracted by TRIzol reagent and then the total RNA was converted to cDNA as described in Chapter 3. The amount of mRNA present in the transfected cells was determined by the Ct value recorded by PCR machine. From the standard curve, the amount of RNA presence in the sample can be found as described in Chapter 3. Results in figure come from one experiment performed in duplicate, data shown are mean ± S.D.



## Chapter 5

### Discussion, Conclusions and Future Plan

#### 5.1 General Discussion and Conclusions

The aim of this project was to examine the role of GHS-R in apoptosis regulation and to define any functional relationship between GHS-R subtypes in transient transfection system and stable expression system in HEK293 cells. In this study, the caspase-3 activity was measured by a colorimetric assay, in order to reflect the apoptotic condition in the cells. BRET<sup>2</sup> and FRET assay were also used to monitor the caspase-3 activity in living HEK293 cells, which uptake and express the target gene and the caspase-3 biosensor.

GHS-R is a G<sub>q</sub>-coupled receptor, so the measurement of inositol phosphate production was used to study the properties of GHS-R. In hGHS-R1a and sbGHS-R1a, there was a receptor concentration-dependent increase in the basal [<sup>3</sup>H]-IP production, it indicating that GHS-R1a is a constitutively active receptor. The constitutive activity of GHS-R1a was further confirmed by the effect of SPa which decreased the basal [<sup>3</sup>H]-IP production of hGHS-R1a. Upon incubation with GHS-R agonists, ghrelin and GHRP-6, there was a further increase in [<sup>3</sup>H]-IP production in hGHS-R1a or sbGHS-R1a expressing HEK293 cells, it indicating that GHS-R1a is responsive to agonists. These properties of GHS-R1a have also been observed in COS-7 cells (Holst *et al.*, 2003). In contrast to GHS-R1a, GHS-R1b did not raise the basal and agonist-stimulated [<sup>3</sup>H]-IP production, indicating that GHS-R1b is not a

constitutively active receptor and is unresponsive to agonists. The epitope-tagged hGHS-R also has these properties, indicating that the epitope tag did not alter the GHS-R signaling properties.

GHS-R1a not only responds to agonist and inverse agonist, it also responds to the partial agonist, adenosine. In HEK293 cells transiently transfected with 2myc-hGHS-R1a and incubated with adenosine or ghrelin, there was adenosine- and ghrelin-stimulated [<sup>3</sup>H]-IP production, but adenosine-stimulated [<sup>3</sup>H]-IP production was smaller than the ghrelin-stimulated [<sup>3</sup>H]-IP production, suggesting that adenosine is a partial agonist of hGHS-R1a. Co-administration of adenosine and ghrelin caused a further increase in the ghrelin-stimulated [<sup>3</sup>H]-IP production. This result is not expected if adenosine is a partial agonist, as the concentration of adenosine that maximized activation of a receptor, another agonist does not provide an additional stimulation. In Smith *et al.* (2000), at the submaximal concentrations of adenosine and MK-0677, there was an additive activation of pig GHS-R1a. At the maximal concentration of adenosine, MK-0677 did not cause a further activation of GHS-R1a. This further suggested that GHS-R responds to adenosine and it is a partial agonist. From the high performance liquid chromatography (HPLC) study of the hGHS-R expressing BHK cells (BHK/GHS-R cells) and adenosine, it showed there was co-elution of adenosine and cell extract from GHS-R expressing cells, and the Fura-2 loaded BHK/GHS-R cells incubated with adenosine caused an increase in the Fura-2 signal, which is a calcium sensitive dye (Tullin *et al.*, 2000). These data indicated that hGHS-R1a responded to adenosine and caused intracellular calcium release. In addition, in the HEK293 cells stably expressing pig GHS-R1a responded



to adenosine, the agonist activation curve reached a plateau at a lower level of activation than that responded to GHSs, such as GHRP-6 (Smith *et al.*, 2000). It indicated that adenosine is a partial agonist of pig GHS-R1a. In contrast to our data, Carreira *et al.* (2004) stated that in HEK293 cells stably expressed hGHS-R1a, they did not have adenosine-stimulated [ $^3\text{H}$ ]-IP production, and adenosine significantly reduced ghrelin-stimulated [ $^3\text{H}$ ]-IP production.

Similar to ghrelin-stimulated [ $^3\text{H}$ ]-IP production, the adenosine-stimulated [ $^3\text{H}$ ]-IP production was inhibited by co-administrated with SPa in 2myc-hGHS-R1a transiently expressed HEK293 cells. It also showed in BHK/hGHS-R cells, preincubation with SPa for 30 seconds before adding adenosine, SPa completely inhibited the adenosine-induced intracellular calcium release (Tullin *et al.*, 2000).

To confirm part of the ghrelin-stimulated [ $^3\text{H}$ ]-IP production was due to the endogenous adenosine, ADA was co-administrated with ghrelin or adenosine. In 2myc-hGHS-R1a expressing cells, there were decreases in basal, ghrelin- and adenosine-stimulated [ $^3\text{H}$ ]-IP production. ADA also inhibited carbachol- and U46619-stimulated [ $^3\text{H}$ ]-IP production in HEK293 cells and hTP $\alpha$  expressing HEK293 cells, respectively. The constitutively active G $_q$  protein-stimulated [ $^3\text{H}$ ]-IP production was also inhibited by ADA. Therefore, the specificity of the ADA was investigated using theophylline. Theophylline did not inhibit any agonist-stimulated [ $^3\text{H}$ ]-IP production, such as ghrelin, adenosine, U46619, carbachol and ATP, on different receptors. These data did not help in concluding that part of the ghrelin- and adenosine-stimulated [ $^3\text{H}$ ]-IP production in HEK293 cells transfected with



hGHS-R1a is due to the endogenous adenosine. Also, there is not enough evidence to show the activation of  $G_q$ -coupled receptor caused a release of endogenous adenosine or is just due to the non-specific activity of ADA. There are contradictory literature mentioned the effect of theophylline in GHS-R transfected cells. Theophylline has been shown to inhibit the activation of pig GHS-R by adenosine (Smith *et al.*, 2000), however, in BHK/GHS-R, theophylline did not show any effect on adenosine- or MK-0677-induced calcium response (Tullin *et al.*, 2000). These contradictory information may be due to the different concentrations of adenosine and theophylline, different sensitivity in the two assays for calcium measurement and different GHS-R1a species.

To investigate the functional relationship of GHS-R in apoptosis regulation, one of the methods is to co-express the GHS-R1a and GHS-R1b in the cells by transient transfection. Therefore, it is necessary to determine whether co-transfection will alter the result which is independent of the function of the target receptor. When HEK293 cells were co-transfected hGHS-R1a with empty vector, the agonist-stimulated [ $^3$ H]-IP production was greater than the cells transfected with hGHS-R1a alone. This was also observed in the cells co-transfected with sbGHS-R1a plus empty vector. These indicated that transfection with additional plasmid DNA potentiated the GHS-R1a agonist-stimulated [ $^3$ H]-IP production, this property was not changed by the addition of epitope tag, as the 2myc-hGHS-R1a and HA-sbGHS-R1a constructs also demonstrated this co-transfection potentiating effect. The basal [ $^3$ H]-IP production was also potentiated by cotransfecting GHS-R1a with empty vector, but seems did not observe in cells transfected with sbGHS-R1a plus empty vector, it

might due to the large variations in some data points, so it needs more experiments to confirm it.

This co-transfection potentiating effect not only occurred with the addition of the empty vector, it also appeared with the addition of other plasmid DNA. When HEK293 cells were co-transfected with hGHS-R1a and hTP $\alpha$  or hGHS-R1b, the ghrelin-stimulated [ $^3$ H]-IP production was greater than when transfected with hGHS-R1a alone. However, the basal [ $^3$ H]-IP production was not potentiated in the cells co-transfected hGHS-R1a plus hGHS-R1b. Besides balancing the DNA concentration with empty vector and G $_q$ -coupled receptor, G $_i$ - and G $_s$ -coupled receptors were tested. It was found that cotransfecting hGHS-R1a with G $_i$ -coupled receptor (MOR) or G $_s$ -coupled receptor (mDP), both the basal and ghrelin-stimulated [ $^3$ H]-IP production was greater than the cells transfected with hGHS-R1a alone. Taken together, co-transfected HEK293 cells with GHS-R1a plus empty vector or other G protein-coupled receptors, the GHS-R1a agonist-stimulated [ $^3$ H]-IP production was potentiated to a variable extent. In some cases, however, the basal [ $^3$ H]-IP production was not potentiated.

The co-transfection potentiating effect was also observed in hTP $\alpha$  agonist-stimulated [ $^3$ H]-IP production. In HEK293 cells co-transfected with hTP $\alpha$  plus other plasmid DNA, such as empty vector or hGHS-R1a or hGHS-R1b, there was a greater increase in U46619-stimulated [ $^3$ H]-IP production. In contrast to GHS-R1a, the basal [ $^3$ H]-IP production of hTP $\alpha$  was not affect, as hTP $\alpha$  is not a constitutively active receptor. In addition, the additional plasmid DNA in transfection caused a potentiated GHS-R1a



agonist-stimulated [<sup>3</sup>H]-IP production, was also observed using various transfection reagents, such as Lipofectamine, Lipofectamine2000, Fugene 6 and Genejuice. However, the additional plasmid DNA in transfection caused a potentiated GHS-R1a basal [<sup>3</sup>H]-IP production was only observed in Lipofectamine and Lipofectamine2000.

Addition of empty vector in co-transfection results in variable potentiated [<sup>3</sup>H]-IP production. One of the possible explanations is the presence of an empty vector increased the transfection efficiency. The transfection efficiency was therefore measured by the expression of EGFP. HEK293 cells co-transfected with 0.1 µg/ml pEGFP plus different concentrations of hGHS-R1a, the fluorescent reading were similar in all groups, however, there was a greater fluorescent reading in the cells co-transfected with 0.1 µg/ml pEGFP plus different concentrations of hGHS-R1a when the concentration of hGHS-R1a was balanced to 1.1 µg/ml by empty vector. In addition, HEK293 cells co-transfected with 0.1 µg/ml pEGFP plus 1 µg/ml empty vector, the fluorescent reading were higher than the cells co-transfected with 0.1 µg/ml pEGFP plus 1 µg/ml hGHS-R1a.

Co-transfection results in a variable potentiating effect in [<sup>3</sup>H]-IP production, therefore, it is good for co-transfecting GHS-R1a plus empty vector, in order to get a greater agonist-stimulated [<sup>3</sup>H]-IP production, than the one transfected with GHS-R1a alone. However, for the study of the GHS-R subtypes functional relationship, co-transfection of two types of plasmid DNAs into HEK293 cells makes the data more complicated for interpretation. Another way to study the relationship of



GHS-R subtypes is to develop a stable cell line which expresses one type of GHS-R, and then only another type of GHS-R needs to be transfected into the cells. This method does not need the co-transfection process, so the potentiating effect in [<sup>3</sup>H]-IP production by co-transfection can be eliminated. Therefore, we tried to develop HEK293 cells stably expressing 2myc-hGHS-R1a or 2myc-hGHS-R1b. The development of the polyclonal stable cell lines was successful, but was unsuccessful in monoclonal stable cell line development. It is unclear why the development of the stable cell line fail, as there are many literatures stated that they are developed a cells stably expressed GHS-R1a (Camina *et al.*, 2004). Instead, HEK-sbGHS-R1a and HEK-sbGHS-R1b cells were obtained from Dr. Chi-Bun Chan (Biochemistry Department, CUHK) and used to study the role of GHS-R in regulation of apoptosis.

Three methods were used to monitor caspase-3 activity in order to study apoptosis, they are colorimetric assay, BRET<sup>2</sup> and FRET assay. The benefit of using BRET and FRET assay rather than colorimetric assay, is they can monitor the caspase-3 activity in the cells which uptake and express the target gene and the caspase-3 biosensor. Also, they are less laborious. However, among these methods, colorimetric assay gave a relatively large increase in both etoposide- and staurosporine-induced caspase-3 activity in HEK293 cells, when compared to BERT<sup>2</sup> and FRET assay. In BRET<sup>2</sup> assay, there was only slightly decrease in BRET<sup>2</sup> signal of the caspase-3 biosensor expressed HEK293 cells, after incubation with staurosporine for 8 h. In FRET assay, the results were not reproducible. Therefore, the colorimetric assay was used in this project.

Preliminary study showed that sbGHS-R1a was anti-apoptotic, while HA-sbGHS-R1b was pro-apoptotic. Therefore, the role of GHS-Rs in regulating apoptosis was further studied using hGHS-Rs. It is necessary to optimize the assay condition in measuring caspase-3 activity, in order to reflect apoptosis. In HEK293 cells, the optimal incubation time for staurosporine and etoposide is 8 and 24 h, respectively.

In the HEK-2myc-hGHS-R1a polyclonal stable cell line, it seems stably expressed 2myc-hGHS-R1a protected the cells against staurosporine-induced caspase-3 activity, but enhanced the cells undergo etoposide-induced caspase-3 activity. However, the staurosporine- and etoposide-induced caspase-3 activity between HEK293 and HEK-2myc-hGHS-R1a is small, it might due to the use of polyclonal stable cell line.

Since the use of polyclonal stable cell line may result in small difference in staurosporine- and etoposide-induced caspase-3 activity between HEK293 and HEK-2myc-hGHS-R1a cells, so instead of using HEK-2myc-hGHS-R1a polyclonal stable cell line, HEK-sbGHS-R1a and HEK-sbGHS-R1b monoclonal stable cell lines were used. In HEK-sbGHS-R1a and HEK-sbGHS-R1b cells, in order to have an optimal staurosporine- and etoposide-induced caspase-3 activity, it is needed to incubate these cells with staurosporine and etoposide for 8 and 24 h. The staurosporine- or etoposide-induced caspase-3 activity was lower in these stable cell lines than in the non-transfected HEK293 cells, it showed that the stably expressed sbGHS-R1a and sbGHS-R1b induced anti-apoptotic effect to the cells. However, transiently transfected sbGHS-R1a or sbGHS-R1b into HEK293, HEK-sbGHS-R1a



and HEK-sbGHS-R1b cells, there was no effect on the staurosporine-induced caspase-3 activity. These results are not expected, as in the preliminary study described in section 4.5, transiently transfected HA-sbGHS-R1b into HEK293 cells, the staurosporine-induced caspase-3 activity was higher than that in HEK293 cells.

The difference between the epitope-tagged and non-tagged sbGHS-R in apoptosis regulation and the presence of serum in staurosporine-induced caspase-3 activity was investigated. The staurosporine-induced caspase-3 activity was larger in the absence of serum and the staurosporine-induced caspase-3 activity was slightly larger in the HEK293 cells transfected with HA-sbGHS-R1a or HA-sbGHS-R1b than in the non-transfected HEK293 cells. HEK293 and HEK-sbGHS-R1a cells transfected with HA-sbGHS-R1b and incubated with staurosporine in the absence of serum. It showed that the HA-sbGHS-R1b caused an increase in the staurosporine-induced caspase-3 activity and this pro-apoptotic effect of HA-sbGHS-R1b was inhibited by stably expressed sbGHS-R1a. It indicated that sbGHS-R1a is anti-apoptotic. These results matched the preliminary results described in section 4.5, except there was no increase in the basal caspase-3 activity in the HA-sbGHS-R1b transfected cells.



## 5.2 Future Plan and Experimental Design

After this project, it shows that in order to study the functional relationship between GHS-R1a and GHS-R1b in apoptosis regulation, using HEK-sbGHS-R1a and HEK-sbGHS-R1b cells and then transfects either one of the GHS-R subtype into these stable cell lines is better than co-transfecting GHS-R subtypes, as co-transfection showed a variable potentiating effect in [<sup>3</sup>H]-IP production. Therefore, HEK-sbGHS-R1a and HEK-sbGHS-R1b cells will be characterized by determining the effect of agonist, GHRP-6 on [<sup>3</sup>H]-IP production and the effect of SPa on basal, GHRP-6-stimulated [<sup>3</sup>H]-IP production. The expected result is HEK-sbGHS-R1a has basal and GHRP-6-stimulated [<sup>3</sup>H]-IP production, while HEK-sbGHS-R1b is unresponsive to GHRP-6.

In this project, two apoptotic inducers were used, staurosporine and etoposide. Although staurosporine gave a good induced caspase-3 activity in colorimetric assay, but staurosporine is a PKC inhibitor, it may affect the signaling of GHS-R1a, so it will just be use as an internal control in the future experiments. Etoposide does not affect the component of G<sub>q</sub>-coupled signaling, but the size of etoposide-induced caspase-3 activity varied. From the preliminary data, 25 μM cadium can induce caspase-3 activity in HEK293 cells. Although the cadium-induced caspase-3 activity was smaller than that induced by staurosporine, it was larger than that induced by etoposide. Therefore, in the future, cadium will also be used.

It had been determined by real-time RT-PCR in Chapter 4 that transiently co-transfected 0.25 μg/ml HA-sbGHS-R1a or HA-sbGHS-R1b and 0.75 μg/ml

empty vector into the cells, the mRNA amount was close to that in HEK-sbGHS-R1a and HEK-sbGHS-R1b, respectively. Therefore, in the future experiments, the transfection groups will be as listed in table 6.1, in order to study the role of sbGHS-R subtypes in regulating apoptosis. HA-sbGHS-R plasmid DNA will be used in transfection because the receptor protein expression level will be quantified in addition to mRNA expression level by real-time RT-PCR.

Briefly, the role of GHS-R in apoptosis regulation will be investigated as the following steps. HEK293, HEK-sbGHS-R1a and HEK-sbGHS-R1b will be transfected with HA-sbGHS-R1a or HA-sbGHS-R1b as described in table 6.1 and then these cells will be incubated with medium, GHRP-6 and SPa with or without apoptosis inducer and then the caspase-3 activity will be measured. At the same time, the total RNA from these transfected cells will be extracted and the amount of transiently expressed HA-sbGHS-R1a and HA-sbGHS-R1b will be quantified by real-time RT-PCR, as the transfection efficiency is slightly different between different experiments. In addition to real-time RT-PCR, Western blot will also be carried out, in order to semi-quantify the amount of HA-sbGHS-R1a and HA-sbGHS-R1b present in the cells.

Cell lines	Transfection plasmid DNA		
	pcDNA3.1/Zeo	HA-sbGHS-R1a	HA-sbGHS-R1b
HEK293	1 $\mu\text{g/ml}$	-	-
	0.75 $\mu\text{g/ml}$	0.25 $\mu\text{g/ml}$	-
	0.75 $\mu\text{g/ml}$	-	0.25 $\mu\text{g/ml}$
HEK-sbGHS-R1a	1 $\mu\text{g/ml}$	-	-
	0.75 $\mu\text{g/ml}$	0.25 $\mu\text{g/ml}$	-
	0.75 $\mu\text{g/ml}$	-	0.25 $\mu\text{g/ml}$
HEK-sbGHS-R1b	1 $\mu\text{g/ml}$	-	-
	0.75 $\mu\text{g/ml}$	0.25 $\mu\text{g/ml}$	-
	0.75 $\mu\text{g/ml}$	-	0.25 $\mu\text{g/ml}$

Table 5.1 Transfection groups in apoptosis study.



---

**References:**

- ADAMS, J.M. (2003). Ways of dying: multiple pathways to apoptosis. *Genes Dev*, **17**, 2481-95.
- ANDREIS, P.G., MALENDOWICZ, L.K., TREJTER, M., NERI, G., SPINAZZI, R., ROSSI, G.P. & NUSSDORFER, G.G. (2003). Ghrelin and growth hormone secretagogue receptor are expressed in the rat adrenal cortex: Evidence that ghrelin stimulates the growth, but not the secretory activity of adrenal cells. *FEBS Lett*, **536**, 173-9.
- ASAKAWA, A., INUI, A., KAGA, T., YUZURIHA, H., NAGATA, T., FUJIMIYA, M., KATSUURA, G., MAKINO, S., FUJINO, M.A. & KASUGA, M. (2001). A role of ghrelin in neuroendocrine and behavioral responses to stress in mice. *Neuroendocrinology*, **74**, 143-7.
- BALDANZI, G., FILIGHEDDU, N., CUTRUPI, S., CATAPANO, F., BONISSONI, S., FUBINI, A., MALAN, D., BAJ, G., GRANATA, R., BROGLIO, F., PAPOTTI, M., SURICO, N., BUSSOLINO, F., ISGAARD, J., DEGHENGI, R., SINIGAGLIA, F., PRAT, M., MUCCIOLI, G., GHIGO, E. & GRAZIANI, A. (2002). Ghrelin and des-acyl ghrelin inhibit cell death in cardiomyocytes and endothelial cells through ERK1/2 and PI 3-kinase/AKT. *J Cell Biol*, **159**, 1029-37.
- BAR-YEHUDA, S., MADI, L., SILBERMAN, D., GERY, S., SHKAPENUK, M. & FISHMAN, P. (2005). CF101, an agonist to the A3 adenosine receptor, enhances the chemotherapeutic effect of 5-fluorouracil in a colon carcinoma murine model. *Neoplasia*, **7**, 85-90.
- BELLONI, A.S., MACCHI, C., REBUFFAT, P., CONCONI, M.T., MALENDOWICZ, L.K., PARNIGOTTO, P.P. & NUSSDORFER, G.G. (2004). Effect of ghrelin on the apoptotic deletion rate of different types of cells cultured in vitro. *Int J Mol Med*, **14**, 165-7.
- BENSO, A., BROGLIO, F., MARAFETTI, L., LUCATELLO, B., SEARDO, M.A., GRANATA, R., MARTINA, V., PAPOTTI, M., MUCCIOLI, G. & GHIGO, E. (2004). Ghrelin and synthetic growth hormone secretagogues are cardioactive molecules with identities and differences. *Semin Vasc Med*, **4**, 107-14.
- BRESSON-BEPOLDIN, L. & DUFY-BARBE, L. (1994). GHRP-6 induces a biphasic calcium response in rat pituitary somatotrophs. *Cell Calcium*, **15**, 247-58.
- BROGLIO, F., BENSO, A., GOTTERO, C., PRODAM, F., GAUNA, C., FILTRI, L., ARVAT, E., VAN DER LELY, A.J., DEGHENGI, R. & GHIGO, E. (2003). Non-acylated



- ghrelin does not possess the pituitary and pancreatic endocrine activity of acylated ghrelin in humans. *J Endocrinol Invest*, **26**, 192-6.
- CAMINA, J.P., CARREIRA, M.C., EL MESSARI, S., LLORENS-CORTES, C., SMITH, R.G. & CASANUEVA, F.F. (2004). Desensitization and endocytosis mechanisms of ghrelin-activated growth hormone secretagogue receptor 1a. *Endocrinology*, **145**, 930-40.
- CARREIRA, M.C., CAMINA, J.P., SMITH, R.G. & CASANUEVA, F.F. (2004). Agonist-specific coupling of growth hormone secretagogue receptor type 1a to different intracellular signaling systems. Role of adenosine. *Neuroendocrinology*, **79**, 13-25.
- CASSONI, P., GHE, C., MARROCCO, T., TARABRA, E., ALLIA, E., CATAPANO, F., DEGHENGI, R., GHIGO, E., PAPOTTI, M. & MUCCIOLI, G. (2004). Expression of ghrelin and biological activity of specific receptors for ghrelin and des-acyl ghrelin in human prostate neoplasms and related cell lines. *Eur J Endocrinol*, **150**, 173-84.
- CASSONI, P., PAPOTTI, M., GHE, C., CATAPANO, F., SAPINO, A., GRAZIANI, A., DEGHENGI, R., REISSMANN, T., GHIGO, E. & MUCCIOLI, G. (2001). Identification, characterization, and biological activity of specific receptors for natural (ghrelin) and synthetic growth hormone secretagogues and analogs in human breast carcinomas and cell lines. *J Clin Endocrinol Metab*, **86**, 1738-45.
- CHAE, I.H., PARK, K.W., KIM, H.S. & OH, B.H. (2004). Nitric oxide-induced apoptosis is mediated by Bax/Bcl-2 gene expression, transition of cytochrome c, and activation of caspase-3 in rat vascular smooth muscle cells. *Clin Chim Acta*, **341**, 83-91.
- CHAN, C.B. & CHENG, C.H. (2004a). Identification and functional characterization of two alternatively spliced growth hormone secretagogue receptor transcripts from the pituitary of black seabream *Acanthopagrus schlegelii*. *Mol Cell Endocrinol*, **214**, 81-95.
- CHAN, C.B., LEUNG, P.K., WISE, H. & CHENG, C.H. (2004b). Signal transduction mechanism of the seabream growth hormone secretagogue receptor. *FEBS Lett*, **577**, 147-53.
- CHOI, K., ROH, S.G., HONG, Y.H., SHRESTHA, Y.B., HISHIKAWA, D., CHEN, C., KOJIMA, M., KANGAWA, K. & SASAKI, S. (2003). The role of ghrelin and growth hormone secretagogues receptor on rat adipogenesis. *Endocrinology*,



144, 754-9.

- CHORNA, N.E., SANTIAGO-PEREZ, L.I., ERB, L., SEYE, C.I., NEARY, J.T., SUN, G.Y., WEISMAN, G.A. & GONZALEZ, F.A. (2004). P2Y receptors activate neuroprotective mechanisms in astrocytic cells. *J Neurochem*, **91**, 119-32.
- COHEN, J.J. (1993). Apoptosis. *Immunol Today*, **14**, 126-30.
- COLIGAN, J.K., AM.; MARGULIES, DH.; SHEVACH, EM.; STROBER, W (1995). Related isolation procedures and functional assays. *Current Protocols in Immunology*, **1**, 3.17.1.
- CRAIG, N.L. (1988). The mechanism of conservative site-specific recombination. *Annu Rev Genet*, **22**, 77-105.
- CRISTALLI, G., COSTANZI, S., LAMBERTUCCI, C., LUPIDI, G., VITTORI, S., VOLPINI, R. & CAMAIONI, E. (2001). Adenosine deaminase: functional implications and different classes of inhibitors. *Med Res Rev*, **21**, 105-28.
- DALBY, B., CATES, S., HARRIS, A., OHKI, E.C., TILKINS, M.L., PRICE, P.J. & CICCARONE, V.C. (2004). Advanced transfection with Lipofectamine 2000 reagent: primary neurons, siRNA, and high-throughput applications. *Methods*, **33**, 95-103.
- DAS, S., CORDIS, G.A., MAULIK, N. & DAS, D.K. (2005). Pharmacological preconditioning with resveratrol: role of CREB-dependent Bcl-2 signaling via adenosine A3 receptor activation. *Am J Physiol Heart Circ Physiol*, **288**, H328-35.
- DATTA, S.R., BRUNET, A. & GREENBERG, M.E. (1999). Cellular survival: a play in three Akts. *Genes Dev*, **13**, 2905-27.
- DATTA, S.R., DUDEK, H., TAO, X., MASTERS, S., FU, H., GOTOH, Y. & GREENBERG, M.E. (1997). Akt phosphorylation of BAD couples survival signals to the cell-intrinsic death machinery. *Cell*, **91**, 231-41.
- DI IORIO, P., BALLERINI, P., TRAVERSA, U., NICOLETTI, F., D'ALIMONTE, I., KLEYWEGT, S., WERSTIUK, E.S., RATHBONE, M.P., CACIAGLI, F. & CICCARELLI, R. (2004). The antiapoptotic effect of guanosine is mediated by the activation of the PI 3-kinase/AKT/PKB pathway in cultured rat astrocytes. *Glia*, **46**, 356-68.
- DJANANI, A., KANEIDER, N.C., STURN, D. & WIEDERMANN, C.J. (2003). Agonist function of the neurokinin receptor antagonist, [D-Arg1,D-Phe5,D-Trp7,9,Leu11]substance P, in monocytes. *Regul Pept*, **115**, 123-9.



- DUXBURY, M.S., WASEEM, T., ITO, H., ROBINSON, M.K., ZINNER, M.J., ASHLEY, S.W. & WHANG, E.E. (2003). Ghrelin promotes pancreatic adenocarcinoma cellular proliferation and invasiveness. *Biochem Biophys Res Commun*, **309**, 464-8.
- EHLERS, R.A., ZHANG, Y., HELLMICH, M.R. & EVERS, B.M. (2000). Neurotensin-mediated activation of MAPK pathways and AP-1 binding in the human pancreatic cancer cell line, MIA PaCa-2. *Biochem Biophys Res Commun*, **269**, 704-8.
- FEOKTISTOV, I., RYZHOV, S., GOLDSTEIN, A.E. & BIAGGIONI, I. (2003). Mast cell-mediated stimulation of angiogenesis: cooperative interaction between A2B and A3 adenosine receptors. *Circ Res*, **92**, 485-92.
- FERNANDEZ-RUIZ, J., GOMEZ, M., HERNANDEZ, M., DE MIGUEL, R. & RAMOS, J.A. (2004). Cannabinoids and gene expression during brain development. *Neurotox Res*, **6**, 389-401.
- FISCUS, R.R., YUEN, J.P., CHAN, S.L., KWONG, J.H. & CHEW, S.B. (2002). Nitric oxide and cyclic GMP as pro- and anti-apoptotic agents. *J Card Surg*, **17**, 336-9.
- FOLEY, J.F., KELLEY, L.P. & KINSELLA, B.T. (2001). Prostaglandin D(2) receptor-mediated desensitization of the alpha isoform of the human thromboxane A(2) receptor. *Biochem Pharmacol*, **62**, 229-39.
- GAVRIELI, Y., SHERMAN, Y. & BEN-SASSON, S.A. (1992). Identification of programmed cell death in situ via specific labeling of nuclear DNA fragmentation. *J Cell Biol*, **119**, 493-501.
- GERMACK, R. & DICKENSON, J.M. (2004a). Characterization of ERK1/2 signalling pathways induced by adenosine receptor subtypes in newborn rat cardiomyocytes. *Br J Pharmacol*, **141**, 329-39.
- GERMACK, R., GRIFFIN, M. & DICKENSON, J.M. (2004b). Activation of protein kinase B by adenosine A1 and A3 receptors in newborn rat cardiomyocytes. *J Mol Cell Cardiol*, **37**, 989-99.
- GHE, C., CASSONI, P., CATAPANO, F., MARROCCO, T., DEGHENGI, R., GHIGO, E., MUCCIOLI, G. & PAPOTTI, M. (2002). The antiproliferative effect of synthetic peptidyl GH secretagogues in human CALU-1 lung carcinoma cells. *Endocrinology*, **143**, 484-91.
- GHIGO, E., BROGLIO, F., ARVAT, E., MACCARIO, M., PAPOTTI, M. & MUCCIOLI, G. (2005). Ghrelin: more than a natural GH secretagogue and/or an orexigenic factor. *Clin Endocrinol (Oxf)*, **62**, 1-17.



- GLAVASKI-JOKSIMOVIC, A., JEFTINIJA, K., SCANES, C.G., ANDERSON, L.L. & JEFTINIJA, S. (2003). Stimulatory effect of ghrelin on isolated porcine somatotropes. *Neuroendocrinology*, **77**, 367-79.
- GNANAPAVAN, S., KOLA, B., BUSTIN, S.A., MORRIS, D.G., MCGEE, P., FAIRCLOUGH, P., BHATTACHARYA, S., CARPENTER, R., GROSSMAN, A.B. & KORBONITS, M. (2002). The tissue distribution of the mRNA of ghrelin and subtypes of its receptor, GHS-R, in humans. *J Clin Endocrinol Metab*, **87**, 2988.
- HAMMAR, S.P. & MOTTET, N.K. (1971). Tetrazolium salt and electron-microscopic studies of cellular degeneration and necrosis in the interdigital areas of the developing chick limb. *J Cell Sci*, **8**, 229-51.
- HATTORI, N., SAITO, T., YAGYU, T., JIANG, B.H., KITAGAWA, K. & INAGAKI, C. (2001). GH, GH receptor, GH secretagogue receptor, and ghrelin expression in human T cells, B cells, and neutrophils. *J Clin Endocrinol Metab*, **86**, 4284-91.
- HEMMINGS, B.A. (1997). Akt signaling: linking membrane events to life and death decisions. *Science*, **275**, 628-30.
- HENGARTNER, M.O. (2000). The biochemistry of apoptosis. *Nature*, **407**, 770-6.
- HOLST, B., CYGANKIEWICZ, A., JENSEN, T.H., ANKERSEN, M. & SCHWARTZ, T.W. (2003). High constitutive signaling of the ghrelin receptor--identification of a potent inverse agonist. *Mol Endocrinol*, **17**, 2201-10.
- HOLST, B., HOLLIDAY, N.D., BACH, A., ELLING, C.E., COX, H.M. & SCHWARTZ, T.W. (2004). Common structural basis for constitutive activity of the ghrelin receptor family. *J Biol Chem*, **279**, 53806-17.
- HOSODA, H., KOJIMA, M., MATSUO, H. & KANGAWA, K. (2000). Ghrelin and des-acyl ghrelin: two major forms of rat ghrelin peptide in gastrointestinal tissue. *Biochem Biophys Res Commun*, **279**, 909-13.
- HOWARD, A.D., FEIGNER, S.D., CULLY, D.F., ARENA, J.P., LIBERATOR, P.A., ROSENBLUM, C.I., HAMELIN, M., HRENIUK, D.L., PALYHA, O.C., ANDERSON, J., PARESS, P.S., DIAZ, C., CHOU, M., LIU, K.K., MCKEE, K.K., PONG, S.S., CHAUNG, L.Y., ELBRECHT, A., DASHKEVICZ, M., HEAVENS, R., RIGBY, M., SIRINATHSINGHI, D.J., DEAN, D.C., MELILLO, D.G., PATCHETT, A.A., NARGUND, R., GRIFFIN, P.R., DEMARTINO, J.A., GUPTA, S.K., SCHAEFFER, J.M., SMITH, R.G. & VAN DER PLOEG, L.H. (1996). A receptor in pituitary and hypothalamus that functions in growth hormone release. *Science*, **273**, 974-7.
- HU, D.E. & BRINDLE, K.M. (2005). Immune cell-induced synthesis of NO and



- reactive oxygen species in lymphoma cells causes their death by apoptosis. *FEBS Lett*, **579**, 2833-41.
- IWAI-KANAI, E. & HASEGAWA, K. (2004). Intracellular signaling pathways for norepinephrine- and endothelin-1-mediated regulation of myocardial cell apoptosis. *Mol Cell Biochem*, **259**, 163-8.
- JALEEL, M.A., TSAI, A.C., SARKAR, S., FREEDMAN, P.V. & RUBIN, L.P. (2004). Stromal cell-derived factor-1 (SDF-1) signalling regulates human placental trophoblast cell survival. *Mol Hum Reprod*, **10**, 901-9.
- JEFFERY, P.L., HERINGTON, A.C. & CHOPIN, L.K. (2002). Expression and action of the growth hormone releasing peptide ghrelin and its receptor in prostate cancer cell lines. *J Endocrinol*, **172**, R7-11.
- JIANG, X.Q., CHEN, J.G., GITTENS, S., CHEN, C.J., ZHANG, X.L. & ZHANG, Z.Y. (2005). The ectopic study of tissue-engineered bone with hBMP-4 gene modified bone marrow stromal cells in rabbits. *Chin Med J (Engl)*, **118**, 281-8.
- KANAMOTO, N., AKAMIZU, T., HOSODA, H., HATAYA, Y., ARIYASU, H., TAKAYA, K., HOSODA, K., SAJO, M., MORIYAMA, K., SHIMATSU, A., KOJIMA, M., KANGAWA, K. & NAKAO, K. (2001). Substantial production of ghrelin by a human medullary thyroid carcinoma cell line. *J Clin Endocrinol Metab*, **86**, 4984-90.
- KATSUMA, S., HATAE, N., YANO, T., RUIKE, Y., KIMURA, M., HIRASAWA, A. & TSUJIMOTO, G. (2005). Free fatty acids inhibit serum deprivation-induced apoptosis through GPR120 in a murine enteroendocrine cell line STC-1. *J Biol Chem*, **280**, 19507-15.
- KATUGAMPOLA, S.D., PALLIKAROS, Z. & DAVENPORT, A.P. (2001). [125I-His(9)]-ghrelin, a novel radioligand for localizing GHS orphan receptors in human and rat tissue: up-regulation of receptors with atherosclerosis. *Br J Pharmacol*, **134**, 143-9.
- KIM, M.S., YOON, C.Y., JANG, P.G., PARK, Y.J., SHIN, C.S., PARK, H.S., RYU, J.W., PAK, Y.K., PARK, J.Y., LEE, K.U., KIM, S.Y., LEE, H.K., KIM, Y.B. & PARK, K.S. (2004). The mitogenic and antiapoptotic actions of ghrelin in 3T3-L1 adipocytes. *Mol Endocrinol*, **18**, 2291-301.
- KINSELLA, B.T., O'MAHONY, D.J. & FITZGERALD, G.A. (1997). The human thromboxane A2 receptor alpha isoform (TP alpha) functionally couples to the G proteins Gq and G11 in vivo and is activated by the isoprostane 8-epi



- prostaglandin F2 alpha. *J Pharmacol Exp Ther*, **281**, 957-64.
- KIPPENBERGER, S., LOITSCH, S., GUSCHEL, M., MULLER, J., KNIES, Y., KAUFMANN, R. & BERND, A. (2005). Mechanical stretch stimulates protein kinase B/Akt phosphorylation in epidermal cells via angiotensin II type 1 receptor and epidermal growth factor receptor. *J Biol Chem*, **280**, 3060-7.
- KOJIMA, M., HOSODA, H., DATE, Y., NAKAZATO, M., MATSUO, H. & KANGAWA, K. (1999). Ghrelin is a growth-hormone-releasing acylated peptide from stomach. *Nature*, **402**, 656-60.
- KOJIMA, M., HOSODA, H. & KANGAWA, K. (2001). Purification and distribution of ghrelin: the natural endogenous ligand for the growth hormone secretagogue receptor. *Horm Res*, **56 Suppl 1**, 93-7.
- KORBONITS, M., GOLDSTONE, A.P., GUEORGUEV, M. & GROSSMAN, A.B. (2004). Ghrelin--a hormone with multiple functions. *Front Neuroendocrinol*, **25**, 27-68.
- KUMAR, M., LIU, Z.R., THAPA, L., WANG, D.Y., TIAN, R. & QIN, R.Y. (2004). Mechanisms of inhibition of growth of human pancreatic carcinoma implanted in nude mice by somatostatin receptor subtype 2. *Pancreas*, **29**, 141-51.
- LIU, Y.Z., BOXER, L.M. & LATCHMAN, D.S. (1999). Activation of the Bcl-2 promoter by nerve growth factor is mediated by the p42/p44 MAPK cascade. *Nucleic Acids Res*, **27**, 2086-90.
- LUO, D., BROAD, L.M., BIRD, G.S. & PUTNEY, J.W., JR. (2001a). Signaling pathways underlying muscarinic receptor-induced  $[Ca^{2+}]_i$  oscillations in HEK293 cells. *J Biol Chem*, **276**, 5613-21.
- LUO, K.Q., YU, V.C., PU, Y. & CHANG, D.C. (2001b). Application of the fluorescence resonance energy transfer method for studying the dynamics of caspase-3 activation during UV-induced apoptosis in living HeLa cells. *Biochem Biophys Res Commun*, **283**, 1054-60.
- MALAGON, M.M., LUQUE, R.M., RUIZ-GUERRERO, E., RODRIGUEZ-PACHECO, F., GARCIA-NAVARRO, S., CASANUEVA, F.F., GRACIA-NAVARRO, F. & CASTANO, J.P. (2003). Intracellular signaling mechanisms mediating ghrelin-stimulated growth hormone release in somatotropes. *Endocrinology*, **144**, 5372-80.
- MOUNIER, C.M., GHOMASHCHI, F., LINDSAY, M.R., JAMES, S., SINGER, A.G., PARTON, R.G. & GELB, M.H. (2004). Arachidonic acid release from mammalian cells transfected with human groups IIA and X secreted phospholipase A(2) occurs



- predominantly during the secretory process and with the involvement of cytosolic phospholipase A(2)-alpha. *J Biol Chem*, **279**, 25024-38.
- MUCCIOLI, G., PAPOTTI, M., LOCATELLI, V., GHIGO, E. & DEGHENGI, R. (2001). Binding of 125I-labeled ghrelin to membranes from human hypothalamus and pituitary gland. *J Endocrinol Invest*, **24**, RC7-9.
- MURATA, M., OKIMURA, Y., IIDA, K., MATSUMOTO, M., SOWA, H., KAJI, H., KOJIMA, M., KANGAWA, K. & CHIHARA, K. (2002). Ghrelin modulates the downstream molecules of insulin signaling in hepatoma cells. *J Biol Chem*, **277**, 5667-74.
- NANZER, A.M., KHALAF, S., MOZID, A.M., FOWKES, R.C., PATEL, M.V., BURRIN, J.M., GROSSMAN, A.B. & KORBONITS, M. (2004). Ghrelin exerts a proliferative effect on a rat pituitary somatotroph cell line via the mitogen-activated protein kinase pathway. *Eur J Endocrinol*, **151**, 233-40.
- PALMA, C. & MAGGI, C.A. (2000). The role of tachykinins via NK1 receptors in progression of human gliomas. *Life Sci*, **67**, 985-1001.
- PALYHA, O.C., FEIGHNER, S.D., TAN, C.P., MCKEE, K.K., HRENIUK, D.L., GAO, Y.D., SCHLEIM, K.D., YANG, L., MORRIELLO, G.J., NARGUND, R., PATCHETT, A.A., HOWARD, A.D. & SMITH, R.G. (2000). Ligand activation domain of human orphan growth hormone (GH) secretagogue receptor (GHS-R) conserved from Pufferfish to humans. *Mol Endocrinol*, **14**, 160-9.
- PAPOTTI, M., GHE, C., CASSONI, P., CATAPANO, F., DEGHENGI, R., GHIGO, E. & MUCCIOLI, G. (2000). Growth hormone secretagogue binding sites in peripheral human tissues. *J Clin Endocrinol Metab*, **85**, 3803-7.
- PETTERSSON, I., MUCCIOLI, G., GRANATA, R., DEGHENGI, R., GHIGO, E., OHLSSON, C. & ISGAARD, J. (2002). Natural (ghrelin) and synthetic (hexarelin) GH secretagogues stimulate H9c2 cardiomyocyte cell proliferation. *J Endocrinol*, **175**, 201-9.
- POMES, A., PONG, S.S. & SCHAEFFER, J.M. (1996). Solubilization and characterization of a growth hormone secretagogue receptor from porcine anterior pituitary membranes. *Biochem Biophys Res Commun*, **225**, 939-45.
- RANG, H.P., DALE, M.M., RITTER, J.M., MOORE, P.K. (2003). *Pharmacology*: CHURCHZLL LIVINGSTONE.
- RENVOIZE, C., BIOLA, A., PALLARDY, M. & BREARD, J. (1998). Apoptosis: identification of dying cells. *Cell Biol Toxicol*, **14**, 111-20.
- RIBBLE, D., GOLDSTEIN, N.B., NORRIS, D.A. & SHELLMAN, Y.G. (2005). A simple technique for quantifying apoptosis in 96-well plates. *BMC Biotechnol*, **5**, 12.



- ROMASHKOVA, J.A. & MAKAROV, S.S. (1999). NF-kappaB is a target of AKT in anti-apoptotic PDGF signalling. *Nature*, **401**, 86-90.
- RUSSELL, J.S.A.D.W. (1998). *Molecular Cloning: A laboratory manual*: Cold Spring Harbor Laboratory (CSHL) Press.
- SAI KRISHNA, A.D., PANDA, G. & KONDAPI, A.K. (2005). Mechanism of action of ferrocene derivatives on the catalytic activity of topoisomerase IIalpha and beta-Distinct mode of action of two derivatives. *Arch Biochem Biophys*, **438**, 206-16.
- SAUER, B. (1994). Site-specific recombination: developments and applications. *Curr Opin Biotechnol*, **5**, 521-7.
- SINGH, K., XIAO, L., REMONDINO, A., SAWYER, D.B. & COLUCCI, W.S. (2001). Adrenergic regulation of cardiac myocyte apoptosis. *J Cell Physiol*, **189**, 257-65.
- SMITH, R.G. (2005). Development of growth hormone secretagogues. *Endocr Rev*, **26**, 346-60.
- SMITH, R.G., GRIFFIN, P.R., XU, Y., SMITH, A.G., LIU, K., CALACAY, J., FEIGNER, S.D., PONG, C., LEONG, D., POMES, A., CHENG, K., VAN DER PLOEG, L.H., HOWARD, A.D., SCHAEFFER, J. & LEONARD, R.J. (2000). Adenosine: A partial agonist of the growth hormone secretagogue receptor. *Biochem Biophys Res Commun*, **276**, 1306-13.
- SMITH, R.G., VAN DER PLOEG, L.H., HOWARD, A.D., FEIGNER, S.D., CHENG, K., HICKEY, G.J., WYVRATT, M.J., JR., FISHER, M.H., NARGUND, R.P. & PATCHETT, A.A. (1997). Peptidomimetic regulation of growth hormone secretion. *Endocr Rev*, **18**, 621-45.
- SNUSTAD, D.P. & SIMMONS, M.J. (1997). *Principles of genetics*.
- SOMAI, S., GOMPEL, A., ROSTENE, W. & FORGEZ, P. (2002). Neurotensin counteracts apoptosis in breast cancer cells. *Biochem Biophys Res Commun*, **295**, 482-8.
- SUGDEN, P.H. & CLERK, A. (1997). Regulation of the ERK subgroup of MAP kinase cascades through G protein-coupled receptors. *Cell Signal*, **9**, 337-51.
- TEJERA, N., GOMEZ-GARRE, D., LAZARO, A., GALLEGO-DELGADO, J., ALONSO, C., BLANCO, J., ORTIZ, A. & EGIDO, J. (2004). Persistent proteinuria up-regulates angiotensin II type 2 receptor and induces apoptosis in proximal tubular cells. *Am J Pathol*, **164**, 1817-26.
- THOMPSON, N.M., GILL, D.A., DAVIES, R., LOVERIDGE, N., HOUSTON, P.A., ROBINSON, I.C. & WELLS, T. (2004). Ghrelin and des-octanoyl ghrelin



- promote adipogenesis directly in vivo by a mechanism independent of the type 1a growth hormone secretagogue receptor. *Endocrinology*, **145**, 234-42.
- TOMEI, L.D. & COPE, F.O. (1991). *Apoptosis: The Molecular Basis of the Cell Death*.
- TRACEY, K.J. & WARREN, H.S. (2004). Human genetics: an inflammatory issue. *Nature*, **429**, 35-7.
- TULLIN, S., HANSEN, B.S., ANKERSEN, M., MOLLER, J., VON CAPPELEN, K.A. & THIM, L. (2000). Adenosine is an agonist of the growth hormone secretagogue receptor. *Endocrinology*, **141**, 3397-402.
- TURNER, P.R., MEFFORD, S., CHRISTAKOS, S. & NISSENSON, R.A. (2000). Apoptosis mediated by activation of the G protein-coupled receptor for parathyroid hormone (PTH)/PTH-related protein (PTHrP). *Mol Endocrinol*, **14**, 241-54.
- UNGRIN, M.D., SINGH, L.M., STOCCO, R., SAS, D.E. & ABRAMOVITZ, M. (1999). An automated aequorin luminescence-based functional calcium assay for G-protein-coupled receptors. *Anal Biochem*, **272**, 34-42.
- VAN DER LELY, A.J., TSCHOP, M., HEIMAN, M.L. & GHIGO, E. (2004). Biological, physiological, pathophysiological, and pharmacological aspects of ghrelin. *Endocr Rev*, **25**, 426-57.
- VASSILIOU, E., SHARMA, V., JING, H., SHEIBANIE, F. & GANEA, D. (2004). Prostaglandin E2 promotes the survival of bone marrow-derived dendritic cells. *J Immunol*, **173**, 6955-64.
- VOLANTE, M., ALLIA, E., FULCHERI, E., CASSONI, P., GHIGO, E., MUCCIOLI, G. & PAPOTTI, M. (2003). Ghrelin in fetal thyroid and follicular tumors and cell lines: expression and effects on tumor growth. *Am J Pathol*, **162**, 645-54.
- VOLANTE, M., ALLIA, E., GUGLIOTTA, P., FUNARO, A., BROGLIO, F., DEGHENGI, R., MUCCIOLI, G., GHIGO, E. & PAPOTTI, M. (2002). Expression of ghrelin and of the GH secretagogue receptor by pancreatic islet cells and related endocrine tumors. *J Clin Endocrinol Metab*, **87**, 1300-8.
- WANG, Y.K. & HUANG, Z.Q. (2005). Protective effects of icariin on human umbilical vein endothelial cell injury induced by H<sub>2</sub>O<sub>2</sub> in vitro. *Pharmacol Res*, **52**, 174-82.
- WIDMANN, C., GIBSON, S., JARPE, M.B. & JOHNSON, G.L. (1999). Mitogen-activated protein kinase: conservation of a three-kinase module from yeast to human. *Physiol Rev*, **79**, 143-80.
- WU-WONG, J.R., CHIOU, W.J. & WANG, J. (2000). Extracellular signal-regulated kinases are involved in the antiapoptotic effect of endothelin-1. *J Pharmacol*

*Exp Ther*, **293**, 514-21.

- WU, D., CLARKE, I.J. & CHEN, C. (1997). The role of protein kinase C in GH secretion induced by GH-releasing factor and GH-releasing peptides in cultured ovine somatotrophs. *J Endocrinol*, **154**, 219-30.
- ZHANG, G., GURTU, V., SMITH, T.H., NELSON, P. & KAIN, S.R. (1997). A cationic lipid for rapid and efficient delivery of plasmid DNA into mammalian cells. *Biochem Biophys Res Commun*, **236**, 126-9.
- ZHU, W.Z., ZHENG, M., KOCH, W.J., LEFKOWITZ, R.J., KOBILKA, B.K. & XIAO, R.P. (2001). Dual modulation of cell survival and cell death by beta(2)-adrenergic signaling in adult mouse cardiac myocytes. *Proc Natl Acad Sci U S A*, **98**, 1607-12.





CUHK Libraries



004278851